

Synthesis, characterization and properties of novel photoactive polysaccharides

Dissertation

zur Erlangung des akademischen Grades doctor rerum naturalium
(Dr. rer. nat.)



seit 1558

vorgelegt dem Rat der Chemisch-Geowissenschaftlichen Fakultät der
Friedrich-Schiller-Universität Jena

von Diplom-Chemiker Holger Wondraczek
geboren am 20. April 1983 in Jena

Gutachter:

1. Prof. Dr. Thomas Heinze (Universität Jena)
2. Prof. Dr. Rainer Beckert (Universität Jena)
3. Prof. Dr. Pedro Fardim (Åbo Akademi University)

Tag der öffentlichen Verteidigung: 12.10.2012

Contents

List of Figures	vii
List of Tables	xi
1. Introduction	1
I. General Part	3
2. Light for the characterization of polysaccharides and polysaccharide derivatives	5
2.1. Structure of polysaccharides	6
2.2. Light absorption by polysaccharides	9
2.3. Fluorescence of polysaccharides and polysaccharide derivatives	11
3. Photoreactions of polysaccharides and polysaccharide derivatives	17
3.1. Photocrosslinking	17
3.2. Photochromic polysaccharide derivatives	19
3.2.1. Polysaccharides containing trans-cis isomerizable chromophores	20
3.2.2. Polysaccharide derivatives forming ionic structures upon irradiation	25
II. Special Part	29
4. UV-Vis spectroscopy for the characterization of novel polysaccharide derivatives	31
4.1. Synthesis of aminocellulose sulfates as novel zwitterionic polymers . .	31
4.2. Characterization of tosyl cellulose sulfates and aminocellulose sulfates	34

5. Tailored synthesis and structure characterization of new highly functionalized photoactive polysaccharide derivatives	39
5.1. Photoactive polysaccharide esters	39
5.1.1. Synthesis	39
5.1.2. Characterization	40
5.2. Synthesis of photoactive polysaccharide polyelectrolytes	47
5.2.1. Mixed 2-[(4-methyl-2-oxo-2 <i>H</i> -chromen-7-yl)oxy]acetic acid- sulfuric acid half esters of dextran and pullulan	48
5.2.2. Mixed 2-[(4-methyl-2-oxo-2 <i>H</i> -chromen-7-yl)oxy]acetic acid- (3-carboxypropyl)trimethylammonium chloride esters of cellulose	54
6. Preparation of nanoparticles from photoactive polysaccharide esters	59
6.1. Nanoparticles from conventional cellulose esters: Evaluation of preparation methods	60
6.1.1. Emulsification-evaporation process	61
6.1.2. Solvent-displacement	64
6.1.3. Conclusions	70
6.2. Nanoparticles from highly substituted dextran 2-[(4-methyl-2-oxo-2 <i>H</i> -chromen-7-yl)oxy] acetates	70
7. Photochemical and photophysical behavior	73
7.1. Photochemical and photophysical behavior of photoactive polysaccharide derivatives in solution	75
7.2. Light absorption and fluorescence for the characterization of photoactive polysaccharide based nanoparticles	78
8. Summary	87
9. Zusammenfassung	89
III. Experimental Part	93
Experimental	94
Materials	94
Measurements	94

Synthesis	96
Tosyl cellulose 2a-c and tosyl cellulose sulfates 3a-c	96
6-deoxy-6-(4-aminoethyl)amino cellulose-2,3(6)-O-sulfate 4a-c , typical example:	96
6-deoxy-6-(2-(bis-N',N'-(2-aminoethyl)aminoethyl)) amino cellulose-2,3(6)-O-sulfate 5a-c , typical example:	96
2-[(4-Methyl-2-oxo-2 <i>H</i> -chromen-7-yl)oxy]acetic acid methyl ester	97
2-[(4-Methyl-2-oxo-2 <i>H</i> -chromen-7-yl)oxy]acetic acid (8)	97
2-[(4-Methyl-2-oxo-2 <i>H</i> -chromen-7-yl)oxy] acetates of cellulose (9), typical example	98
2-[(4-Methyl-2-oxo-2 <i>H</i> -chromen-7-yl)oxy] acetates of dextran (10) and pullulan (11), general procedure	98
Perpropionylation, general procedure	99
Sulfation of 2-[(4-methyl-2-oxo-2 <i>H</i> -chromen-7-yl)oxy] acetates of dextran (12) and pullulan (13), general procedure	99
Mixed [(4-methyl-2-oxo-2 <i>H</i> -chromen-7-yl)oxy] acetic acid- (3-carboxypropyl)trimethylammonium chloride esters of cellulose (15), typical example	99
Nanoparticle preparation methods	100
Emulsification-evaporation	100
Solvent-displacement	100
IV. Back matter	101
Bibliography	102
Publication List	122
Scientific publications in peer reviewed journals	122
Oral presentations	123
Posters	124
Acknowledgements/Danksagung	126
Declaration of Authorship / Selbständigkeitserklärung	129

List of Figures

1.	Jablonski-type diagram.	6
2.	Molecular structure of cellulose.	7
3.	Molecular structure of dextran.	8
4.	Molecular structure of pullulan.	9
5.	Chromophores isolated from cellulosic materials.	10
6.	UV/Vis spectra and picture of a film of a lyotropic mixture of cellulose carbanilate and diethylene glycol dimethacrylate.	11
7.	Structure of oxidized functionalities in polysaccharides and schematic presentation of pathways for their determination by fluorescence labeling.	13
8.	Synthesis of sulforhodamin B and fluorescein labeled dextran propionate and the preparation of nano sized spheres for pH-sensing.	15
9.	Schematic model of the use of a Langmuir-Blodgett assembly as a primer for surface modification.	19
10.	Sol-gel transition behaviour of azobenzene functionalized hydroxypropyl methylcellulose in the absence and presence of α -cyclodextrin.	24
11.	Three-dimensional view of a photoinduced surface relief grating on an azo-cellulose film.	25
12.	Photochromic transformation of spiro benzopyran to a resonance hybrid of a quinoid and a bipolar structure.	26
13.	Synthesis scheme for the preparation of different amino cellulose sulfates	33
14.	FT-IR- and ^{13}C NMR spectra: cellulose, p-toluenesulfonyl (tosyl) cellulose, tosyl cellulose sulfate, and 6-deoxy-6-(2-(bis- N',N' -(2-aminoethyl)aminoethyl)) amino cellulose-2,3(6)- O -sulfate.	36
15.	UV spectra of the methyl 6- O -tosyl- α -D-glucopyranoside and corresponding calibration curve	38
16.	Synthesis scheme for the preparation of cellulose-, dextran- and pullulan 2-((4-methyl-2-oxo-2 <i>H</i> -chromen-7-yl)oxy) acetates.	41

17.	^1H - and ^{13}C NMR spectra of perpropionylated dextran 2-((4-methyl-2-oxo-2 <i>H</i> -chromen-7-yl)oxy) acetate	43
18.	UV spectra of 2-((4-methyl-2-oxo-2 <i>H</i> -chromen-7-yl)oxy)acetic acid methyl ester and corresponding calibration curve	44
19.	^{13}C NMR spectra of cellulose, dextran, pullulan, and the corresponding polysaccharide 2-((4-methyl-2-oxo-2 <i>H</i> -chromen-7-yl)oxy) acetates	46
20.	Synthesis scheme of the sulfation of the 2-((4-methyl-2-oxo-2 <i>H</i> -chromen-7-yl)oxy) acetates of dextran and pullulan	49
21.	IR spectra of pullulan 2-((4-methyl-2-oxo-2 <i>H</i> -chromen-7-yl)oxy) acetate sulfated pullulan 2-((4-methyl-2-oxo-2 <i>H</i> -chromen-7-yl)oxy) acetate	52
22.	^{13}C NMR spectra of pullulan, pullulan 2-((4-methyl-2-oxo-2 <i>H</i> -chromen-7-yl)oxy) acetate and sulfated pullulan 2-((4-methyl-2-oxo-2 <i>H</i> -chromen-7-yl)oxy) acetate	53
23.	Synthesis scheme of the esterification of the cellulose 2-[(4-methyl-2-oxo-2 <i>H</i> -chromen-7-yl)oxy] acetates (9a-f) with (3-carboxypropyl)trimethylammonium chloride (14) in <i>N,N</i> -dimethylacetamide (DMA)/LiCl	55
24.	^{13}C NMR spectra of cellulose, cellulose 2-((4-methyl-2-oxo-2 <i>H</i> -chromen-7-yl)oxy) acetate and mixed 2-((4-methyl-2-oxo-2 <i>H</i> -chromen-7-yl)oxy)-acetic acid- (3-carboxypropyl)trimethylammonium chloride esters of cellulose	57
25.	Principle of the preparation of cellulose ester nanoparticles by the emulsification–evaporation process.	62
26.	Principle of the preparation of polysaccharide nanoparticles by solvent–displacement process.	65
27.	Dependency of the particle size (<i>z</i> -Average) and polydispersity index (PDI) of nanoparticles obtained via dialysis (top) and reduced viscosity (η_{red} , bottom) on the concentration of a) cellulose triacetate (16) and b) cellulose acetate (17 , DS 2.49) dissolved in <i>N,N</i> -dimethylacetamide; c^* denotes for the critical overlapping concentration.	68
28.	Scanning electron microscopy images from nanoparticles obtained by dialysis of dextran ((4-methyl-2-oxo-2 <i>H</i> -chromen-7-yl)oxy)acetates	72
29.	Light-induced processes of coumarins.	73
30.	Structure of different isomers obtained by $2\pi+2\pi$ cycloaddition of coumarin	74

31.	Results of the UV-Vis spectroscopic investigation of the photodimerization of the perpropionylated dextran 2-((4-methyl-2-oxo-2 <i>H</i> -chromen-7-yl)oxy) acetate	76
32.	Results of the viscosity measurements upon photodimerization of dextran 2-((4-methyl-2-oxo-2 <i>H</i> -chromen-7-yl)oxy) acetate	77
33.	Absorption-, fluorescence emission-, and fluorescence excitation spectra of dextran 2-((4-methyl-2-oxo-2 <i>H</i> -chromen-7-yl)oxy) acetate nanoparticles	79
34.	Fluorescence decay curves and average fluorescence lifetimes of dextran 2-((4-methyl-2-oxo-2 <i>H</i> -chromen-7-yl)oxy) acetate nanoparticles.	80
35.	Decay associated fluorescence spectra of dextran 2-((4-methyl-2-oxo-2 <i>H</i> -chromen-7-yl)oxy) acetate nanoparticles	82
36.	Fluorescence lifetime distribution of dextran 2-((4-methyl-2-oxo-2 <i>H</i> -chromen-7-yl)oxy) acetate nanoparticles	83
37.	Fluorescence spectra of dextran 2-((4-methyl-2-oxo-2 <i>H</i> -chromen-7-yl)oxy) acetate nanoparticles before and after illumination	85

List of Tables

1.	Structures of polysaccharides of different origin	7
2.	Typical photoisomerizations	20
3.	Polysaccharides with trans-cis isomerizable moieties	21
4.	Polysaccharides forming ionic structures upon irradiation	26
5.	Conditions for and results of the synthesis of tosyl cellulose (TC) and tosyl cellulose sulfates (TCS)	32
6.	Conditions for and results of the synthesis of 6-deoxy-6-(ω -aminoethyl)amino cellulose-2,3(6)- <i>O</i> -sulfate and 6-deoxy-6-(2-(bis- <i>N'</i> , <i>N'</i> -(2-aminoethyl) aminoethyl))amino cellulose-2,3(6)- <i>O</i> -sulfate	34
7.	Conditions for and results of the esterification of cellulose, dextran and pullulan with 2-[(4-methyl-2-oxo-2 <i>H</i> -chromen-7-yl)oxy] acetic acid (8) via activation with <i>N,N</i> -carbonyldiimidazole (CDI)	42
8.	Conditions for and results of the sulfation of the 2-[(4-methyl-2-oxo-2 <i>H</i> -chromen-7-yl)oxy] acetates of dextran (10) and pullulan (11) with SO ₃ /DMF complex in <i>N,N</i> -dimethylformamide (DMF) as reaction media.	50
9.	Conditions for and results of the synthesis of mixed 2-[(4-methyl-2-oxo-2 <i>H</i> -chromen-7-yl)oxy]	56
10.	Degree of substitution (DS) and weight average molecular weight (\overline{M}_W) of cellulose acetate (CA), cellulose acetate propionate (CAP), -butyrate (CAB), and -phthalate (CAPH) samples applied in the current study.	61
11.	Conditions for and results of the preparation of nanoparticles by emulsification-evaporation.	63
12.	Conditions for and results of the preparation of nanoparticles by the dropping technique.	69
13.	Conditions for and results of the preparation nanoparticles from of photoactive dextran derivatives via dialysis.	71

1. Introduction

Light can be a non-invasive stimulus or probe for the control or analytics of polymer properties. While the analytics rest on the photophysical processes resulting from the interaction of polymers with light the control of polymer properties is generally based on light triggered chemical alterations in the polymer structure. However, both fields of application benefit from the special characteristics of light, that are, high velocity of propagation and in particular the possibility to adjust its energy content as well as its intensity and localization (both spatial and temporal).

Applications based on light-polymer interactions are known for more than 4000 years now. For example, the ancient Egyptians and Babylonians utilized sunlight to photocrosslink linen during mummification and to prepare waterproof papyrus boats via the photopolymerization of an asphalt oil.^[1] Also the first permanent photograph prepared by Joseph Nicéphore Niépce in 1822 was based on the light induced hardening of polymeric bitumen.^[2] Since the design of the first artificial photoreactive polymers by Minsk and co-workers in the 1950s,^[3] the development of different technical applications related to such polymers has become beneficial for daily life.^[4,5] To mention a few examples, photoresponsive polymers are used in photostructuring,^[6] as photoswitches,^[7] and for optical information recording.^[8-10] Moreover, fundamental light triggered biological processes, e.g., vision, photosynthesis, photomorphogenesis, and photomovement at various biological levels, are of great academic and practical interest.^[11,12]

The common feature of photoresponsive polymers is a chromophore incorporated in the macromolecular matrix. Therefore, light absorption and the involved electronic transitions can cause a series of transformations in the polymeric material. Some excellent review articles are published, dealing with various aspects of polymers showing light-induced conformational changes, photostimulated variations of viscosity and solubility, photocontrol of membrane functions, and photomechanical effects.^[13-17]

Polysaccharides are a highly promising class of biopolymers owing to their enormous structural diversity, functional versatility and ubiquity. They are formed biosynthetically by many organisms as storage or as structural polymers and display an extraordinary ability for the formation of supramolecular assemblies of variable

types. In terms of their potential for the development of advanced materials, the outstanding properties of naturally occurring polysaccharides can be specifically exploited or even improved by chemical modification.^[18]

However, in contrast to the enormous interest regarding photoresponsive synthetic polymers, polypeptides and proteins, only a few publications deal with the synthesis and characterization of photosensitive polysaccharide derivatives. The potential arising from the chemical and physical characteristics of polysaccharides is far from being exhausted. For example, to the best of the authors knowledge no work is reported so far utilizing the multifunctional character of polysaccharides to prepare highly functionalized photoactive derivatives that bear additional functional groups. Moreover, only a very few investigations are reported studying photoactive polysaccharide derivatives with regard to the broad structural diversity, i.e. there is neither an information about the influence of the polysaccharide backbone on the functionalization with a specific chromophore nor on its influence on the photochemistry of the functional group. Last but not least, the design of photo-controllable biopolymeric nanostructures is of recent interest for the design of advanced materials, e.g., the development of stimuli responsive drug delivery systems.

The essential objective reported in this thesis was the synthesis and detailed characterization of photoactive polysaccharide derivatives. Advanced methods for the chemical modification of polysaccharides in particular modern esterification techniques were used for the synthesis of well defined polysaccharide derivatives decorated with both photoactive and ionic functionalities. Following the unambiguous structural characterization of the derivatives they were applied for the preparation of nanostructures and their photochemistry was investigated.

Part I.
General Part*

*This part is based on the review article “Photoactive polysaccharides” by Holger Wondraczek, Anne Kotiaho, Pedro Fardim, and Thomas Heinze published in *Carbohydrate Polymers* 83 (2011) 1048–1061

2. Light for the characterization of polysaccharides and polysaccharide derivatives

Light absorption of a chromophore incorporated in a macromolecular matrix results in electronic transitions similar to those of low molecular weight compounds. These transitions involved in photoexcitation and relaxation of the excited states can be schematically summarized in a modified Jablonski diagram (Fig. 1). As a result of absorption (abs) of light, the chromophore reaches a higher energy state. The energy gained can be released either radiatively or non-radiatively. The non-radiative relaxation processes include internal conversion (ic), vibrational relaxation (vr), and intersystem crossing (isc). The relaxation processes including emission of light are fluorescence (fl) and phosphorescence (phos). While fluorescence is a spin-allowed transition, taking place in the picosecond-timescale, phosphorescence is a spin-forbidden transition, and thus a slow process taking place in the millisecond- or even second-timescale. The energy of the excited molecule can also be released via interaction with other molecules by the direct transfer of energy or electrons as well as by the formation of excited complexes. Absorption of light can also trigger photochemical reactions like isomerization, dissociation or crosslinking (react). However, some properties of polymers like relatively high rigidity, orderliness or anisotropy may cause unusual spectroscopic properties and special effects within the deactivation processes.

While conventional UV/Vis spectroscopy can be applied to analyze and to identify polymers containing chromophors regarding their molecular constitution, sophisticated absorption methods provide powerful tools to study supramolecular structures as well. For example, circular dichroism (CD) spectroscopy allows the determination of different structural types as well as the detection of the alterations in the supramolecular structure of macromolecular systems. To mention a few examples, the secondary structure of proteins (α -helix, parallel and anti-parallel β -pleated sheets, and β -turns) can be designated in type and relative content, the thermal denaturation of superstructures such as those of DNA or collagen can be monitored, and the chirality of newly synthesized polymers can be characterized.^[19,20] The rele-

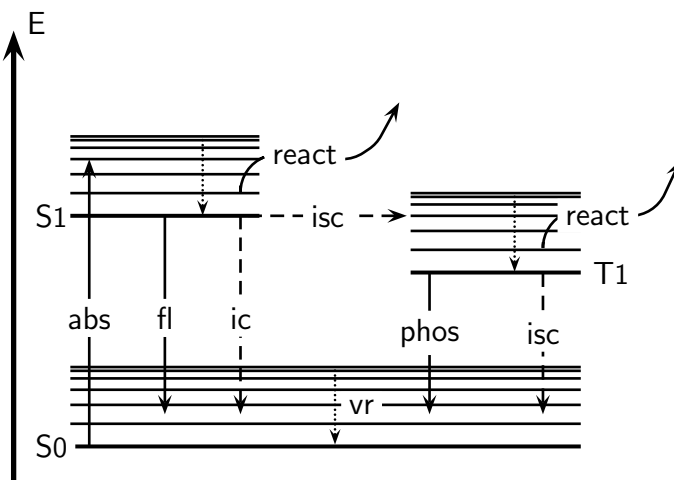


Figure 1: Jablonski-type diagram. Abbreviations: abs: absorption, fl: fluorescence, phos: phosphorescence, ic: internal conversion, isc: intersystem crossing, vr: vibrational relaxation, react: other deactivation processes (see text).

vance of UV/Vis spectroscopy and related spectroscopic methods for polysaccharide chemistry is discussed in the following. However, it appears appropriate to focus on some aspects of polysaccharide structure before.

2.1. Structure of polysaccharides

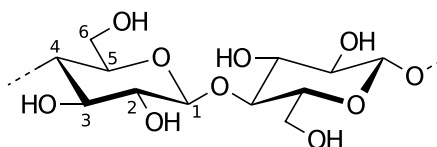
There is a wide range of naturally occurring polysaccharides derived from plants, microorganisms, fungi, marine organisms, and animals as storage and structure forming macromolecules. The polysaccharides most commonly used for polymeranalogous reactions are summarized in Tab. 1. The common motifs are the polymer backbone, consisting of O-linked pyranose or furanose rings, and different functionalities, e.g., primary and secondary OH-groups, carboxylic acid moieties, and NH_2 groups, accessible to chemical modifications. Comprehensive reviews about important methods of modification, including esterification, etherification, and oxidation, are available^[21–26].

Cellulose, the most abundant organic compound on earth, is the most prominent polysaccharide among the biopolymers mentioned in Tab. 1. It stands out due to its unique structure characterized by regio- and enantioselectively $\beta - (1 \rightarrow 4)$ linked anhydro-D-glucose units composing a polydisperse linear homopolymer (Fig. 2). Beside the rather simple molecular structure, complex supramolecular structures are formed, which have remarkable influence on both physical and chemical properties

Table 1 : Structures of polysaccharides of different origin^[21]

Polysaccharide	Source	Structure	Ref.
Cellulose	Plants	β -(1→4)-anhydro-D-glucose	[27]
Curdlan	Bacteria	β -(1→3)-anhydro-D-glucose	[28]
Scleroglucan	Fungi	β -(1→3)-anhydro-D-glucose main chain, β -(1→6)-anhydro-D-glucose branches	[29]
Schizophyllan	Fungi	β -(1→3)-anhydro-D-glucose main chain, anhydro-D-glucose branches	[30]
Dextran	Bacteria	α -(1→6)-anhydro-D-glucose main chain, anhydro-D-glucose branches	[25]
Pullulan	Fungi	α -(1→6) linked maltotriosyl units	[31,32]
Starch	Plants		[33,34]
Amylose		α -(1→4)-anhydro-D-glucose	
Amylopectin		α -(1→4) and α -(1→6)-anhydro-D-glucose	
Xylan	Plants	β -(1→4)-anhydro-D-xylose main chain, complex branches	[35]
Guar	Plants	β -(1→4)-anhydro-D-mannose main chain, anhydro-D-galactose branches	[36]
Inulin	Plants	β -(1→2)-anhydrofructofuranose	[37]
Chitin	Animals	β -(1→4)-anhydro-D-(N-acetyl)glucosamine	[38]
Chitosan	Fungi	β -(1→4)-anhydro-D-glucosamine	
Alginate	Algae	α -(1→4)-anhydro-L-guluronic acid, β -(1→4)-anhydro-D-mannuronic acid	[39]

of the polymer.^[40,41] An important consequence of its supramolecular structure is the insolubility of the macromolecule in water and in common organic liquids, which still stimulates the search for solvents appropriate for shaping and for homogeneous phase reactions of cellulose.^[42–44] The carbon atoms at the positions 2, 3, and 6 possess hydroxyl groups, which are, in general, accessible to the typical conversions of primary and secondary -OH groups.

**Figure 2** : Molecular structure of cellulose including numbering of C-atoms

Dextran, a family of neutral polysaccharides, find widespread use in medicinal and pharmaceutical applications, e.g., as blood plasma substitutes or coating material

to prevent protein opsonization.^[45] The polymer, produced by numerous bacterial strains (*Leuconostoc* and *Streptococcus*), consists of a α -(1 \rightarrow 6) linked anhydro-D-glucose main chain with varying branches. The content of α -(1 \rightarrow 6) linkages may vary from 97 to 50% of total glycosidic bonds. The number and type of branches, bound by α -(1 \rightarrow 2), α -(1 \rightarrow 3), and α -(1 \rightarrow 4) glycosidic bonds, depends on the origin.^[32] The commercially applied bacteria strain *Leuconostoc mesenteroides* NRRL B-512(F) produces a dextran that is predominately α -(1 \rightarrow 6) linked and contains a relatively low level (< 5%) of randomly distributed α -(1 \rightarrow 3) linked branches (Fig. 3).^[46] This dextran is generally soluble in water and organic solvents such as dimethyl sulfoxide and it can be utilized for chemical conversion into unconventional derivatives, like dextran pyroglutamate or dextran furoate, which show formation of nano-scaled particles.^[47]

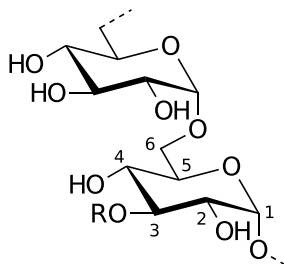


Figure 3: Structure of dextran obtained from *Leuconostoc mesenteroides* NRRL B-512(F) including numbering of C-atoms. R = predominately H and 5% glucose or α -(1 \rightarrow 6) linked glucopyranosyl- α -D-glucopyranoside

Pullulan is also a neutral, water soluble polysaccharide produced extracellularly by certain strains of the polymorphic fungus *Aureobasidium pullulans* via the fermentation of sugars like maltose, xylose, arabinose, glucose, and sucrose. It is a non-branched glucan consisting of α -(1 \rightarrow 6) linked maltotriosyl repeating units^[32,48]. In the repeating unit three anhydro-D-glucose moieties are joined by α -(1 \rightarrow 4) linkages. The polysaccharide possesses primary hydroxyl groups at position 6 of the anhydro-D-glucose moieties b and c as well as secondary hydroxyl groups at position 2 and 3 (AGU a, b and c) and position 4 (AGU a). The current knowledge on biosynthesis, biological activity, and chemical modification of pullulan are summarized in recent review articles.^[31,49]

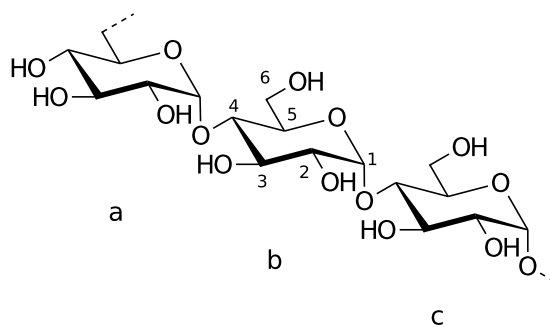


Figure 4: Molecular structure of pullulan including numbering of C-atoms and of the three different anhydro-D-glucose units of the α -(1 \rightarrow 6) linked maltotriosyl repeating units.

2.2. Light absorption by polysaccharides

Chemically pure glucans, like bacterial cellulose are poor absorbers of UV and visible light on one hand. On the other, cellulosic pulps contain different chromophores that are formed from polysaccharides because of thermal-oxidative stress during the common process stages of pulping and bleaching. Moreover, subsequent processing including fiber spinning and derivatization or even natural aging may lead to additional chromophores in products manufactured from cellulosic pulps.

The chemical nature of the chromophores in cellulose has been studied utilizing reference model compounds since the 1960's.^[50,51] The weak absorption bands in the 210-320 nm UV range were assigned to carbonyl and acetal groups as well as various impurities such as trace amounts of transition metal ions.^[52] So far, the reason for the visible yellowing effect of cellulosic fibers and derivatives was largely unclear, since the overall discoloration effect is caused by a large number of chromophores. In addition, the concentration of these chromophores is generally extremely low, mostly in the ppb range. By a chromophore release and identification procedure, which applies boron trifluoride-acetic acid complexes in combination with sodium sulfite, a number of hydroxybenzoquinone, hydroxyacetophenone, and naphthoquinone structures were isolated from different cellulosic materials (Fig. 5).^[53,54] Some of these compounds, so called Theander products, arise from cellulose degradation starting from keto structures, e.g., oxidized spots in cellulose. They are formed mainly upon acidic, basic, and thermal treatment of polysaccharide fragments in the presence of air and thus their formation is largely independent of origin of the cellulosic material.^[55-58] Moreover secondary, mainly process-specific, chromophores are present in cellulose II products such as fibers, which are more prominent and color-intensive.^[54] Recent

studies using UV-resonance Raman spectroscopy also demonstrate the formation of aromatic structures from the reducing end groups of polysaccharide chains.^[59]

Due to the consumer notion, that only "really white" materials are clean, both the optical properties of cellulosic materials and the formation of chromophores are still a focus of research.^[60,61] In particular, the role of aromatic structures in brightness reversion is studied by applying sophisticated analytical tools including reflectance UV/Vis spectroscopy, UV-resonance Raman spectroscopy, gel permeation chromatography, and chemical methods.^[62-64] A thorough knowledge about the chemical structure of the chromophores and their origin might help to develop strategies to reduce the formation of these impurities in the processes of the paper and textile industries from the outset, and thus for example, save bleaching costs and reduce the environmental impact of pulp production.

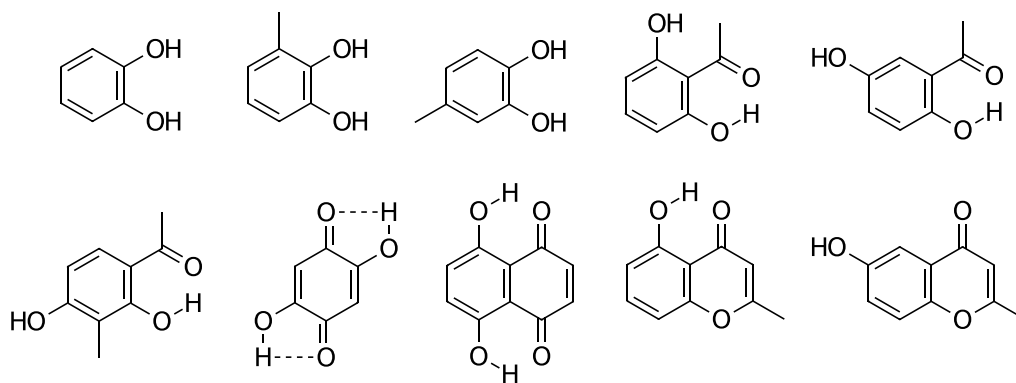


Figure 5: Chromophores isolated from cellulosic materials by a chromophore release and identification procedure.^[53,54]

Absorption spectroscopy is also a valuable tool especially for analytics of cellulose derivatives. First of all, the success of functionalization with a light absorbing moiety can be proofed and the degree of substitution (DS) can be determined by utilizing an appropriate reference compound. Moreover, the elucidation of supramolecular structures is possible. For example, cellulose derivatives displaying lyotropic or thermotropic cholesteric phases can be characterized by means of absorption spectroscopy. By measuring the cholesteric reflection peaks, the pitch height of the helicoidal arrangement was determined for a series of cellulose derivatives.^[65-69] Fig. 6 shows the UV/Vis spectra of a lyotropic mixture of cellulose carbanilate with a $-CF_3$ moiety in *meta*-position and diethylene glycol dimethacrylate. After crosslinking the mixture at different temperatures, the cholesteric helix and thus their pitch was fixed. The spectra, subsequently recorded at room temperature, illustrate the

selective reflection of the cholesteric sample and allow the determination of the pitch height according to literature.^[70] Beside the selective reflection, the cholesteric state is optically uniaxial and therefore displays optical rotation dispersion and circular dichroism. These features could be used for the determination of further structural parameters, including handedness of the cholesteric helix. The combination of the optical effects sketched above, make lyotropic and thermotropic cellulose derivatives interesting materials for opto-electronic applications as well as for opalescent cholesteric films.^[69,71,72] Moreover, these issues reveal the potential of absorption spectroscopy for the understanding of supramolecular structures.

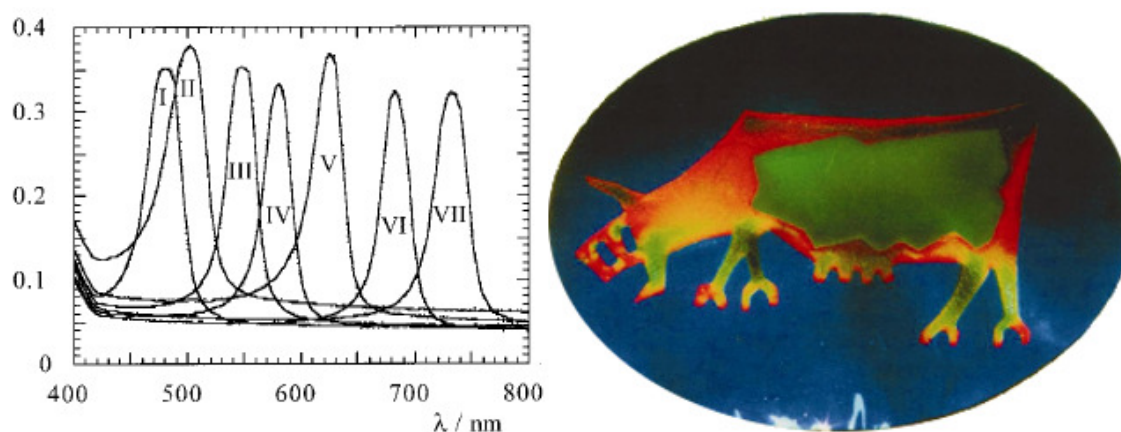


Figure 6: Left: UV/Vis spectra of a cholesteric mixture containing 3-(trifluoromethyl)phenyl urethane of cellulose (45 wt.-%) and diethylene glycol dimethacrylate crosslinked at I: 20 °C, II: 25 °C, III: 30 °C, IV: 35 °C, V: 40 °C, VI: 45 °C, VII: 50 °C. Right: Picture of a film prepared from the cholesteric mixture photo-crosslinked at different temperatures (blue: 20 °C, green: 30 °C, orange: 45 °C). Adapted from “Cholesteric phases and films from cellulose derivatives” with permission from Wiley-VCH Verlag GmbH & Co. KGaA.^[69]

2.3. Fluorescence of polysaccharides and polysaccharide derivatives

The absorption of light results in an electronically excited state of the polymer itself or only the attached/incorporated chromophores. From the different deactivation processes that can occur, fluorescence is one of the most prominent pathways.^[73] This section will give some examples that connect the phenomenon of fluorescence with the field of polysaccharide chemistry.

Fluorescence typically occurs from highly conjugated polycyclic aromatic molecules. For polysaccharides in general, and cellulose in particular, different impurities like lignin appear to be the main contributors to fluorescence emission. Thus the fluorescences of lignocellulose have been extensively studied and the nature of the fluorescent chromophores in lignin was investigated by means of lignin model molecules.^[74-76] Coniferyl alcohol, biphenyl, stilbene, phenylcoumarone and structures similar to coniferyl aldehyde are widely considered to be the main structural elements responsible for the fluorescence emission of wood and lignin-rich pulps.

Nevertheless, fluorescence could still be observed in different cellulose samples, even when lignin was removed by pulping and bleaching.^[77] In view of their universal presence in all living organisms, proteins have been suggested as the source of fluorescence emission as well as residual lignin.^[74] However, Castellan et al. pointed out that the presence of contaminants (protein, tyrosine, etc.) in microcrystalline cellulose is very unlikely.^[78] Moreover, the lignification process for cotton linters is quite limited. Thus, it is puzzling that fluorescence could still be observed in both cases. Although phenolic and quinoid chromophores are proposed to be the source of fluorescence emission, the exact chemical structure of fluorophores in cellulose remains unclear (Fig. 5). However, since fluorescence techniques are highly sensitive, they are suitable for detailed investigations of residual lignin in bleached pulps. Moreover, they are useful tools for the observation of bleaching and brightness reversion.^[79]

Beside the continuing research regarding the nature of fluorescent chromophores in cellulose themselves, fluorescence spectroscopy provides the possibility to analyze the molecular structure of the polymer backbone. For example, Fig. 7a shows different oxidized functionalities, which may occur in polysaccharides in general and in cellulose in particular. Oxidized positions in cellulose are main reasons for strength loss and decreased performance parameters in textiles, paper, and other cellulosic materials. Moreover, they are responsible for general aging and are assumed to be the promoter of thermal and light induced yellowing processes.^[80,81] The reliable and accurate determination of aldehyde-, keto-, and carboxyl groups in cellulose and other polysaccharides represented a largely unsolved problem in polysaccharide research. Recently, different methods to quantify small amounts of oxidized structures via fluorescence spectroscopy in cellulosic pulps were developed. As shown in Fig. 7b, a carbazole fluorophore decorated with a spacer and an appropriate anchor group was used to label carbonyl groups selectively.^[82,83] The derivatization presented proceeds

completely over the whole molecular weight range in the "exotic" solvent *N,N*-dimethylacetamide/lithium chloride, which is one of a limited number of solvents dissolving high molecular weight polysaccharides. Moreover, the fluorophore does not interfere with the multi angle laser light scattering (MALLS) detection of chromatographic procedures and the spacer avoids any shift of the fluorescence emission, which might be caused by the spatial environment of the fluorophore. By implementing these method into gel permeation chromatography (GPC), it became possible to determine not only the carbonyl content as a sum parameter, but also with regard to the molecular weight distribution for the first time.^[84-86] Moreover, a similar method for the determination of the carboxyl content and carboxyl profile was developed applying 9*H*-fluoren-2-yl-diazomethane as selective fluorescence label (Fig. 7c).^[87,88]

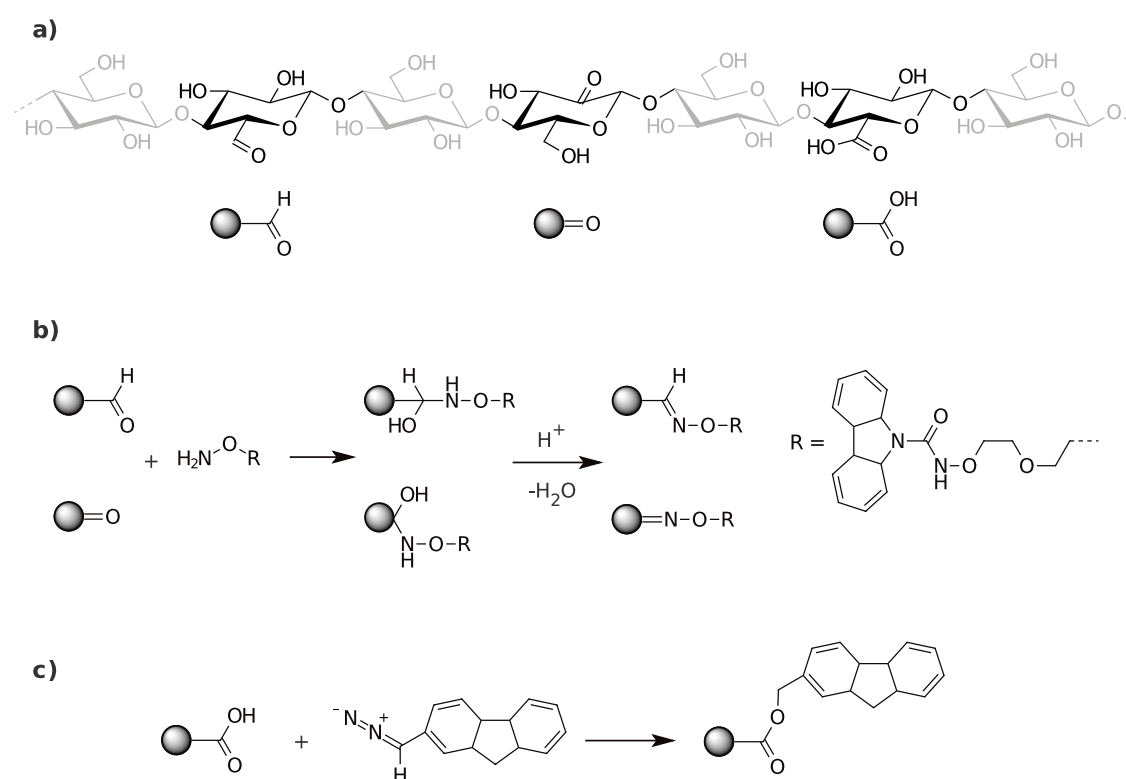


Figure 7: a) Schematic representation of oxidized functionalities in polysaccharides, including aldehyde-, keto-, and carboxyl groups (end groups not shown); b) Reaction pathway for the determination of the carbonyl content in cellulose by fluorescence labeling; c) Reaction pathway for the determination of the carboxyl content in cellulose by fluorescence labeling.^[82,87]

The combination of polysaccharides or polysaccharide derivatives with fluorescence methods also leads to promising applications in the biomedical field. Here dextran is

of particular interest. For example, the exploration of chemical micro environments in organisms as well as on the cellular level can be realized with dextran based fluorescent nanoparticles. A sensor system for pH monitoring in living cells is based on nano-scaled particles prepared from dextran decorated with propionic acid, sulforhodamine B acid, and the pH indicator dye fluorescein (Fig. 8).^[89] The use of the natural polymer as a basis for such functionalized nanoparticles may benefit from the inherent biocompatibility of polysaccharides and thus overcome drawbacks like toxicity due to monomer and surfactant residues in synthetic polymers or the need of stimulating agents for cell uptake.

Fluorescence is one example of photoluminescence, but light emission can also be initiated by applying voltage. An application, taking advantage of electroluminescence, are devices like Organic Light Emitting Diodes (OLEDs). Cellulose and starch were mainly used as a supporting material in order to provide biocompatibility,^[90] to improve mechanical properties,^[91,92] or to enhance photoluminescence and electroluminescence efficiency of OLEDs.^[93] However, the application of functionalized cellulose as active luminescent material for both OLEDs and an organic memory device is reported as well.^[94,95] Different regioselectively substituted derivatives were prepared using 9-(4-bromobutyl)-9H-carbazole and p-methoxytrityl cellulose. These fluorescent cellulose compounds show properties similar to poly(N-vinylcarbazole), widely used for OLEDs. However, the results indicate that the packing manner of the carbazole moieties as a consequence of the substitution pattern greatly affects optical properties like the emission intensity and spectrum or the luminance voltage.

The preparation of chromophore films without scaffolding can lead to quenching of fluorescence due to aggregation and thus to an reduced performance as sensitizers or photocurrent generators. Therefore, polysaccharide scaffolds have also been considered for the preparation of solid structures of precisely organized chromophores, which retain the fluorescence properties even at high concentrations of chromophores. Typical examples are cellulose derivatives that are regioselectively functionalized in position 6 with porphyrin moieties (DS 0.6). The chirality and the stiff backbone of cellulose combined with the strictly defined regiochemistry lead to a helical arrangement of the cellulose-bound porphyrins as shown by CD spectroscopy. Moreover, porphyrin cellulose was studied by means of spectroelectrochemistry and picosecond laser fluorescence in context with the application as an optoelectronic material.^[96,97] Langmuir-Blodgett films of porphyrin-cellulose show improved photocurrent generation in electrochemical cells compared to porphyrin films, indicating the beneficial

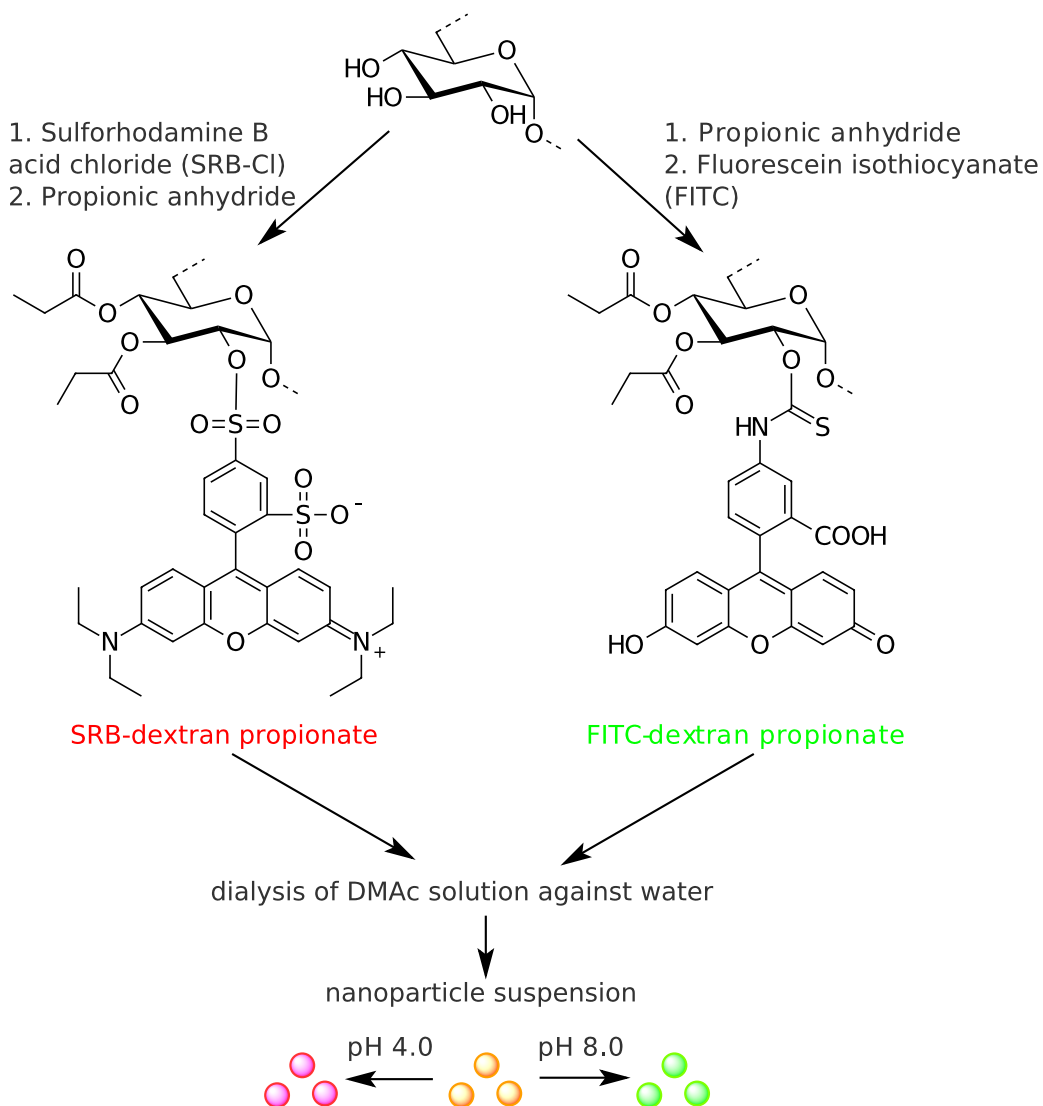


Figure 8: Synthesis of sulforhodamin B and fluorescein labeled dextran propionate and the preparation of nano sized spheres for pH-sensing; one anhydro-D-glucose unit is schematically presented. ^[89]

role of cellulose as a scaffold.^[98] The chromophores are spaced at a fixed distance by using cellulose with its rigid structure and thus the photocurrent quantum yields for the LB films are increased.^[99] A further improvement of photocurrent performance was obtained by the incorporation of fullerene (C_{60}) in porphyrin-cellulose films.^[100]

A further indication of the ability of polysaccharides to act as an efficient scaffold can be concluded from studies of anthracene molecules attached to dextran.^[101] The polymers are water soluble at low DS of anthracene moieties. Quenching of fluorescence after addition of suitable energy or electron acceptors in the water solution is observed, indicating photoinduced energy or electron transfer. Thus, these are promising polymers for photosensitization of reactions of organic compounds in aqueous solutions.^[102]

3. Photoreactions of polysaccharides and polysaccharide derivatives

In the discussion about photoreactions of polymer based systems, in particular polysaccharides, different aspects must be considered: the polysaccharide itself, low molecular weight compounds hosted by the polysaccharide matrix, and chromophores covalently attached to the polymer backbone. These aspects cannot be strictly separated from each other at any time and the following section will give an overview about photochemical processes such as photodegradation, photocrosslinking, and photochromic effects.

The absorption of light can cause photolysis in cellulose and its derivatives.^[81] In general, a decrease of the degree of polymerization and an increase of the copper number, that is, an increase of the carbonyl content, as well as an increase of alkali solubility can be observed. Moreover, the light induced degradation is accompanied by yellowing and the formation of carbonyl- and carboxyl groups along the polymer chain. Carbon monoxide, carbon dioxide, and hydrogen are the main gaseous products formed during photolysis of polysaccharides. Since society invests considerable resources in the preservation of cultural heritage a detailed understanding of photoinduced degradation of polysaccharides and in particular of cellulose is of major interest.^[103–107] Moreover, light stability is of growing importance in material sciences, where a revival of interest on polysaccharides by researchers and industrialists occurred recently. The destructive nature of UV and visible light, in particular in case of high intensity or long exposure time, must be kept in mind for the discussion of photoreactions.

3.1. Photocrosslinking

In polysaccharide chemistry light induced crosslinking is applied for the improvement of material properties,^[108] the stabilization of supramolecular structures,^[109] and the immobilization of biomolecules.^[110] Some aspects of these fields will be pointed out.

Polysaccharides in particular starch were investigated as a promising raw material in order to replace synthetic polymers and thus reduce the environmental impact of plastic wastes especially from packing. For example, thermoplastic starch mixtures have found application in the polymer market as loose filler materials. Nevertheless, the hydrophilic nature of thermoplastic starch seriously limits its wider applications. Thermoplastic starch is sensitive to water and since the water content of the materials changes with environmental humidity, mechanical properties change during use and storage. Photocrosslinking is one interesting attempt to overcome these disadvantages. A solid state crosslinking procedure of sensitized starch films using UV irradiation and sodium benzoate as water-soluble photo additive was described.^[111] In contrast to conventional crosslinking procedures, there was no need of organic solvents and toxic crosslinking agents like epichlorohydrine or phosphoryl chloride. The crosslinking kinetics were studied by the determination of the degree of swelling and gel fraction, in order to characterize the created network. The results indicate that mechanical properties like Young's moduli and ultimate strength can be improved by UV treatment. Additional investigations describe the influence of photocrosslinking on the retrogradation of starch based materials.^[112] It was shown that the crosslinking treatment partially inhibits retrogradation of starch films by limiting crystallization and thus partially prevents aging and the decrease of the ultimate mechanical properties (elongation and stress at break, Young's moduli). Sodium benzoate was also used as sensitizer for surface modifications of starch sheets, in order to improve the surface properties without changing the bulk composition and characteristics.^[113,114] Compared with the bulk photocrosslinking, the required amount of sensitizer was significantly lower and the crosslinking reaction occurred much easier in the surface layer. One primary result of these investigations was a significant increase of the surface water contact angle indicating an enhancement of the hydrophobic character of the surface and a lower value for the polar component of the surface energy. Moreover, the surface modification led to notably lower moisture uptake and an overall improvement of water resistance.

The preparation of composite materials by means of photochemical methods is also an approach to enhance existing properties or impart new properties in polysaccharide based polymers. UV irradiation and sodium benzoate as a photo sensitizer were used in order to crosslink films of cellulose reinforced starch and the obtained biocomposites show remarkably improved physical and mechanical properties.^[115] Moreover, the synthesis of interpenetrating polymer networks and polysaccharide based copolymers

is a valuable tool to gain new materials with promising properties. In this sense, photocrosslinking was applied to graft synthetic polymers onto polysaccharides, ^[116,117] or to preserve the structures possessed by the polysaccharide during the preparation of the composite material. ^[118] Cinnamoylisopentylcellulose is one interesting hairy-rod-like polysaccharide (HRP) derivative that can be utilized to create Langmuir-Blodgett (LB) assemblies of defined thickness on the nanometer scale. By crosslinking the cinnamoyl groups, stable LB films with properties such as isotopic selectivity or a certain swelling degree are obtained. ^[109] As shown in Fig. 9 such LB assemblies were used as a primer for surface modification by polymerization. ^[119] The incorporation of methyl methacrylate as typical monomer (Fig. 9a) and a subsequent polymerization led to homogeneous nano-scaled composite films (Fig. 9b).

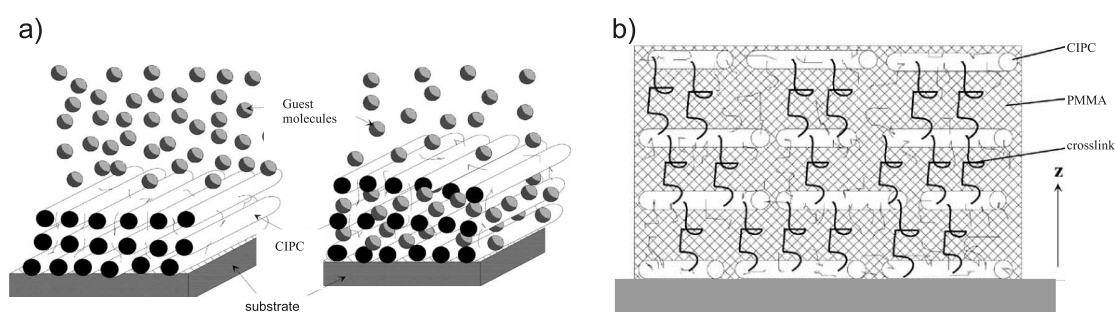
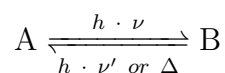


Figure 9: a) Schematic model of a swellable LB film of photocrosslinked cinnamoylisopentylcellulose (CIPC). Guest molecules can be solvent, dye molecules or monomers. b) Schematic picture of the composite multilayered CIPC and poly-methyl methacrylate (PMMA) incorporated via vapor phase photopolymerization. The scale of the CIPC hairy-rods and periodic spacing is only schematically represented. Adapted from “Multilayered Assembly of Cellulose Derivatives as Primer for Surface Modification by Polymerization”. ^[119] With permission from Wiley-VCH Verlag GmbH & Co. KGaA.

3.2. Photochromic polysaccharide derivatives

Photochromic compounds undergo a reversible change of color upon illumination. As the compound is interconverted between two states by means of irradiation or a thermal stimulus, the absorption spectrum and the physical properties of the compound change. The interconversion between the two forms can schematically be expressed as:



Typical examples of chromophores, which show photochromic behavior upon irradiation with light of an appropriate wavelength, are summarized in Tab. 2. In the following subsections some photochromic polysaccharide derivatives are discussed.

Table 2: Typical photoisomerizations

Reaction type	Example
(a) Trans-cis isomerization of double bonds	<p>The diagram shows the photoisomerization of a trans-azobenzene derivative (left) to its cis form (right). The trans isomer has a dipole moment of 9.0 Å, and the cis isomer has a dipole moment of 5.5 Å. Both molecules have R groups on the phenyl rings.</p>
(b) Zwitter ion formation	<p>The diagram shows the photoisomerization of a spirocyclic compound (left) to a zwitterionic form (right). The zwitterionic form features a positively charged nitrogen atom (N+) and a negatively charged oxygen atom (O-).</p>
(c) Ionic dissociation	<p>The diagram shows the photoisomerization of a neutral carbonium ion salt (left) to a zwitterionic form (right). The zwitterionic form features a positively charged carbon atom (C+) and a negatively charged halide ion (X-).</p>
(d) Ring formation and ring cleavage	<p>The diagram shows the photoisomerization of a coumarin derivative (left) to a spirocyclic form (right).</p>

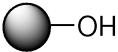
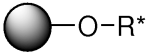
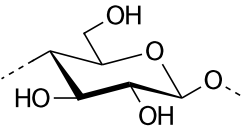
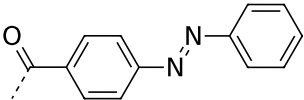
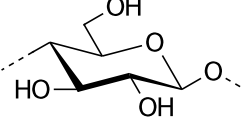
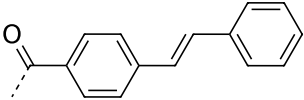
3.2.1. Polysaccharides containing trans-cis isomerizable chromophores

The introduction of photoisomerizable compounds (Tab. 2a) in polymers may yield a photoinduced conformational change of the polymer chain induced by the conformational change of the chromophore. Azobenzene compounds (azos), characterized by an azo linkage (-N=N-) joining two phenyl rings, are the most prominent photoisomerizable molecules. The azobenzene photochemistry gives rise to numerous photoswitching and photostructuring applications due to the fact that azobenzene chromophores undergo a large change both in structure and dipole moment during the

isomerization. Moreover, a photoinduced orientation of the azobenzene chromophores in polymers and, therefore, a mass transport process is possible when irradiating with polarized light. Additionally, azos are chemically robust molecules and can easily be incorporated into a polymer matrix or even covalently attached.^[120,121]

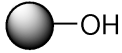
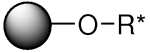
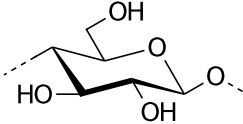
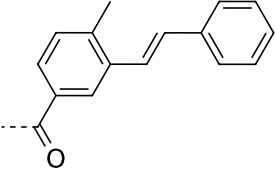
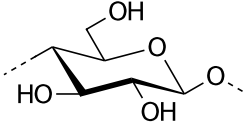
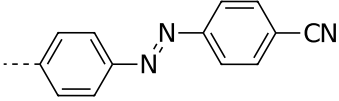
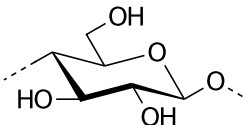
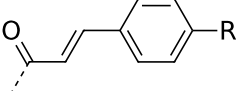
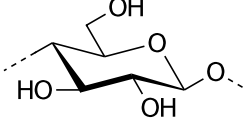
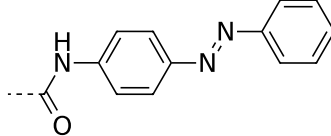
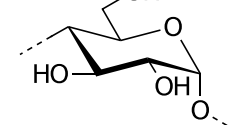
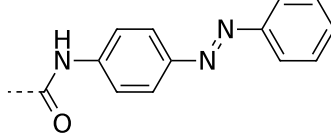
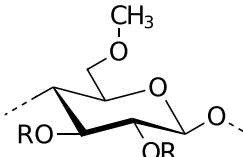
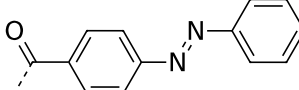
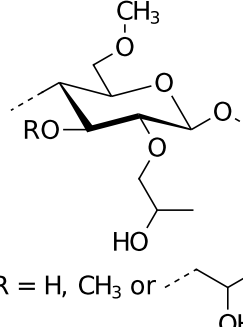
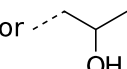
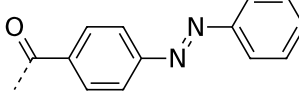
In Tab. 3, a series of polysaccharide derivatives decorated with trans-cis isomerizable moieties are summarized. Beside azobenzene chromophores (Tab. 3 entry 1, 4 & 6-11) stilbene (Tab. 3 entry 2 & 3) and cinnamic acid (Tab. 3 entry 5 & 12) were linked to the polymer backbone. Cellulose was the most common starting polymer at the beginning of the research on modification of polysaccharides with isomerizable substituents (Tab. 3 entry 1-6). Recently, other polysaccharides in particular dextran and starch (Tab. 3 entry 7 & 10-12) came into focus as well as commercial polysaccharide derivatives like methylcellulose or hydroxypropyl methylcellulose (Tab. 3 entry 8 & 9). The linkage between the polymer backbone and the photoresponsive moieties was realized in different ways. For example, esterification,^[108,122-129] etherification,^[130,131] and the formation of carbamates were applied.^[132] However, esterification was the most important path for introducing photoactive functionalities up to now. In general, a conventional esterification procedure was employed, using the acyl chloride either heterogeneously or homogeneously. Recently, *N,N*-carbonyldiimidazole was established as an efficient activating agent for the homogeneous acylation of polysaccharides in non-aqueous systems for substituents like azobenzene- and cinnamic acid.^[129]

Table 3: Polysaccharides with trans-cis isomerizable moieties

No.	Starting polymer	Photoresponsive moiety ^a	Reference
			
1			[122]
2			[123]

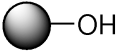
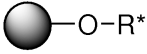
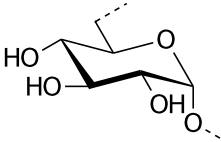
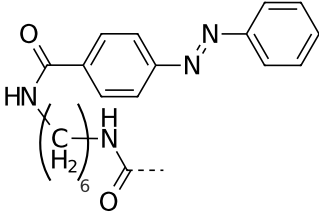
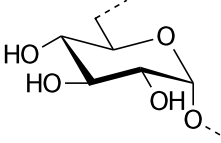
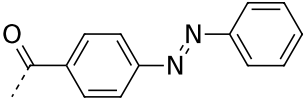
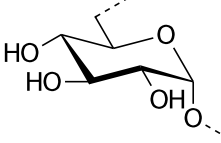
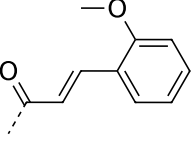
^a including linkage to the polymer backbone

Table 3: Polysaccharides with trans-cis isomerizable moieties (continued)

No.	Starting polymer 	Photoresponsive moiety ^a 	Reference
3			[124]
4			[130,131]
5		 R = H, NO ₂ , O-(C(CH ₂) _{5 or 15})-CH ₃	[108]
6			[132]
7			[132]
8	 R = H or -CH ₃		[125]
9	 R = H, CH ₃ or 		[126-128]

^a including linkage to the polymer backbone

Table 3: Polysaccharides with trans-cis isomerizable moieties (continued)

No.	Starting polymer 	Photoresponsive moiety ^a 	Reference
10			[133]
11			[129]
12			[129]

^a including linkage to the polymer backbone

Cellulose derivatives containing azobenzene groups (Azo-cellulose) were prepared for the first time heterogeneously by the reaction of microcrystalline cellulose with 4-phenylazobenzoyl chloride in pyridine.^[122] Similar cellulose-stilbene derivatives were synthesized using stilbene-4-carbonyl chloride.^[123] Using these derivatives as the adsorbent in thin layer chromatography, the photoregulation of the rate of flow of different compounds was possible.

Since these first attempts to control the special properties of polysaccharides by means of trans-cis isomerizable substituents, a series of other approaches was developed. The photocontrolled separation of several neutral racemates by enantioselective adsorption on solid [4-(phenylazo)phenyl]carbamoylated cellulose and amylose membranes was reported.^[132] Moreover, liquid crystalline phase formation and the sol-gel transformation behaviour of different cellulose derivatives were regulated by light induced trans-cis isomerization.^[125,134] The sol-gel transformation could be influenced not only by the conversion of the photochromic group but also by additives like α -cyclodextrin.^[126-128] Fig. 10 shows the thermoreversible sol-gel transition of an aqueous solution of azobenzene functionalized hydroxypropyl methylcellulose monitored by turbidity measurements. Thus, isothermal and reversible regulation of

the sol-gel transition of the Azo-cellulose polymer can be realized by photoirradiation. The difference in gelation temperature between the *trans*- and *cis* isomers can also be influenced by addition of α -cyclodextrin, which selectively forms inclusion complexes with the *trans* azobenzene.^[135]

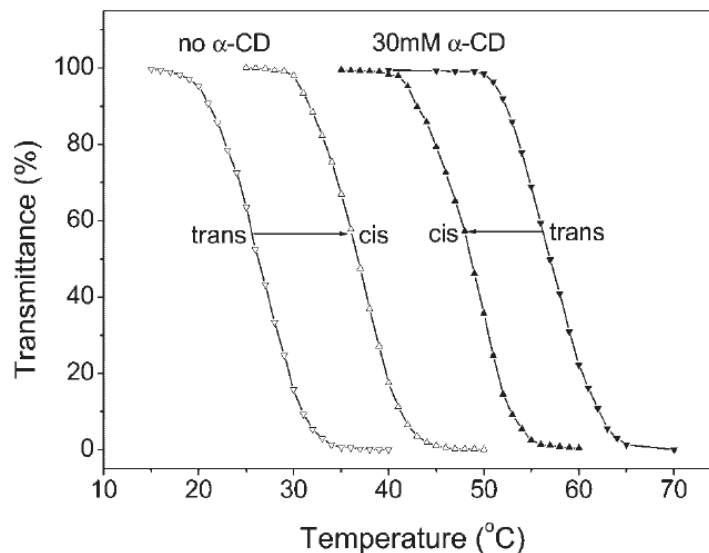


Figure 10: Sol-gel transition behaviour of azobenzene functionalized hydroxypropyl methylcellulose in the absence and presence of α -cyclodextrin (α -CD). *trans*: sample irradiated with visible light; *cis*: sample irradiated with UV light. Adapted from “Photoregulated Sol-Gel Transition of Novel Azobenzene-Functionalized Hydroxypropyl Methylcellulose and Its alpha-Cyclodextrin Complexes”.^[126] With permission from Wiley-VCH Verlag GmbH & Co. KGaA.

Another approach, impressively demonstrating the enormous potential of polysaccharides decorated with *trans*-*cis* isomerizable moieties, was reported by Yang and co-workers.^[130,131,136] Applying a Mitsunobu type ether formation, 4-cyanophenylazophenol was linked to cellulose with ultrahigh molecular weight. The irradiation with linearly polarized light led to the *trans*-*cis*-*trans* isomerization accompanied by reorientation. The orientation redistribution of the azobenzene chromophores finally drives the *cis*-isomer predominantly oriented perpendicular to the polarization of the irradiating light. This procedure results in a net dichroism and birefringence of the material. Moreover, holographic gratings can be developed by irradiating the photoanisotropic films by two polarized interfering beams (Fig. 11). The experiments reported clearly demonstrate how to inscribe volume gratings to a ultrahigh molecular weight polymer exhibiting no glass transition temperature even up to the temperature of decomposition.

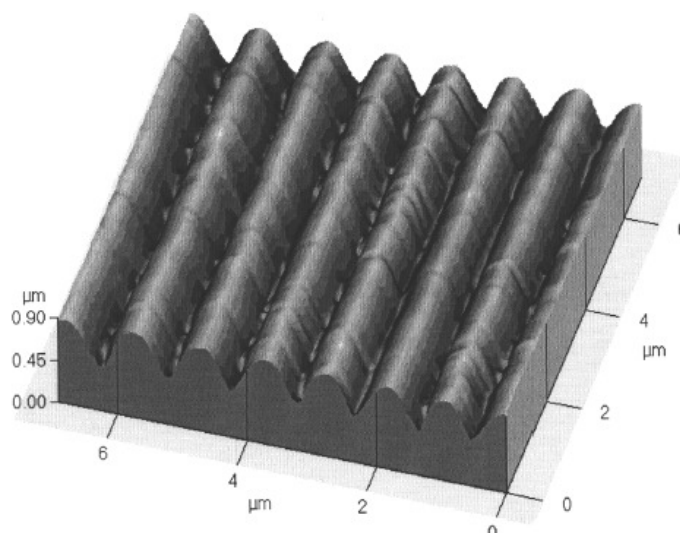


Figure 11: Three-dimensional view of a photoinduced surface relief grating on an azo-cellulose film. Adapted from “Photoinduced Surface Relief Gratings on Azocellulose Films”.^[136] With permission from Taylor & Francis.

3.2.2. Polysaccharide derivatives forming ionic structures upon irradiation

The light induced formation of a zwitterion (Tab. 2b) provides the possibility of creating strong dipoles. Thus, a change of the polymer conformation and properties can be obtained photochemically, by introducing compounds like spiro benzopyran. The spiro benzopyran chromophores as well as the closely related spiro benzoxazines and spiro naphthoxazines are well known for the formation of a merocyanine zwitterion, by a ring-opening reaction.^[137–139] Upon irradiation with UV light, the rupture of the C-O linkage takes place, according to the mechanism shown in Fig. 12. This reaction can be reversed either thermally or photochemically. The second way to form ionic structures under UV irradiation is the dissociation to ions as known for triphenylcarbinol or related compounds Tab. 2c.

In Tab. 4 different polysaccharides bearing moieties with a photochromic character similar to triphenylcarbinol (entry 1 & 2) and spiro benzopyran (entry 3-6) are summarized. Cellulose (Tab. 4 entry 1 & 2), methylcellulose (entry 3 & 4), cellulose acetate (entry 5), and dextran (entry 6) were applied as starting polymer for the modification with these chromophores. The linkage between polymer backbone and the chromophoric group was realized by etherification (Tab. 4 entry 1, 2, 5) or esterification (entry 3, 4, 6). All products were obtained under homogeneous reaction conditions.

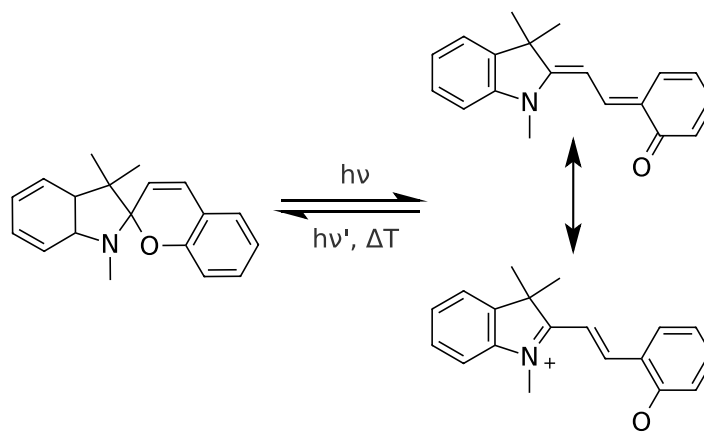


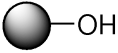
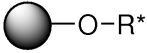
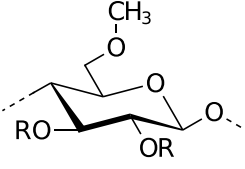
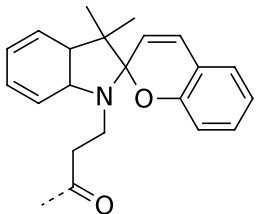
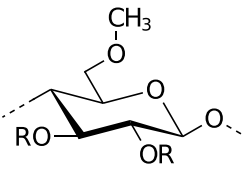
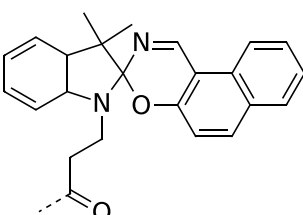
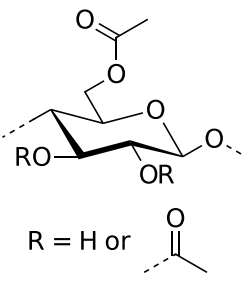
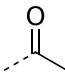
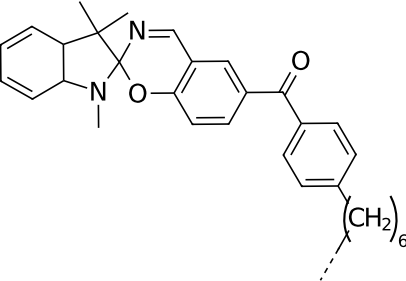
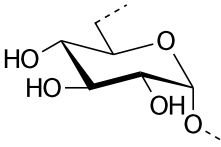
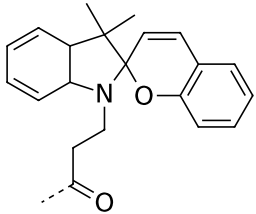
Figure 12: Photochromic transformation of spiro benzopyran to a resonance hybrid of a quinoid and a bipolar structure.

Table 4: Polysaccharides forming ionic structures upon irradiation

No.	Starting polymer	Photoresponsive moiety ^a	Reference
1			[140]
2			[141]

^a including linkage to the polymer backbone

Table 4: Polysaccharides forming ionic structures upon irradiation (continued)

No.	Starting polymer 	Photoresponsive moiety ^a 	Reference
3	 <p>R = H or ---CH₃</p>		[142]
4	 <p>R = H or ---CH₃</p>		[143]
5	 <p>R = H or </p>		[144]
6			[145]

^a including linkage to the polymer backbone

In the beginning of research, the control of material properties like degree of swelling and contact angle was the main ambition of linking photochromic substituents, displaying formation of ionic structures, to polysaccharides.^[141–143] Photoconductive cellulosic films were also prepared applying cellulose decorated with 4,4'-bis(dimethylamino) diphenylmethyl groups.^[140] Edahiro et al. developed a system, which exists in a uniform single phase at room temperature in the dark, and separates into two aqueous phases through blue light irradiation.^[145] The system

was composed of an aqueous solution of photochromic 6-nitrospiropyran modified dextran and polyethylene glycol, which are the first studies about the control of the affinity of photoresponsive and non-photoresponsive polymers in aqueous solution.

Part II.
Special Part

4. UV-Vis spectroscopy for the characterization of novel polysaccharide derivatives

Currently there is a substantial research activity towards advanced materials by the chemical modification of polysaccharides. A prerequisite for these developments is to reveal the structure property relationships of the novel polysaccharide derivatives and thus their synthesis needs to be connected with a detailed characterization. In particular, the characterization of multifunctional polysaccharide derivatives requires improvements or combinations of the techniques established so far. This chapter will illustrate how UV-Vis spectroscopy was utilized to gain the degree of substitution (DS) as an important structural parameter of novel multifunctional polysaccharide derivatives.

4.1. Synthesis of aminocellulose sulfates as novel zwitterionic polymers

Zwitterionic polymers possess both cationic and anionic groups either on different (polyampholytes) or on the same repeating units (polybetaines).^[146] Since they display unique physicochemical characteristics, polyampholytes and polybetaines are of certain interest for various applications including protein separation and purification, binding and recovery of metal ions, and enhanced oil recovery.^[147] Therefore, the theoretical basis and simulation approaches for polyzwitterions are currently of great academic interest and there is an ongoing research on synthetic methods for the preparation of unconventional zwitterionic macromolecules.^[146,148,149]

Amino cellulose sulfates (ACS) are a novel class of polysaccharide based polyzwitterions that are accessible via a convenient three step synthesis (Fig 13).^[150] Namely 6-deoxy-6-(ω -aminoethyl) amino cellulose-2,3(6)-*O*-sulfate (AECS) and 6-deoxy-6-(2-(bis-*N*'*N*'-(2-aminoethyl)aminoethyl)) amino cellulose-2,3(6)-*O*-sulfate (BAECS) were obtained starting with the reaction of cellulose **1** with *p*-toluenesulfonyl chloride in the presence of triethylamine in *N,N*-dimethylacetamide (DMA)/LiCl as solvent.^[151] In order to achieve different DS values of *p*-toluenesulfonyl (tosyl) groups

(DS_{Tos}), the molar ratio of p-toluenesulfonyl chloride to anhydroglucose units (AGU) was varied. The subsequent reaction of the tosyl cellulose (TC, **2a-c**, DS_{Tos} between 0.55 and 1.37) with SO_3 pyridine complex to tosyl cellulose sulfates (TCS, **3a-c**) was carried out homogeneously in DMA.^[152] The molar ratio of 1:5 (modified AGU: SO_3 pyridine) results in products with DS_{SO_3Na} values between 1.09 and 1.27 depending on the DS_{Tos} of starting TC (Tab. 5). The sulfuric acid half esters were converted into their sodium salts to avoid polymer degradation and hydrolysis of the functional groups. As shown in Tab. 5, the DS_{Tos} of the TCS is slightly decreased compared to the DS of the initial TC.

Table 5: Conditions for and results of the synthesis of tosyl cellulose (TC) and tosyl cellulose sulfates (TCS)

TC ^a					TCS ^b		
No.	Molar ratio			DS ^c	No.	DS ^d	
	AGU ^e	TEA	TosCl			Tos	Tos
2a	1	1.6	0.8	0.55	3a	0.43	1.27
2b	1	2.6	1.3	0.85	3b	0.61	1.14
2c	1	4.0	2.0	1.37	3c	1.08	1.09

^aPrepared by the reaction of cellulose with p-toluenesulfonyl chloride (TosCl) and triethylamine (TEA) as a base within 24 h at 8 °C in *N,N*-dimethylacetamide (DMA)/LiCl; ^bprepared by the reaction of TC with sulfur trioxide pyridine complex (5 mol per mol modified anhydroglucose unit) in DMA as solvent; ^cdegree of substitution, calculated on basis of the sulfur content determined by means of elemental analysis; ^dcalculated on basis of the sulfur content and of UV-Vis spectroscopic measurements, ^eanhydroglucose unit.

In general, tosyl moieties are good leaving groups for nucleophilic displacement reactions. However, in the case of TC and TCS only position 6 is accessible, since the replacement of tosylate groups by weak nucleophiles (e.g. amines) follows the S_N2 mechanism.^[153] The homogeneous reaction of TCS **3a-c** with the multifunctional amines 1,2-diaminoethane (DAE) or tris(2-aminoethyl) amine (TAEA) leads to AECS (**4a-c**) and BAECS (**5a-c**). To avoid intermolecular cross-linking the bifunctional DAE and trifunctional TAEA were applied in a molar excess of 25 equivalents.^[154] The nucleophilic attack of the NH_2 groups to the tosyl functionalized C6 of the repeating units led to the formation of C–NH–linkage between the polymer and the oligo amine. With increasing DS_{Tos} of the TCS the DS values of the corresponding

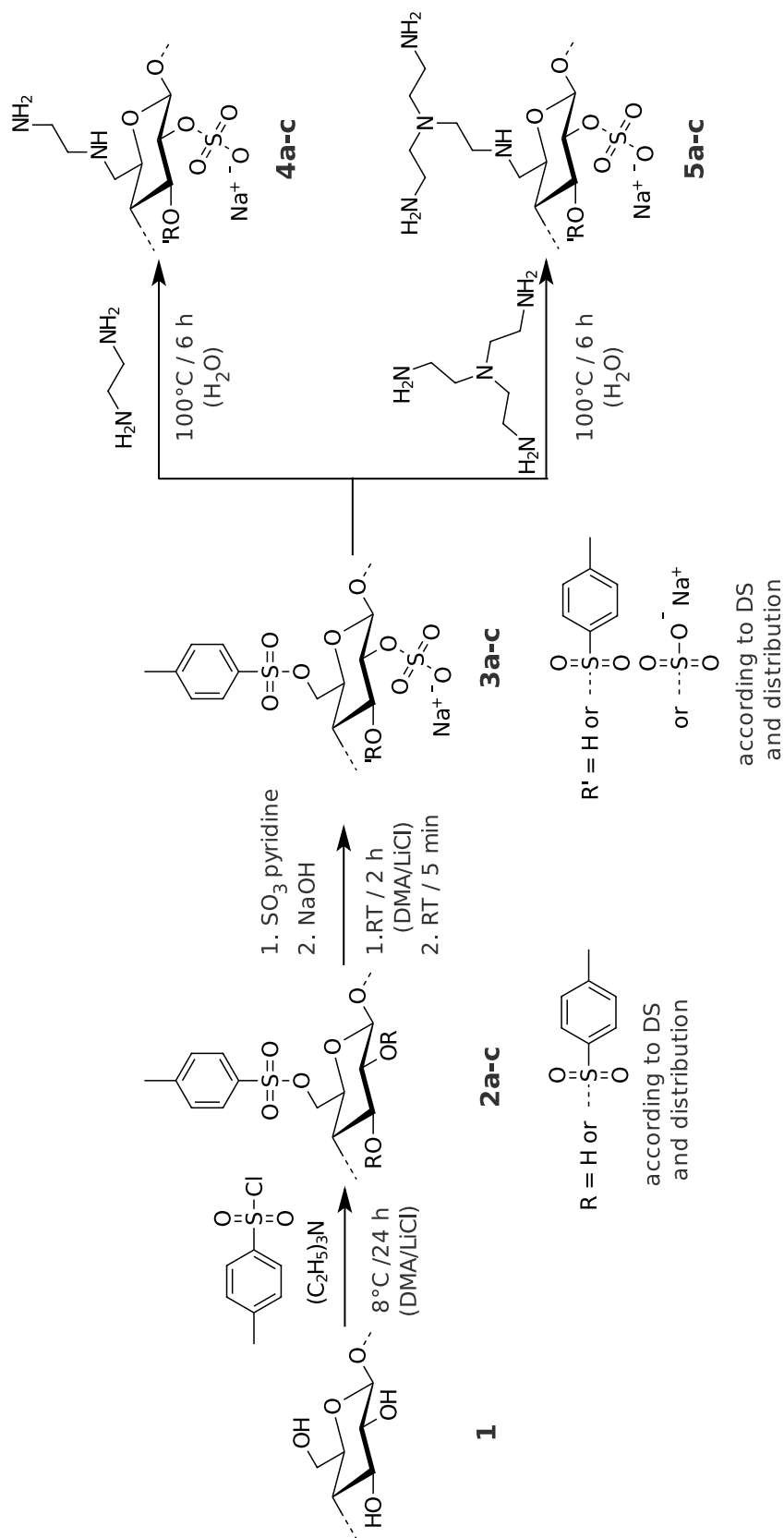


Figure 13 : Synthesis scheme for the preparation of 6-deoxy-6-(ω -aminoethyl)amino cellulose-2,3(6)-O-sulfate (**4a-c**) and 6-deoxy-6-(2-(bis- N' , N' -(2-aminoethyl)aminoethyl)amino cellulose-2,3(6)-O-sulfate (**5a-c**) via p-toluenesulfonyl (tosyl) cellulose (**2a-c**) and tosyl cellulose sulfate (**3a-c**). Presentation of possible variations of the regiochemistry were left out for clarity.

amine increases (Tab. 6). Moreover, it can be noticed that no tosyl moieties remain in the ACS synthesized starting from TCS **3a** and **3b** with $DS_{\text{Tos}} < 1$. In case of using TCS **3c** $DS_{\text{Tos}} > 1$, a low quantity of tosyl groups can be detected in the final ACS (**4c** and **5c**, $DS_{\text{Tos}} \approx 0.2$). The maximal DS_{BAEA} and DS_{AEA} achieved could not exceed 0.74 and 0.86, respectively. Obviously, a small amount of tosyl moieties is cleaved off during reaction without replacement by amino groups. It is suggested in literature that the cleavage is driven by the basic character of the amine, which may act as catalyst for the reaction of the tosyl groups with impurities or the solvent.^[155] In particular, carrying out the reaction in water this explanation holds true.

Table 6: Conditions for and results of the synthesis of 6-deoxy-6-(ω -aminoethyl)amino cellulose-2,3(6)-*O*-sulfate (AECS) and 6-deoxy-6-(2-(bis- N' , N' -(2-aminoethyl) aminoethyl)) amino cellulose-2,3(6)-*O*-sulfate (BAECS) starting from tosyl cellulose sulfates (TCS)

TCS			AECS ^a				BAECS ^b			
No.	DS		No.	DS ^c			No.	DS ^c		
	Tos	SO ₃		Tos	SO ₃	AEA		Tos	SO ₃ Na	BAEA
3a	0.43	1.27	4a	0	1.25	0.41	5a	0	1.21	0.32
3b	0.61	1.14	4b	0	1.14	0.58	5b	0	1.12	0.45
3c	1.08	1.09	4c	0.19	1.08	0.86	5c	0.21	0.70	0.74

^aPrepared by the reaction TCS with 1,2-diaminoethane (25 mol per mol modified anhydroglucose unit) at 100 °C in H₂O within 6 h; ^bprepared by the reaction TCS with tris(2-aminoethyl) amine (25 mol per mol modified anhydroglucose unit) at 100 °C in H₂O within 6 h; ^cdegree of substitution, calculated on basis of the sulfur, nitrogen, and carbon content determined by means of elemental analysis.

4.2. Characterization of tosyl cellulose sulfates and aminocellulose sulfates

The success of functionalization and the structural entities of the cellulose derivatives **2a-c**, **3a-c**, **4a-c**, and **5a-c** can be visualized as well by FTIR- as by ¹³C-NMR spectroscopy. For example, the direct comparison of the FTIR spectra (Fig. 14a) of cellulose **1**, TC **2a**, TCS **3a** and BAECS **5a** allows to identify the starting material, the intermediate products and the final ACS's. Starting from the spectrum of **1** the

functionalization with tosyl groups is clearly proofed by the typical signals in the spectrum of **2a**. Namely, the signals arising from the $\nu_{CH_{arom}}$ (3063 cm^{-1}), $\nu_{C-C_{arom}}$ (1600 cm^{-1}), $\nu_{(as)SO_2(Tos)}$ (1360 cm^{-1}), and $\nu_{(sy)SO_2(Tos)}$ (1176 cm^{-1}) are visible. The subsequent conversion with SO_3 pyridine complex generates sulfate moieties and therefore the corresponding $\nu_{(as)SO_2(Sulf)}$ (1260 cm^{-1}) and $\nu_{(sy)SO_2(Sulf)}$ (1015 cm^{-1}) are visible in the spectra of **3a**. Moreover, the signals resulting from the tosyl groups (described above) are visible in the spectra of **3a** as well. The final S_N2 reaction of TCS **3a** with TAEA lead to the formation of BAECs **5a**. As a consequence the signals arising from the tosyl groups disappear from the spectrum of **5a**. The new signals, which became visible, can be assigned to the ν_{NH_2} (3100 cm^{-1}) and δ_{NH_2} (1490 cm^{-1}) stretching. Fig. 14b shows the ^{13}C -NMR spectra of cellulose **1** dissolved in DMSO- d_6 /tetrabutylammonium fluoride, TC **2a** dissolved in DMSO- d_6 , TCS **3a**, and BAECs **5a** both dissolved in D_2O . All signals could be assigned on basis of literature data.^[151,152,156,157] The spectrum of **2a** reveals the success of the tosylation of cellulose. The ^{13}C resonances of the sp_2 carbon atoms of the aromatic residue of the tosyl group are visible in the range from 128 to 145 ppm. Moreover, the signal at 22 ppm can be assigned to the methyl group of the tosyl substituent. The direct comparison of the spectra of cellulose **1** and TC **2a** shows that the signals of C1-C5 are almost unaffected while a shift of C6 to lower field (C6-Tos) is visible after the esterification. The ^{13}C -NMR spectrum of TCS **3a** obtained by the conversion of TC **2a** with SO_3 pyridine complex shows the same peaks assigned to the tosyl substituents as described above. The sulfation is proved by the typical resonance of C6-O- SO_3^- at 66 ppm. Moreover, a larger line width could be noticed resulting from a short lifetime of the longitudinal and transversal magnetization. This typical phenomenon observed in NMR spectroscopy of polyelectrolytes is caused by the electrostatic repulsion forces and the resulting decrease in flexibility of the polymer chain. Unfortunately, the large line width impede the clear detection and assignment of the signals of C2-O- SO_3^- or C3-O- SO_3^- that must be present since the total DS of **3a** is about 1.7 and therefore other positions than C6 must be functionalized. The spectrum of **5a** was recorded after the reaction of TCS **3a** with TAEA. It is obvious that all resonances assigned to the tosyl substituents disappeared. The new signals, which became visible at 37 and 52 ppm, can be assigned to the methylene carbon atoms of the BAEA substituents. Additionally the signal at 45 ppm, which results from C6-NH- proofs the covalent linkage between the BAEA substituents and the

cellulose backbone. Comparable analytical details can be observed in the IR- and NMR spectra of the samples **4a-c**.

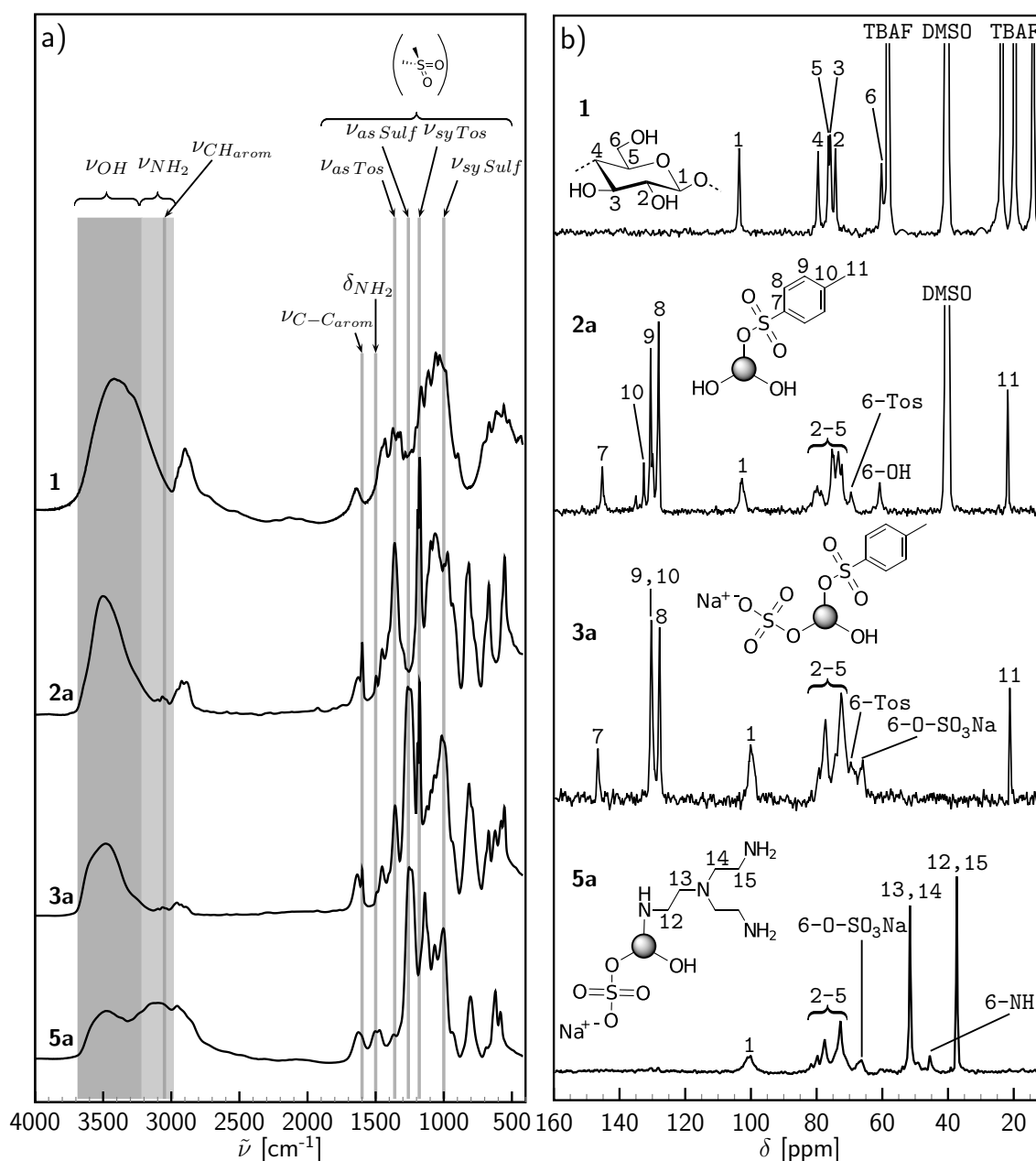


Figure 14: a) FTIR- and b) ^{13}C NMR spectra of: cellulose (**1**), p-toluenesulfonyl (tosyl) cellulose (**2a**, $\text{DS}_{\text{Tos}} = 0.55$), tosyl cellulose sulfate (**3a**, $\text{DS}_{\text{Tos}} = 0.43$, $\text{DS}_{\text{SO}_3\text{Na}} = 1.27$), and 6-deoxy-6-(2-(bis- N',N' -(2-aminoethyl)aminoethyl)) amino cellulose-2,3(6)- O -sulfate (**5a**, $\text{DS}_{\text{BAEA}} = 0.32$, $\text{DS}_{\text{SO}_3\text{Na}} = 1.21$). NMR spectrum of **1** recorded in DMSO- d_6 / tetrabutylammonium fluoride (TBAF), of **2a** in DMSO- d_6 and of **3a** and **5a** in D_2O .

Although FTIR- and NMR spectroscopy gave good qualitative information about the constitution of the polymeric repeating units, the DS as a quantitative measure of functionalization is not accessible by these methods in case of the cellulose derivatives **2a-c**, **3a-c**, **4a-c**, and **5a-c**. The DS_{Tos} can be almost surely calculated from the sulfur content determined by elemental analysis in case of **2a-c**:

$$DS_{Tos} = \frac{M_{AGU} \cdot w_S(\%)}{M_S \cdot 100\% - M_{Tos} \cdot w_S(\%)} \quad (4.1)$$

M_{AGU} denotes the molar mass of the anhydroglucose unit (AGU), M_S the molar mass of sulfur, M_{Tos} the molar mass of the tosyl group, and $w_S(\%)$ the mass fraction of sulfur in the samples determined by elemental analysis.

In case of the water soluble polyelectrolytes **3a-c**, the calculation of DS_{Tos} and the DS_{SO_3Na} is in principle possible from sulfur and carbon content determined by elemental analysis. However, this calculation would not be reliable, since same heteroatoms are introduced by both substituents and the carbon content changes in an unfavorable way for this combination of substituents.

Therefore, the calculation of DS_{Tos} and DS_{SO_3Na} in tosyl cellulose sulfates was carried out on the basis of UV-Vis measurements and elemental analysis. First, the UV-Vis spectra of standard solutions of methyl-6-*O*-tosyl- α -D-glucopyranoside (MTG) in deionized water in a concentration range from 0.010 and 0.045 g/L were measured (Fig 15a) and the absorbance at 227 nm (where only the tosyl moieties absorb) over the concentration was plotted in order to obtain a calibration curve (Fig 15b). Utilizing this calibration curve the concentration of tosyl moieties c_{Tos} of a given solutions of the tosyl cellulose sulfate sample in water can be calculated from the absorbance A_{227} :

$$c_{Tos} = \frac{A_{227} + 0.0086}{12451} \quad (4.2)$$

From c_{Tos} , the mass concentration of the tosyl cellulose sulfate sample (c_W) and the molar mass of sulfur M_S , the mass fraction of sulfur in the sample arising from tosyl groups can be calculated:

$$w_S(\%)_{Tos} = \frac{c_{Tos} \cdot M_S \cdot 100\%}{c_W} \quad (4.3)$$

Elemental analysis yields the overall sulfur content $w_S(\%)$ arising from both tosyl and sulfate moieties of the tosyl cellulose sulfate was obtained. The difference between the overall sulfur content $w_S(\%)$ and $w_S(\%)_{Tos}$ yields the sulfur content arising from

the sulfate groups:

$$w_S(\%)_{Sulf} = w_S(\%) - w_S(\%)_{Tos} \quad (4.4)$$

and subsequently the concentration of sulfate groups:

$$c_{Sulf} = \frac{w_S(\%)_{Sulf} \cdot c_W}{M_S \cdot 100\%} \quad (4.5)$$

The concentration of modified anhydroglucose units (AGU), c_{AGU} can be calculated from:

$$c_{AGU} = \frac{c_W - c_{Tos}(M_{Tos} - M_H) - c_{Sulf}(M_{Sulf} - M_H)}{M_{AGU}} \quad (4.6)$$

Combining the results of eq. (4.2), eq. (4.5), and eq. (4.6) lead to the degrees of substitution in tosyl cellulose sulfates:

$$DS_{Tos} = \frac{c_{Tos}}{c_{AGU}} \quad \text{and} \quad DS_{Sulf} = \frac{c_{Sulf}}{c_{AGU}} \quad (4.7)$$

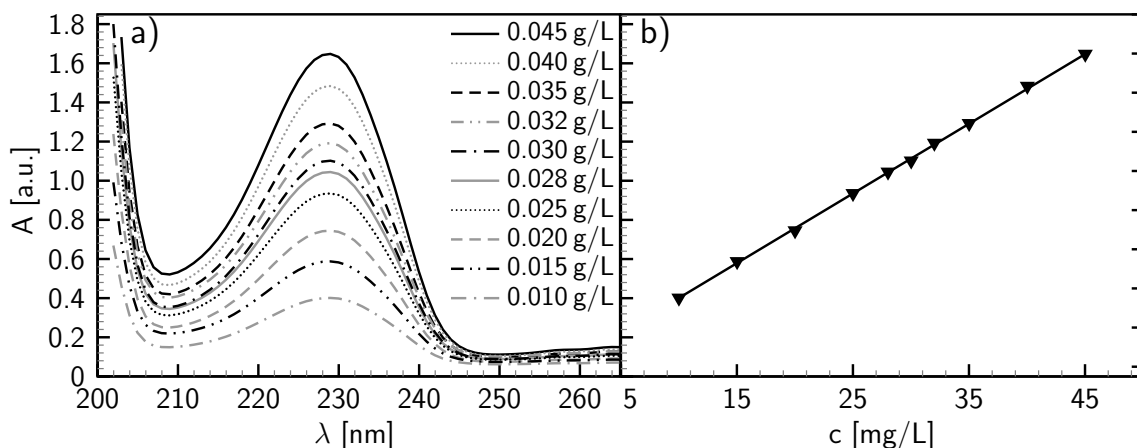


Figure 15: **a)** UV spectra of the methyl 6-*O*-tosyl- α -D-glucopyranoside (MTG) dissolved in deionized water at different concentrations. **b)** Calibration curve calculated from the absorbance at wave length 227 nm as a function to concentration of MTG.

In case of the cellulose derivatives AECS and BAECS the calculation of DS_{AEA} and DS_{BAEA} as well as DS_{SO_3Na} can be carried out on basis of elemental analysis, since the different substituents possess different heteroatoms.

5. Tailored synthesis and structure characterization of new highly functionalized photoactive polysaccharide derivatives

As highlighted in Part I, there is a substantial interest in the synthesis of photoresponsive polysaccharide derivatives and the development of novel functional materials thereof. In this context polysaccharides do not only afford a renewable alternative to synthetic polymers but also feature properties like polyfunctionality and biocompatibility. However, the potential arising from the chemical and physical characteristics of polysaccharides is far from being exhausted. For example, the influence of regioselectivity of photoresponsive polysaccharide derivatives on their properties has only been touched on in the literature. Moreover, only a very few investigations are reported studying photoresponsive polysaccharide derivatives with regard to the broad structural diversity. Up to now, there is neither an information about the influence of the polysaccharide backbone on the functionalization with photoactive moieties nor about its impact on the photochemistry.

The first section of this chapter is focusing on the synthesis and characterization of highly functionalized photoactive derivatives starting from different polysaccharides. In the second section, the preparation of water soluble photoactive polyelectrolytes is described as an example of utilizing the polyfunctionality of polysaccharides to achieve not only a high degree of functionalization but also different functionalities within one polymeric structure.

5.1. Photoactive polysaccharide esters

5.1.1. Synthesis

Acylation of polysaccharides is an important path to design the structure and hence the properties by introducing new functionalities. Conventional esterification of polysaccharides employs acyl chlorides and acid anhydrides. Because of the limited compatibility of the acyl chlorides with common polysaccharide solvents, the limited

availability of the carboxylic acid anhydrides and due to loss of half of the acid (i.e., one mol acid is formed as by-product of the reaction per mol acid anhydride) as well as due to the formation of acidic by-products, novel acylation systems applying the carboxylic acid are required. In particular, for the synthesis of unconventional polysaccharide derivatives with complex or sensitive functional groups a mild and efficient activation of the carboxylic acid is necessary. Therefore, coupling reagents known from peptide chemistry have been studied and *N,N*-carbonyldiimidazole (CDI) was found to be an efficient activating agent for the acylation of polysaccharides in non-aqueous systems.^[25]

CDI was applied as activating agent for 2-[(4-methyl-2-oxo-2*H*-chromen-7-yl)oxy]acetic acid (**8**) and the intermediately generated imidazolide was allowed to react with cellulose (**1**), dextran (**6**), and pullulan (**7**). The reaction of the dissolved polymers (**1** in DMA/LiCl, **6** and **7** in DMSO) yields the corresponding polysaccharide 2-[(4-methyl-2-oxo-2*H*-chromen-7-yl)oxy] acetates **9a-f**, **10a-f**, **11a-f** (Fig 16). The DS of the polysaccharide derivatives can easily be adjusted by the molar ratio of the AGU:CDI:**8** (Table 7). However, cellulose, dextran and pullulan possess a different reactivity. In case of dextran and pullulan the lowest molar ratio of 1:0.125:0.125 (**10a** and **11a**) lead to quantitative conversion of the carboxylic acid into the corresponding ester. With increasing molar ratio to 1:1:1 (**10f** and **11f**), the efficiency of conversion to the ester decreases to $\approx 90\%$ for dextran and to $\approx 75\%$ for pullulan. In case of cellulose, about the half of the amount of the carboxylic acid is converted into the corresponding ester at all molar ratios applied. The differences in reactivity observed might be a result of both different molecular structures of the polymers and their different molar masses. Anyhow, the reaction efficiency achieved is still high for a polymeranalogous conversion of polysaccharides. In particular, when dextran is applied the reaction can be termed as highly efficient, since even at a molar ratio of 1:3:3 (**10h**) $\approx 66\%$ of the carboxylic acid are converted to the corresponding ester.

5.1.2. Characterization

The structure of the different polysaccharide 2-[(4-methyl-2-oxo-2*H*-chromen-7-yl)oxy] acetates **9a-f**, **10a-f**, **11a-f** was evaluated by ¹H- and ¹³C NMR spectroscopy. To eliminate intra- and intermolecular interactions of the polymer chains by hydrogen bonds and any overlap of the signals of the protons of the polysaccharide backbone and the hydroxyl groups, the remaining OH groups were perpropionylated. Thus,

the completely functionalized polysaccharide esters were used for NMR studies in case of the samples **9a-f**, **10a-f**, **11a-f** that gave well resolved spectra.

Fig. 17 shows the ^1H - and ^{13}C NMR spectra of perpropionylated dextran 2-[(4-methyl-2-oxo-2*H*-chromen-7-yl)oxy] acetate **10c** as a representative example. The proton resonances of the substituents appear at 7.6 (H11), 6.9 (H18), 6.8 (H10), 6.1 (H15), and 4.8 ppm (H8). The signal of the methyl group (H14) overlaps with the resonance of the methylene protons of the propionate moiety. Furthermore, the

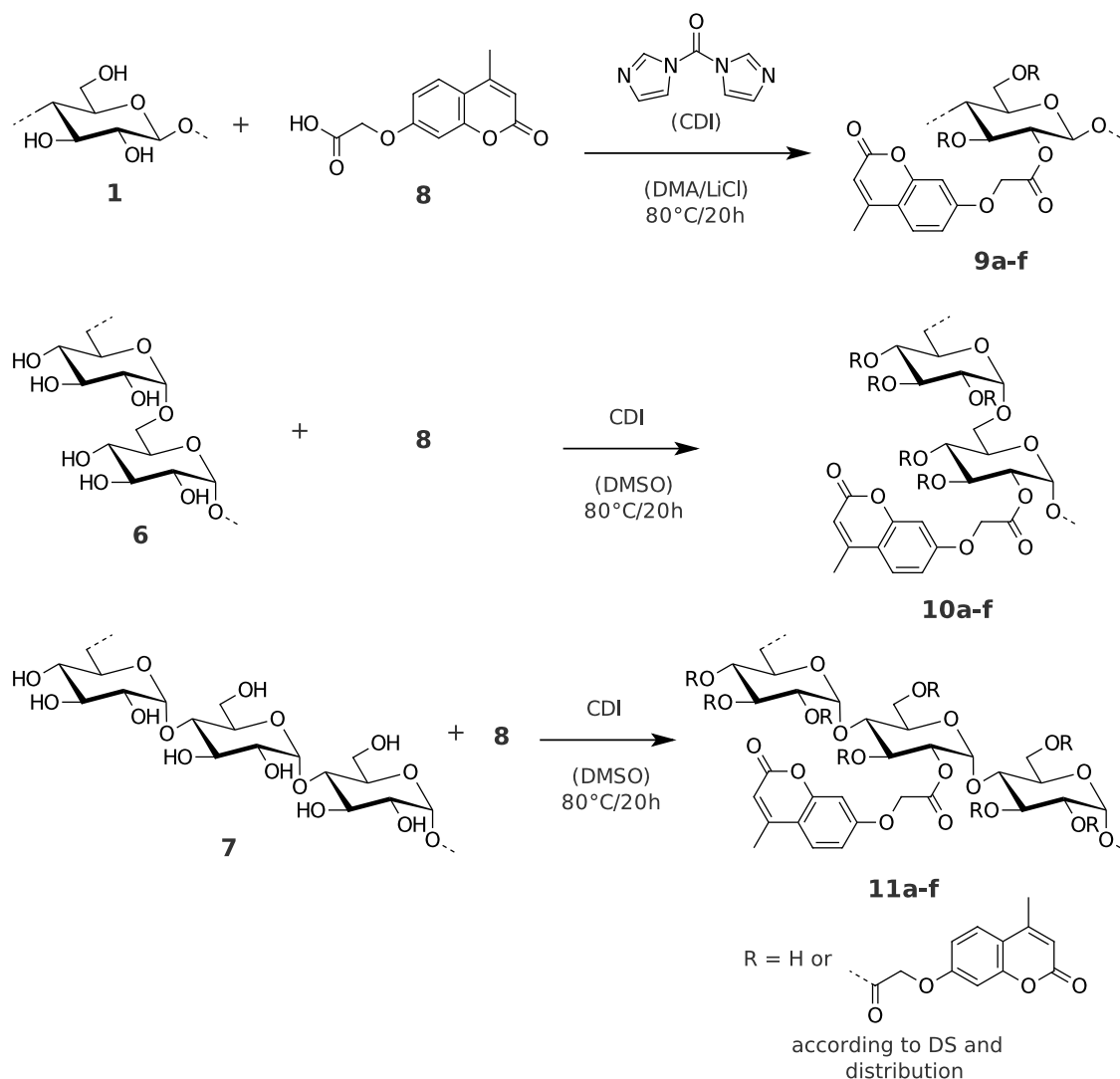


Figure 16: Synthesis scheme for the preparation of cellulose-, dextran- and pullulan 2-[(4-methyl-2-oxo-2*H*-chromen-7-yl)oxy] acetates via the activation of the carboxylic acid with *N,N*-carbonyldiimidazole (CDI) in *N,N*-dimethylacetamide (DMA)/LiCl or DMSO.

Table 7: Conditions for and results of the esterification of cellulose, dextran and pullulan with 2-[(4-methyl-2-oxo-2*H*-chromen-7-yl)oxy] acetic acid (**8**) via activation with *N,N*-carbonyldiimidazole (CDI)

Polysaccharide	Molar ratio			No.	DS	
	AGU ^a	CDI	8		UV ^b	NMR ^c
cellulose	1	0.125	0.125	9a	0.06	0.05
cellulose	1	0.250	0.250	9b	0.16	0.16
cellulose	1	0.375	0.375	9c	0.25	0.24
cellulose	1	0.500	0.500	9d	0.33	0.33
cellulose	1	0.750	0.750	9e	0.38	0.37
cellulose	1	1.000	1.000	9f	0.49	0.51
dextran	1	0.125	0.125	10a	0.12	0.11
dextran	1	0.250	0.250	10b	0.25	0.25
dextran	1	0.375	0.375	10c	0.38	0.38
dextran	1	0.500	0.500	10d	0.47	0.48
dextran	1	0.750	0.750	10e	0.71	0.69
dextran	1	1.000	2.000	10f	0.90	0.93
dextran	1	2.000	3.000	10g	1.45	1.44
dextran	1	3.000	1.000	10h	2.01	1.99
pullulan	1	0.125	0.125	11a	0.12	0.11
pullulan	1	0.250	0.250	11b	0.19	0.21
pullulan	1	0.375	0.375	11c	0.24	0.25
pullulan	1	0.500	0.500	11d	0.37	0.37
pullulan	1	0.750	0.750	11e	0.57	0.51
pullulan	1	1.000	1.000	11f	0.74	0.76

^a Anhydroglucose unit; ^b degree of substitution, determined by means of UV-Vis spectroscopy in DMA; ^c degree of substitution, determined by means of ¹H NMR spectroscopy after perpropionylation.

proton signals of the AGU are visible in the range from 3.7 to 5.7 ppm (Fig. 17a). The well resolved ¹³C NMR spectrum (Fig. 17b) allows the assignment of the carbon atoms by comparison with spectra of both the methyl ester of **8** and dextran propionate reported.^[25] The NMR spectra prove the success of the functionalization with the photoactive moiety. Moreover, the DS value can be calculated from the ¹H NMR spectrum out of the relation of the spectral integrals of the protons of the aromatic

system (5.9 to 7.9 ppm) versus the CH₃ protons of the propionate moiety (1.0 ppm):

$$DS = \frac{3 \cdot I_{H,10+11+15+18}}{4 \cdot \left(\frac{I_{H,10+11+15+18}}{4} + \frac{I_{H,21}}{3} \right)} \quad (5.1)$$

The DS values can also be calculated on basis of UV-Vis spectroscopic measurements. Applying the methyl ester of **8** as reference compound a calibration curve was obtained (Fig. 18), which allows the determination of the concentration of the photoactive moieties c_{Photo} in a solution of the polysaccharide 2-[(4-methyl-2-oxo-2*H*-chromen-7-yl)oxy] acetates:

$$c_{\text{Photo}} = \frac{A_{320} + 0.0044}{13669} \quad (5.2)$$

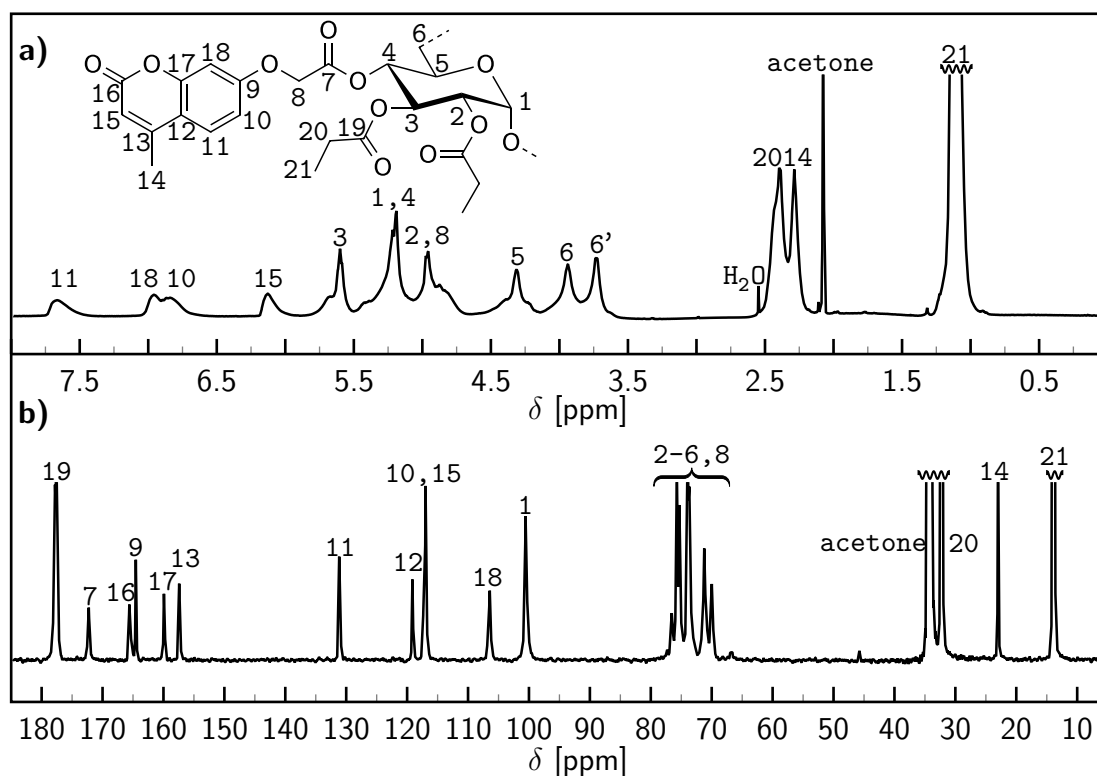


Figure 17: a) ¹H- and b) ¹³C NMR spectra of perpropionylated dextran 2-[(4-methyl-2-oxo-2*H*-chromen-7-yl)oxy] acetate (**10c**, DS 0.38) both acquired in acetone-d₆.

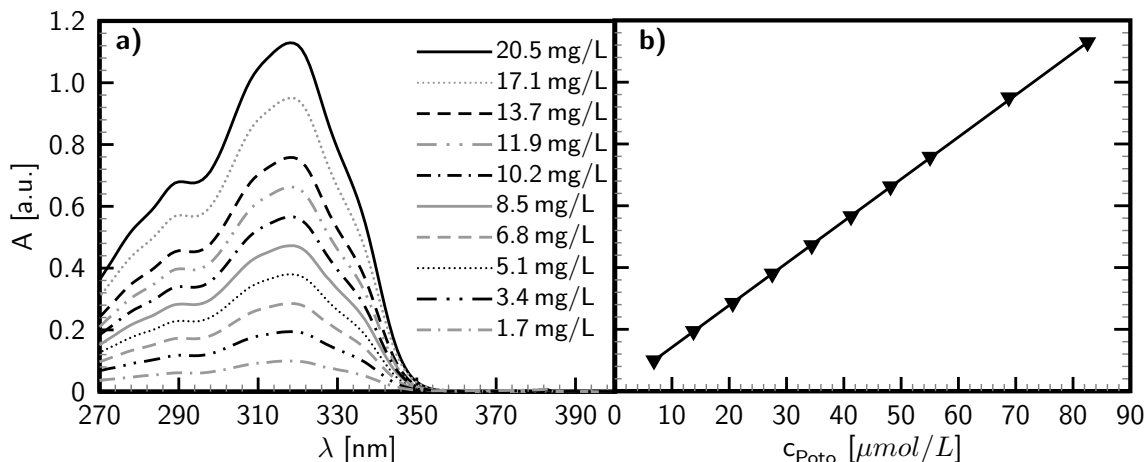


Figure 18: a) UV spectra of 2-[(4-methyl-2-oxo-2*H*-chromen-7-yl)oxy]acetic acid methyl ester (**8-Me**) dissolved in *N,N*-dimethylacetamide at different concentrations. b) Calibration curve calculated from the absorbance at wave length 320 nm as a function of the concentration of **8-Me**.

For a known mass concentration c_w the concentration of modified anhydroglucose units (AGU), c_{AGU} can be calculated:

$$c_{AGU} = \frac{c_w - c_{Photo}(M_{Photo} - M_H)}{M_{AGU}} \quad (5.3)$$

Combining the results of eq. (5.1) and (5.3) the DS of photoactive 2-[(4-methyl-2-oxo-2*H*-chromen-7-yl)oxy] acetate moieties can be obtained:

$$DS_{Photo} = \frac{c_{Photo}}{c_{AGU}} \quad (5.4)$$

It is important to note that the DS values calculated on basis of NMR- and UV-Vis spectroscopic measurements agree very well (Tab. 7). In comparison, UV-Vis spectroscopy is a much faster method and lower DS values can be accurately determined. The NMR spectroscopic determination of the DS according to eq. 5.1 requires an additional functionalization of the polymer (perpropionylation) and its sensitivity is at least one order of magnitude lower. However, the prerequisites for the UV-Vis spectroscopic determination of the DS in general are a high purity of the polymer (other chromophores must not be present), the polymer must be soluble in a solvent, which is appropriate for UV-Vis spectroscopy at the desired wavelength, and

the absorption characteristics must not be changed by the linkage to the polymer compared to the model compound.

The knowledge of the DS as an average parameter allows a more detailed analysis of the structure of the polymers **9-11**. Fig. 19a shows the ^{13}C NMR spectra of cellulose **1** dissolved in DMSO-d₆/tetrabutylammonium fluoride and cellulose 2-[(4-methyl-2-oxo-2*H*-chromen-7-yl)oxy]acetate **9e** in DMSO-d₆. Again, all signals could be assigned by two dimensional measurements (HSQC-DEPT, TOCSY) and comparison with the spectra of the methyl ester of **8**. The spectrum of **9e** reveal the success of the esterification with the photoactive moiety. As discussed above, the ^{13}C resonances of the coumarin moiety (C9-C18) are visible in the range from 162 ppm to 102 ppm. The signal of C18 appears as shoulder beside the resonance of C1 of the repeating unit. The signal of the methylene group of the acetate linker (C8) overlaps with the resonances of C3 and C5 at about 75 ppm and the resonance of the methyl group (C14) appears at about 18 ppm. The direct comparison of the spectra of cellulose and **9e** shows that the signals of C2-C5 are almost unaffected, while a shift of C6 to lower field (C6s) is visible after the esterification. Although it is not possible to give an exact measure from ^{13}C NMR spectra as it is possible from the spectral integrals of proton NMR, the relative intensities of the signals of C6 and C6s reveal that both species appear in almost same quantity. Keeping in mind that the DS of the sample measured is about 0.38 it may be concluded that the esterification takes place predominantly at position 6 of the repeating unit. However, the small peak appearing at about 100 ppm (assigned to C1_{2s}) indicates also a esterification of the hydroxyl groups at position 2, although the resonance of C2s is not resolved.

The direct comparison of the spectra of dextran and **10c** also reveals the success of the functionalization (Fig. 19b). The peak at about 100 ppm (assigned to C1_{2s}) and the signal at 77 ppm (assigned to C2s) prove the ester linkage at position 2. However, compared to cellulose no preference of the esterification for the hydroxyl groups at any specific position can be concluded, since the resonances of C3 and C4 or C3s and C4s cannot be resolved under the measurement conditions applied.

Pullulan and the corresponding polymer **11d** display even more complex ^{13}C NMR spectra (Fig. 19c). The single positions of the three different α -(1→4) linked AGUs, which are joined by α -(1→6) linkages to the maltotriosyl repeating units, have an individual chemical shift. Therefore, 18 signals appear already in the ^{13}C NMR spectrum of pullulan and various additional resonances related to the polymer backbone appear in case of functionalization. However, the most significant changes

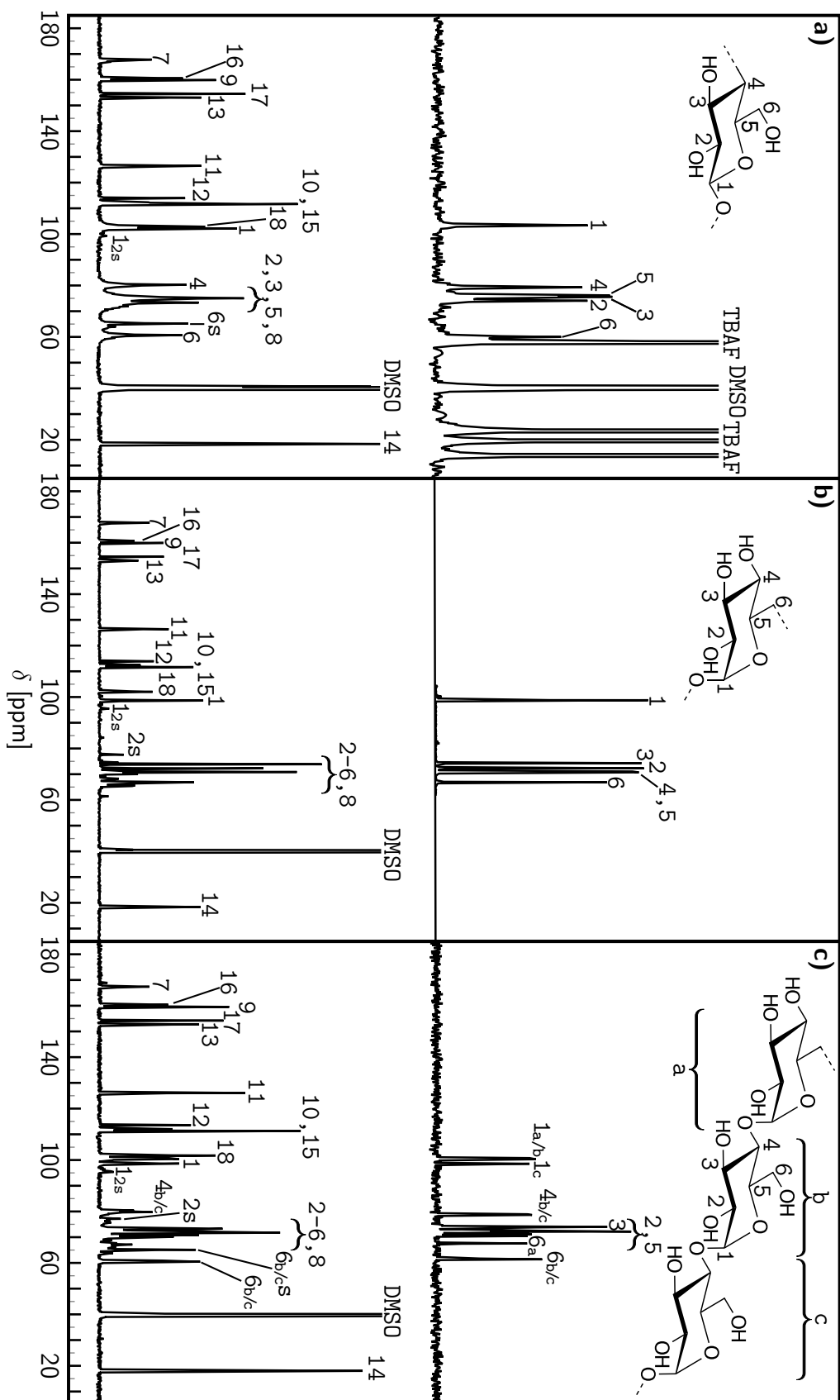


Figure 19: ^{13}C NMR spectra of **a)** cellulose recorded in DMSO-d₆ / tetrabutylammonium fluoride (TBAF), **b)** dextran (D₂O), **c)** pullulan (D₂O) and the corresponding polysaccharide 2-[(4-methyl-2-oxo-2H-chromen-7-yl)oxy] acetates **9e**, **10c**, and **11d** all with a DS of 0.38 (DMSO-d₆). Numbering of the substituent according to Fig. 17

in the spectra allow more detailed conclusions about the structure of **11d** and thus reveal some trends for the functionalization of pullulan. For example, it can be noticed that the functionalization of primary hydroxyl groups located in position C6_b and C6_c results in a similar shift to lower field (C6_{b/c}s) as described above for cellulose. The signals of C6_{b/c} and C6_{b/c}s have almost the same relative intensities and again, it can be concluded (keeping in mind the uncertainties mentioned above) that esterification of the primary hydroxyl groups is preferred. However, the signal assigned to C1_{2s} at about 100 ppm is more pronounced than in case of cellulose and the resonance assigned to C2s is clearly visible at about 76 ppm. In difference to the spectrum of **10c** it can be noticed that this signal consists of three individual peaks that maybe result from the different AGUs of pullulan. The field strength applied for the NMR measurements is too low for a definitive assignment by two dimensional measurements of the derivative **11d**. Nevertheless, from lower to higher field the order C2_as, C2_bs and C2_cs can be assumed, since signals resulting from the corresponding carbon atoms of the unmodified pullulan appear in that order.

5.2. Synthesis of photoactive polysaccharide polyelectrolytes

Among the enormous diversity of polysaccharide derivatives polysaccharide-based polyelectrolytes are of great practical and academical interest.^[23] For example, polysaccharide sulfates (PSS) are an abundant class of naturally occurring carbohydrate compounds containing anionic sulfuric acid half ester moieties. As recently highlighted, they are widespread structure forming materials and play an important regulatory role in living organisms. Moreover, they possess a number of biological activities, making them promising antimicrobial or antiviral agents and potent pharmaceuticals e.g. for prevention of blood coagulation and inflammation reactions.^[158] Semi-synthetic PSS, derived from homopolysaccharides such as dextran or cellulose, can mimic the beneficial properties of naturally occurring substances but have the advantage that they are available in larger quantities with defined structural features and purity^[156,159,160]. The following subsection is focusing on the synthesis of photoactive polysaccharide sulfates starting from the dextran and pullulan 2-[(4-methyl-2-oxo-2*H*-chromen-7-yl)oxy] acetates **10**, and **11** described in section 5.1. The aim was to obtain multifunctional derivatives that should be able to respond to disparate stimuli, namely ionic strength and light, and thus allow the photocontrol of solution properties or the control of properties of modified surfaces.

5.2.1. Mixed 2-[(4-methyl-2-oxo-2*H*-chromen-7-yl)oxy]acetic acid- sulfuric acid half esters of dextran and pullulan

Several homogeneous and heterogeneous synthesis pathways for sulfation of polysaccharides have been developed^[25]. In all cases the strongly acidic protonated form of the sulfuric acid half ester must be converted to its sodium salt, to avoid the auto catalytic hydrolysis of the ester moieties and chain degradation of the polysaccharide backbone. A gentle method to produce well-defined polysaccharide sulfuric acid half esters is the application of SO₃ complexes of organic bases (e.g. pyridine) or aprotic dipolar solvents like *N,N*-dimethylformamide (DMF).^[156,161]

Synthesis

In the present work the easily manageable SO₃/DMF complex was applied as reagent for the sulfation of the polysaccharide esters **10a-f** and **11a-f** (Fig. 20). By carrying out the reaction under homogeneous conditions in DMF as solvent, an uniform distribution of the sulfate moieties along the polymer chain can be guaranteed.^[156] Therefore, water soluble products were obtained even at low DS values of sulfate groups (DS_{SO₃Na}). The proton scavenger 2-methyl-2-butene was added to prevent undesired polymer degradation and as can be noticed from the values summarized in Tab. 8, the cleavage of the 2-[(4-methyl-2-oxo-2*H*-chromen-7-yl)oxy]acetate moieties was prevented (DS_{Photo} remains constant). The DS_{SO₃Na} was adjusted by varying the molar ratio of modified AGU to sulfating agent and thus the hydrophilic/hydrophobic balance of the resulting mixed polysaccharide esters was controlled. However, the exact value of DS_{SO₃Na} is depended on the reaction conditions as well as on the DS_{Photo} of the initial polysaccharide ester. The DS_{SO₃Na} values increase in case of all samples with increasing molar ratio of modified AGU to SO₃/DMF complex from 1:1 to 1:3. Moreover, a higher DS_{Photo} of the initial polysaccharide ester lead to products with an increased DS_{SO₃Na} until a limiting DS_{Photo} is exceeded. For example, DS_{SO₃Na} increases from 0.24 to 0.69 if the polysaccharide esters **10a-e** (DS_{Photo} 0.12 to 0.71) are converted to the corresponding mixed 2-[(4-methyl-2-oxo-2*H*-chromen-7-yl)oxy]acetic acid- sulfuric acid half esters applying equimolar amounts of SO₃/DMF complex (samples 12a1-12e1). In contrast, the DS_{SO₃Na} value of sample **12f1** is remarkable lower. The same behavior can be observed in case of the conversion of the pullulan esters **11a-f**, but the limiting DS_{Photo} is about 0.25 and beyond this point DS_{SO₃Na} starts to decrease again. The direct comparison of the DS_{SO₃Na} values of

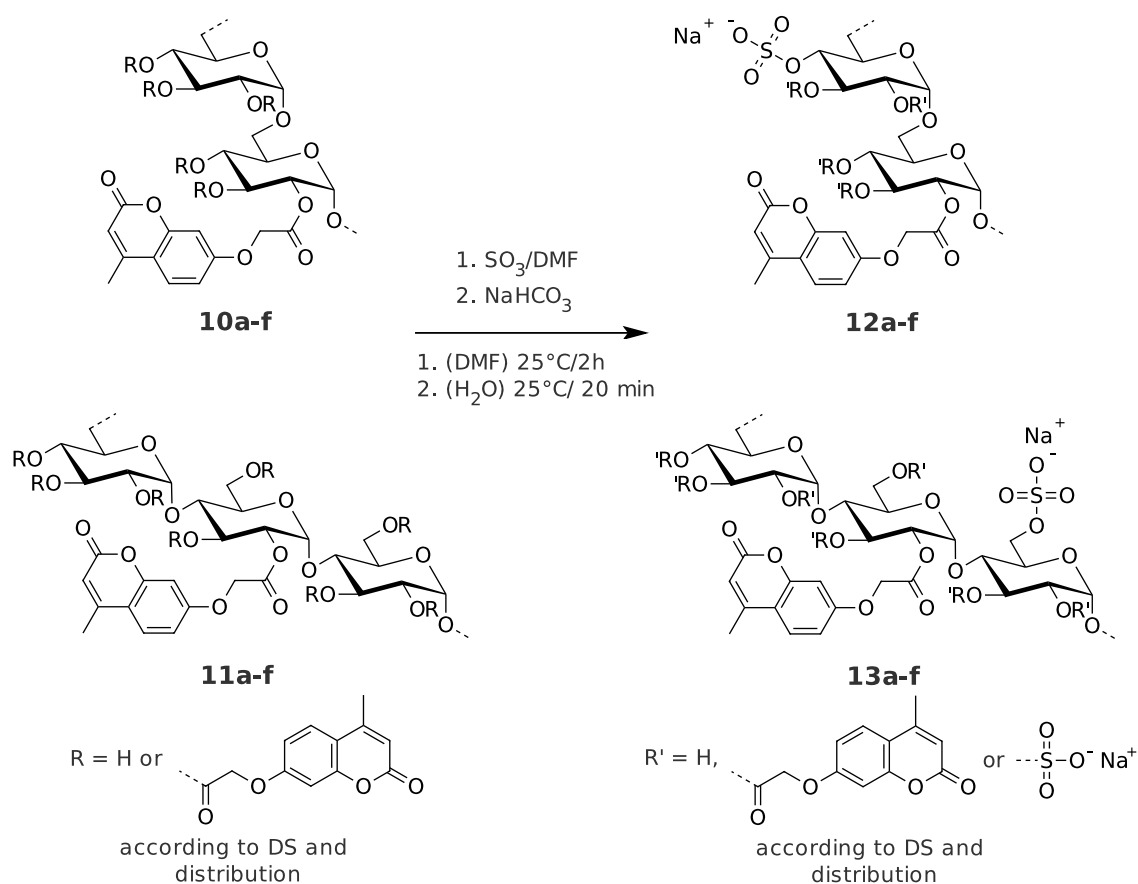


Figure 20 : Synthesis scheme of the sulfation of the 2-[(4-methyl-2-oxo-2H-chromen-7-yl)oxy] acetates of dextran (**10**) and pullulan (**11**) with SO_3/DMF complex in *N,N*-dimethylformamide (DMF)

mixed 2-[(4-methyl-2-oxo-2*H*-chromen-7-yl)oxy]acetic acid- sulfuric acid half esters of dextran and pullulan, which were prepared starting from polysaccharide esters with similar DS_{Photo} (e.g. **12b1-3** and **13e1-3** prepared from **10b** and **11e**), reveals a higher reactivity of pullulan.

Although it is difficult to give a definitive interpretation of the findings described above, they need to be attributed to the properties of the starting polysaccharide esters **10a-f** and **11a-f**. On one hand, it seems contradictorily that the $\text{DS}_{\text{SO}_3\text{Na}}$ is increasing when the DS_{Photo} of the initial polymer increases, since less hydroxyl groups are available for modification. On the other, aspects like polymer interactions and the conformation of the polymers chains must be considered. For example, at lower DS_{Photo} more intra- and intermolecular hydrogen bonds can be expected. As a consequence the flexibility of the polymer chains is reduced and the solvating power

of DMF might be not high enough to guarantee a molecularly dispersed solution of the polymers. Both effects reduce the accessibility of the hydroxyl groups for modification. At higher values of DS_{Photo} hydrogen bonding is less pronounced and the number of hydroxyl groups available become the ruling parameter and thus the $DS_{\text{SO}_3\text{Na}}$ values decrease. The differences in reactivity of dextran and pullulan may arise from the different primary structure. The higher $DS_{\text{SO}_3\text{Na}}$ values of the pullulan samples can be explained by the higher reactivity of the primary hydroxyl groups, which are present in the polymer. Moreover, the different glycosidic linkages in pullulan (α -(1 \rightarrow 4) and α -(1 \rightarrow 6)) might affect hydrogen bonding and flexibility in the terms mentioned above.

Table 8: Conditions for and results of the sulfation of the 2-[(4-methyl-2-oxo-2*H*-chromen-7-yl)oxy] acetates of dextran (**10**) and pullulan (**11**) with SO_3/DMF complex in *N,N*-dimethylformamide (DMF) as reaction media.

Educt		Molar ratio		Product		
No.	$DS_{\text{Photo}}^{\text{a}}$	AGU ^b	SO_3/DMF	No.	$DS_{\text{Photo}}^{\text{a}}$	$DS_{\text{SO}_3\text{Na}}^{\text{c}}$
10a	0.12	1	1	12a1	0.12	0.24
10a	0.12	1	2	12a2	0.12	0.53
10a	0.12	1	3	12a3	0.11	0.77
10b	0.25	1	1	12b1	0.25	0.29
10b	0.25	1	2	12b2	0.24	0.54
10b	0.25	1	3	12b3	0.25	0.82
10c	0.38	1	1	12c1	0.38	0.47
10c	0.38	1	2	12c2	0.38	0.79
10c	0.38	1	3	12c3	0.38	1.06
10d	0.47	1	1	12d1	0.46	0.68
10d	0.47	1	2	12d2	0.46	1.06
10d	0.47	1	3	12d3	0.45	1.20
10e	0.71	1	1	12e1	0.71	0.69
10e	0.71	1	2	12e2	0.70	1.04
10e	0.71	1	3	12e3	0.69	1.11
10f	0.93	1	1	12f1	0.91	0.41
10f	0.93	1	2	12f2	0.91	0.79
10f	0.93	1	3	12f3	0.90	0.75

^a Degree of substitution (DS) of photoactive 2-[(4-methyl-2-oxo-2*H*-chromen-7-yl)oxy] acetate moieties; ^b modified anhydroglucose unit; ^c DS of sulfuric acid half ester (sodium salt) moieties.

Table 8: Conditions for and results of the sulfation of the 2-[(4-methyl-2-oxo-2*H*-chromen-7-yl)oxy] acetates of dextran (**10**) and pullulan (**11**) with SO₃/DMF complex in *N,N*-dimethylformamide (DMF) as reaction media (continued).

Educt		Molar ratio		Product		
No.	DS _{Photo} ^a	AGU ^b	SO ₃ /DMF	No.	DS _{Photo} ^a	DS _{SO₃Na} ^c
11a	0.12	1	1	13a1	0.12	0.42
11a	0.12	1	2	13a2	0.11	0.84
11a	0.12	1	3	13a3	0.12	1.27
11b	0.20	1	1	13b1	0.20	0.50
11b	0.20	1	2	13b2	0.20	1.00
11b	0.20	1	3	13b3	0.20	1.37
11c	0.25	1	1	13c1	0.24	0.59
11c	0.25	1	2	13c2	0.25	1.15
11c	0.25	1	3	13c3	0.25	1.40
11d	0.37	1	1	13d1	0.37	0.45
11d	0.37	1	2	13d2	0.35	1.11
11d	0.37	1	3	13d3	0.36	1.38
11e	0.54	1	1	13e1	0.54	0.44
11e	0.54	1	2	13e2	0.53	1.02
11e	0.54	1	3	13e3	0.53	1.35
11f	0.75	1	1	13f1	0.74	0.39
11f	0.75	1	2	13f2	0.75	0.96
11f	0.75	1	3	13f3	0.73	1.34

^a Degree of substitution (DS) of photoactive 2-[(4-methyl-2-oxo-2*H*-chromen-7-yl)oxy] acetate moieties; ^b modified anhydroglucose unit; ^c DS of sulfuric acid half ester (sodium salt) moieties.

Characterization

The degrees of substitution (DS_{Photo} and DS_{SO₃Na}) of the mixed 2-[(4-methyl-2-oxo-2*H*-chromen-7-yl)oxy]acetic acid- sulfuric acid half esters of dextran and pullulan were calculated on the basis of elemental analysis and UV-Vis spectroscopic measurements analogous to the procedure described in section 4.2. As well the content of sulfur as of carbon was used for calculation, since it is difficult to obtain water free polysaccharide

sulfates. For the UV-Vis measurements sample **8** was applied as reference compound and the spectra of all compounds were measured in a boronic acid/borate Clark and Lubs standard buffer solution at pH 9.

The structural characterization of the compounds **12** and **13** was carried out by means of FTIR- and ^{13}C NMR spectroscopy. Fig. 21 exemplarily shows the FTIR spectra of pullulan 2-[(4-methyl-2-oxo-2*H*-chromen-7-yl)oxy] acetate (**11d**, DS_{Photo} 0.37) and of its sulfated derivative (**13d3**, DS_{Photo} 0.37, $\text{DS}_{\text{SO}_3\text{Na}}$ 1.38). In both spectra typical signals arising from $\nu_{\text{C}=\text{O}}$ stretchings are visible at about 1720 cm^{-1} and 1610 cm^{-1} . The signal at 1720 cm^{-1} can be assigned to the carbonyl group of the ester linkage of the coumarin chromophor (C7 according to Fig. 17) and the carbonyl group of the lactone like structure of the substituent (C16 according to Fig. 17) gives rise to the signal at 1610 cm^{-1} . These signals prove the presence of 2-[(4-methyl-2-oxo-2*H*-chromen-7-yl)oxy] acetate moieties and their covalent linkage to the polymer backbone. In the spectrum of **13d3** two additional distinct signals can be noticed. The first one at about 1260 cm^{-1} results from the $\nu_{(\text{as})\text{SO}_2}$ stretching of the sulfate groups and the second at about 1015 cm^{-1} from the corresponding $\nu_{(\text{sy})\text{SO}_2}$ vibration.

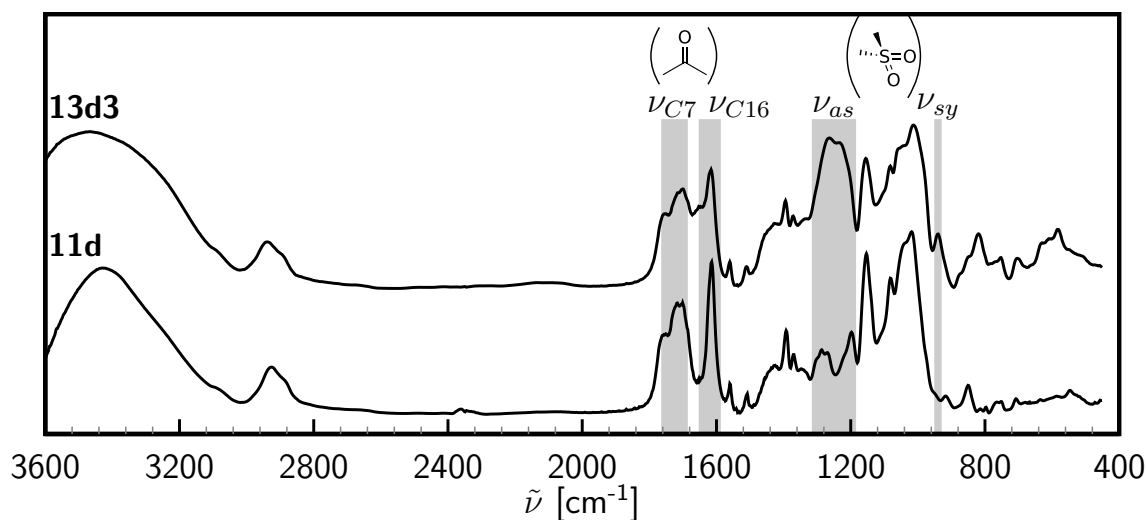


Figure 21 : IR spectra of pullulan 2-[(4-methyl-2-oxo-2*H*-chromen-7-yl)oxy] acetate (**11d**, DS_{Photo} 0.37, bottom) and sulfated pullulan 2-[(4-methyl-2-oxo-2*H*-chromen-7-yl)oxy] acetate (**13d3**, DS_{Photo} 0.37, $\text{DS}_{\text{SO}_3\text{Na}}$ 1.38, top); numbering of carbonyl atoms see Fig. 22

Figure 22 shows the ^{13}C NMR spectra of pullulan (Fig. 22a), pullulan 2-[(4-methyl-2-oxo-2*H*-chromen-7-yl)oxy] acetate (**11d**, DS_{Photo} 0.37, Fig. 22b), and sulfated pullulan 2-[(4-methyl-2-oxo-2*H*-chromen-7-yl)oxy] acetate (**13d3**, DS_{Photo} 0.37, $\text{DS}_{\text{SO}_3\text{Na}}$ 1.38,

Fig. 22c). In the spectra of **11d** and **13d3** the typical signals of the 2-[(4-methyl-2-oxo-2*H*-chromen-7-yl)oxy] acetate moiety are visible indicating its covalent attachment to the polymer backbone and the stability of the ester moieties during sulfation. In Fig. 22c a larger line width can be noticed resulting from the short lifetime of longitudinal and transversal magnetization; a typical phenomenon observed in polyelectrolytes caused by the electrostatic repulsion forces and thus a decrease in

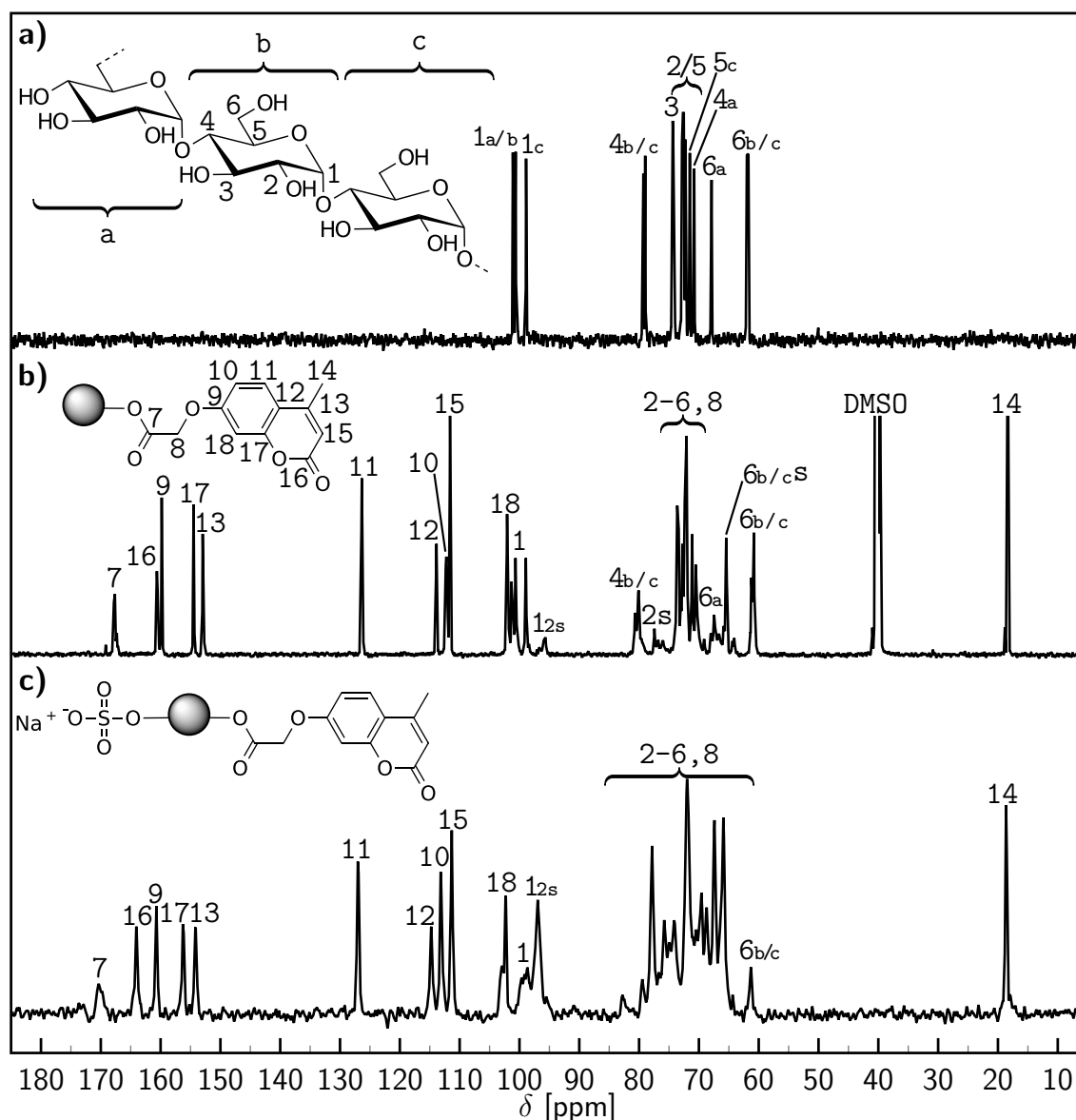


Figure 22: ^{13}C NMR spectra of: **a)** pullulan (**7**) in D_2O , **b)** pullulan 2-[(4-methyl-2-oxo-2*H*-chromen-7-yl)oxy] acetate (**11d**, DS_{Photo} 0.37) in DMSO-d_6 , **c)** sulfated pullulan 2-[(4-methyl-2-oxo-2*H*-chromen-7-yl)oxy] acetate (**13d3**, DS_{Photo} 0.37, $\text{DS}_{\text{SO}_3\text{Na}}$ 1.38) in D_2O .

flexibility. Although these effects hamper a clear and definitive assignment some general effects can be noticed. First, the group of signals at about 76 ppm, which can be assigned to C2s are of much larger intensity than in the spectra of **11d**. Moreover, the signal arising from C6_{b/c} is of very low intensity. Keeping in mind the discussion on the limiting DS_{Photo} and the availability of hydroxyl groups to the modification by SO₃/DMF complex it can be assumed that the sulfation predominately occurs in position 2 and 6 in case of pullulan.

5.2.2. Mixed 2-[(4-methyl-2-oxo-2*H*-chromen-7-yl)oxy]acetic acid-(3-carboxypropyl)trimethylammonium chloride esters of cellulose

Cationic polyelectrolytes derived from polysaccharides also display unconventional properties like protein-like oligomerization^[162] and are currently in the focus of research as flocculation agents in several industrial fields,^[163] for self assembly onto different surfaces,^[164,165] and for delivery of therapeutic or imaging agents.^[157,166] This section describes the synthesis and characterization of multifunctional cellulose derivatives bearing both photoactive 2-[(4-methyl-2-oxo-2*H*-chromen-7-yl)oxy]acetate residues and cationic (3-carboxypropyl)trimethylammonium chloride ester moieties.

Synthesis

The photoactive cellulose esters **9a-f** were allowed to react with (3-carboxypropyl)trimethylammonium chloride (**14**) in order to prepare the cationic photoactive cellulose derivatives (**15a-f**, Fig. 23). As in case of the synthesis of **9a-f**, CDI was applied for the activation of the carboxylic acid **14** and the corresponding imidazolide was added to **9a-f** dissolved in DMA/LiCl. As summarized in Tab. 9 the molar ratio of **9:14:CDI** of 1:0.5:0.5 yields DS values of the cationic group in the range from 0.19 to 0.36. Moreover, the DS of the photoactive group remains almost constant during the second esterification. The products **15a-f** are well soluble in water and aprotic dipolar solvents including DMSO and DMF.

Characterization

The degrees of substitution (DS_{Photo} and DS₁₄ of all mixed 2-[(4-methyl-2-oxo-2*H*-chromen-7-yl)oxy]acetic acid-(3-carboxypropyl)trimethylammonium chloride esters of cellulose were calculated on the basis elemental of analysis and UV-Vis spectroscopic measurements analogous to the procedure described in section 4.2. As

well the content of nitrogen as of carbon was used for calculation, since the samples are hygroscopic and therefore it is difficult to obtain them in a water free form. The UV-Vis measurements were carried out as described in subsection 5.2.1.

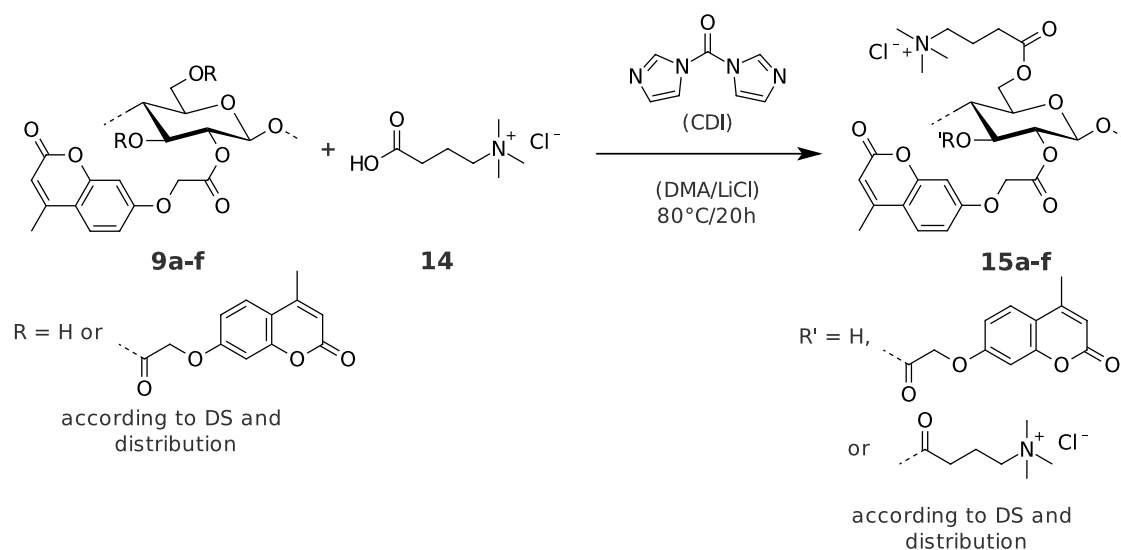


Figure 23 : Synthesis scheme of the esterification of the cellulose 2-[(4-methyl-2-oxo-2*H*-chromen-7-yl)oxy] acetates (**9a-f**) with (3-carboxypropyl)trimethylammonium chloride (**14**) in *N,N*-dimethylacetamide (DMA)/LiCl

The structural characterization of the compounds **15a-f** was carried out by means of ^{13}C NMR spectroscopy. Fig. 24 exemplarily shows the ^{13}C NMR spectra of cellulose (**1**) dissolved in DMSO- d_6 /tetrabutylammonium fluoride (Fig. 24a), cellulose 2-[(4-methyl-2-oxo-2*H*-chromen-7-yl)oxy]acetate **9e** in DMSO- d_6 (Fig. 24b), and the mixed 2-[(4-methyl-2-oxo-2*H*-chromen-7-yl)oxy]acetic acid- (3-carboxypropyl)trimethylammonium chloride ester of cellulose **15e** in DMSO- d_6 (Fig. 24c). All signals could be assigned by two dimensional measurements (HSQC-DEPT, TOCSY) and comparison with the spectra of the methyl ester of **8** and **14**, respectively. In the spectra of **9e** and **15e** the typical signals of the 2-[(4-methyl-2-oxo-2*H*-chromen-7-yl)oxy] acetate moiety are visible indicating its covalent attachment to the polymer backbone and the stability of the ester moieties during the cationization reaction. In the spectrum of the polyelectrolyte (Fig. 24c) again a larger line width could be noticed for the reasons mentioned above. However, all ^{13}C resonances of the 3-carboxypropyl)trimethylammonium chloride ester are visible. The signal arising from the C-atom of the carbonyl group of the linking ester moiety (C19) is visible at 172 ppm and the resonance of the methylene group C21 appears at 30 ppm. The signals of the other

methylene groups of the propyl spacer C20 and C22 overlap with the resonances of the repeating unit (C2, 3, 5) from 70–77 ppm and the methyl group C23 at 53 ppm respectively. From the NMR spectra of **15e** is obvious that esterification with **14** predominately takes place in position C6 as described in discussion on the structure of **9e** (section 5.1.2, page 45ff). The relative intensities of the resonances assigned to C6 and C6s are roughly in agreement with the total DS of 0.75. Moreover, the signal assigned to C1_{2s} have almost the same intensity as in the spectrum of **9e** indicating that no further functionalization at position 2 occurs.

Table 9:

acetic acid- (3-carboxypropyl)trimethylammonium chloride esters of cellulose] Conditions for and results of the synthesis of mixed 2-[(4-methyl-2-oxo-2*H*-chromen-7-yl)oxy]acetic acid- (3-carboxypropyl)trimethylammonium chloride esters of cellulose (**15a-f**) via activation of (3-carboxypropyl)trimethylammonium chloride (**14**) with *N,N*-carbonyldiimidazole (CDI) carried out in *N,N*-dimethylacetamide/LiCl

Educt		Molar ratio			Product		
No.	DS _{Photo} ^a	AGU ^b	CDI	14	No.	DS _{Photo} ^a	DS _{14} ^c
9a	0.06	1	0.5	0.5	15a	0.05	0.19
9b	0.16	1	0.5	0.5	15b	0.16	0.34
9c	0.25	1	0.5	0.5	15c	0.25	0.32
9d	0.33	1	0.5	0.5	15d	0.32	0.34
9e	0.38	1	0.5	0.5	15e	0.37	0.36
9f	0.49	1	0.5	0.5	15f	0.48	0.35

^a Degree of substitution (DS) of photoactive 2-[(4-methyl-2-oxo-2*H*-chromen-7-yl)oxy] acetate moieties; ^b modified anhydroglucose unit; ^c DS of sulfuric acid half ester (sodium salt) moieties.

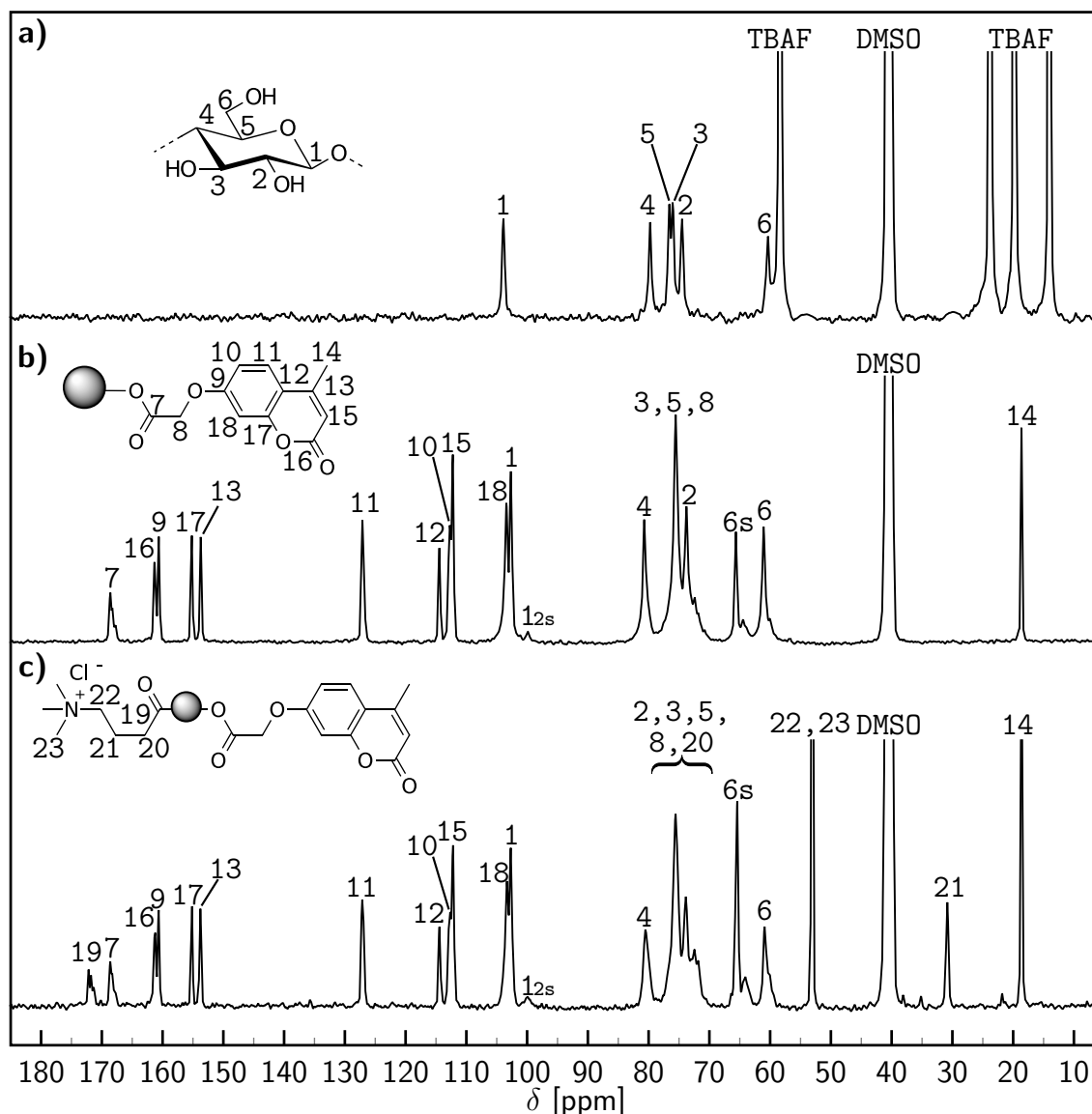


Figure 24: ^{13}C NMR spectra of: **a)** cellulose (1) in DMSO- d_6 / tetrabutylammonium fluoride (TBAF), **b)** cellulose 2-[(4-methyl-2-oxo-2H-chromen-7-yl)oxy] acetate (9e, DS_{Photo} 0.38) in DMSO- d_6 , **c)** mixed 2-[(4-methyl-2-oxo-2H-chromen-7-yl)oxy]acetic acid-(3-carboxypropyl)trimethylammonium chloride esters of cellulose (15e, DS_{Photo} 0.37, DS_{14} 1.38) in DMSO- d_6 .

6. Preparation of nanoparticles from photoactive polysaccharide esters

Cellulose esters like cellulose acetate are known since the middle of the 19th century and were commercially produced since roughly hundred years now. Edgar et al. highlighted that in spite of their long history, there is still a substantial research activity around cellulose esters and creative ways to exploit them in novel commercial applications were found recently.^[167,168] The authors illustrate the conventional shaping of cellulose esters and their performance in modern coatings, controlled release applications, plastics, composites, optical films, and membranes. However, nanostructures may possess properties that are dramatically different from their bulk material and thus there is an emerging interest on the engineering of polysaccharide based nanoassemblies during the last decade.^[169] Especially nanoscaled particles are of certain interest for the application as nanomaterials, particularly for controlled delivery of active principles.^[170–174] Nevertheless, the hydrophilic character of many polysaccharides applied for the preparation of nanoparticles so far makes it difficult to entrap hydrophobic substances such as certain drugs or dyes. Therefore, polysaccharide esters decorated with a broad variety of functional ester moieties came into focus for the preparation of nanoparticulate assemblies. For example, pharmacologically active-,^[161,175] sensor-,^[89] and reactive functionalities^[176] were covalently attached to different polysaccharides via esterification and the resulting hydrophobic derivatives were applied for the preparation of nanoparticles. Although highly engineered, the derivatives and the particles obtained so far can be termed as static or passive systems, since their properties are governed by the intrinsic polymer properties and the preparation conditions. For example, the pH value for a drug release can be predetermined by introducing acid labile acetal moieties into the polymer structure.^[177] However, neither the exact location nor the timing can be adjusted to patient needs or the changing of physiological circumstances. A stimuli responsive particulate system whose properties can be actively controlled would for example allow a spatial- and temporal on-demand dosing independently from

the administration. Therefore, the preparation of nanoparticles from photoactive polysaccharide derivatives is a highly promising pathway for triggerable systems.

The current chapter first is focusing on some general aspects of the preparation of nanoparticles from polysaccharide esters. The adaptation of different concepts (emulsification-evaporation and solvent-displacement) known for the generation of nanoparticles from hydrophobic polymers to the commercially available cellulose esters including cellulose acetate (CA), cellulose acetate propionate (CAP), and -butyrate (CAB) is described. The specific requirements, advantages, and disadvantages of the different methods will be highlighted with respect to the properties of the particular polysaccharide ester applied. In the second part the preparation of nanoparticles from selected photoactive polysaccharide esters will be described.

6.1. Nanoparticles from conventional cellulose esters: Evaluation of preparation methods

The two main concepts adapted for the preparation of nanoparticles from hydrophobic cellulose esters, are the emulsification-evaporation process from a lipophilic solution of the polymer and the solvent-displacement processes from a hydrophilic solution. These techniques for nanoparticle generation can be divided in high- and low-energy procedures, according to the mechanical and thermal energy applied. Depending on the properties of the particular cellulose esters both procedures were applied in order to provide a pool of nanoparticles meeting the specific aims of particular applications. The method of emulsification-diffusion lies somewhere in between the both other methods and this procedure will not be discussed in the following. For a detailed survey about the theory of the preparation methods of organic nanoparticles including polymeric particles the reader is referred to the excellent work from Horn and Rieger.^[178]

As conventional cellulose esters cellulose triacetate (**16**, CTA), cellulose acetate (**17**, CA), cellulose acetate propionate (**18**, CAP), and cellulose acetate butyrate (**19**, CAB) were applied. The compounds were characterized by means of ¹H-NMR spectroscopy after p-nitrobenzylation^[179] and size exclusion chromatography. The analytical values are summarized in Table 10.

Table 10: Degree of substitution (DS) and weight average molecular weight (\overline{M}_W) of cellulose acetate (CA), cellulose acetate propionate (CAP), -butyrate (CAB), and -phthalate (CAPH) samples applied in the current study.

No.	Substance	DS	\overline{M}_W^c [g/mol]
16	CA	2.95 ^a	304 000
17	CA	2.49 ^a	97 900
18	CAP	0.10 / 2.17 ^a	191 100
19	CAB	0.15 / 2.10 ^a	57 300

^aDetermined by means ¹H-NMR spectroscopy after pernitrobenzylation; ^bdetermined by means ¹H-NMR spectroscopy after perpropionylation; ^cdetermined by means of size exclusion chromatography with dimethyl sulfoxide as eluent.

6.1.1. Emulsification-evaporation process

The emulsification-evaporation process is a common method for the preparation of water dispersed nanoparticles from water insoluble organic compounds including hydrophobic polymers. Since the resulting nanoparticle formulations are effectively based on nanometric-scaled emulsions the procedure is frequently termed as nanoemulsion- or miniemulsion process. Anton et al. offer a comprehensive review about the theoretical and practical aspects of the preparation of nanoemulsions and the formation of nanoparticles thereof.^[180]

The basic procedure adapted in this work for cellulose esters can be described as follows: In the first step the nanoemulsion template is generated by sonification from a solution of the cellulose ester in a not water mixable volatile organic solvent and a solution of polyvinyl alcohol as a stabilizing surfactant in water. Subsequently the organic solvent is evaporated from the polymer containing nanodroplets and a stable suspension of cellulose ester nanoparticles is generated (Figure 25). Typical organic solvents applied for this procedure are chlorinated solvents in particular dichloromethane (CH₂Cl₂). Therefore, only the cellulose triacetate **16**, cellulose acetate propionate **18**, -butyrate **19** were used for the emulsification-evaporation technique, which possess the required solubility in CH₂Cl₂.

Since the final nanoparticle properties are governed by properties of the nanoemulsion template the focus was on the optimization of particle properties by the directly controllable formulation parameters of the emulsification. Tab. 11 summarizes the

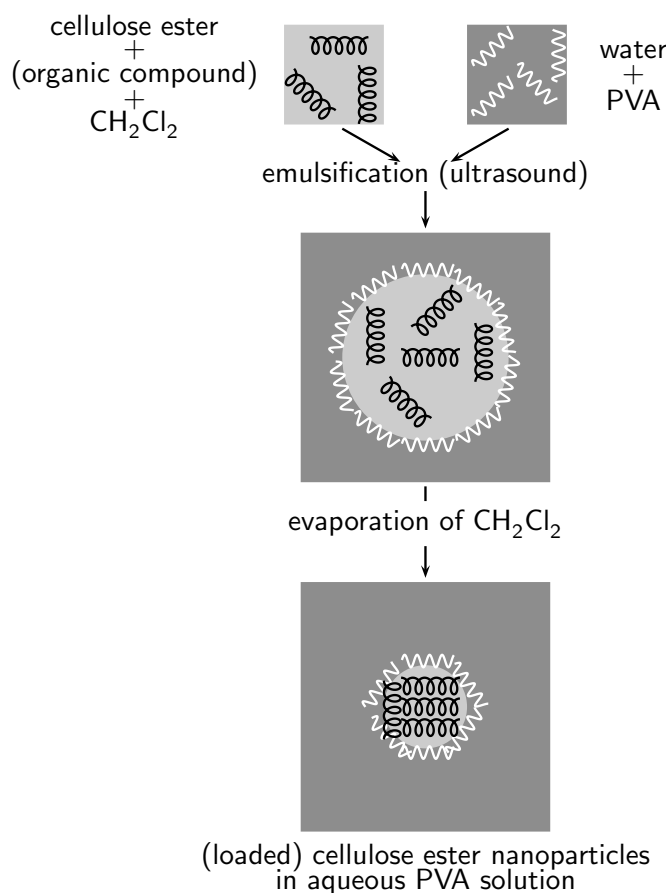


Figure 25: Principle of the preparation of cellulose ester nanoparticles by emulsification–evaporation process applying dichloromethane (CH_2Cl_2) as organic solvent and polyvinyl alcohol (PVA) as stabilizer; adapted from^[178].

conditions applied for emulsification-**evaporation** of **16** and the properties of the nanoparticles obtained. A first set of experiments was carried out to determine the quantity of energy of sonification, which is necessary to create nanoparticles (Tab. 11 **16a-d**). It turned out that below 100 W no nanoemulsion and thus no nanoparticles are obtained. Obviously the energy provided mostly dissipated, generating heat and being wasted in viscous friction.^[181] Therefore, the additional free energy needed to generate the enormous interfacial area of the nanoemulsion is not obtained. An energy of sonification above 100 W finally yields particles of a size approximately 250 nm (**16a**) and there are no remarkable effects on the size in case of a further increase of the energy. However, applying 150 W a minimum of particle size (206 nm) is reached and the most uniform particles are obtained (PDI 0.049). Therefore, this energy was used in all further experiments. The time of sonification was the second formulation parameter, which was optimized (Tab. 11 **16e-k**). It turned out that

the minimal time needed for the generation of a nanoemulsion template is about 5 sec and the resulting particles have a size of approximately 250 nm (**16e**). An increase of sonification time to 10 sec reduces the droplet- and thus the nanoparticle

Table 11: Conditions for and results of the preparation of nanoparticles (NP) from cellulose triacetate (CTA, **16**), cellulose acetate propionate (CAP, **18**), and cellulose acetate butyrate (CAB, **19**) by emulsification-evaporation; not water mixable organic solvent: dichloromethane (CH_2Cl_2); aqueous phase: polyvinyl alcohol (PVA, 3% w/v, $M_w=13\,000\text{-}23\,000$ g/mol).

No.	Preparation conditions					NP properties ^a	
	E [W]	$t_{\text{sonification}}$ [sec] ^b	$m_{\mathbf{16}}$ [mg]	$V_{\text{CH}_2\text{Cl}_2}$ [mL]	V_{PVA} [mL] ^c	Z-average [nm]	PDI
16a	100	10	25	1	2	249	0.095
16b	125	10	25	1	2	256	0.056
16c	150	10	25	1	2	206	0.049
16d	175	10	25	1	2	246	0.051
16e	150	5	25	1	2	242	0.039
16f	150	15	25	1	2	206	0.017
16g	150	20	25	1	2	209	0.023
16h	150	25	25	1	2	211	0.020
16i	150	30	25	1	2	204	0.023
16j	150	35	25	1	2	208	0.021
16k	150	40	25	1	2	208	0.035
16l	150	10	5	1	2	203	0.033
16m	150	10	10	1	2	200	0.043
16n	150	10	15	1	2	213	0.026
16o	150	10	20	1	2	212	0.036
16p	150	10	30	1	2	218	0.031
16q	150	10	35	1	2	241	0.046
16r	150	10	40	1	2	250	0.033
16s	150	10	50	1	2	250	0.027
16t	150	20	250	10	20	253	0.052
18a	150	10	25	1	2	210	0.054
19a	150	10	25	1	2	215	0.060

^a Mean values of whole sample determined by dynamic light scattering using cumulants method assuming spherical particle shape; ^b pulsed ultrasound (1 s puls followed by 0.5 s stop); ^c after sonification all samples were diluted 3 : 10 with PVA_{aq} (0.3% w/v).

size by about 20% (**16c**, 206 nm). However, a further increase has almost no effects on size and distribution and since longer sonification times might have negative consequences (e.g. degradation) 10 sec was considered as most efficient sonification time. In order to study the effects of the amount of cellulose ester applied for the emulsification-evaporation the concentration of the polymer solution was varied from 5 to 50 mg/mL (Tab. 11 **16l-s**). A trend of an increasing size of the final particles with increasing polymer concentration became obvious. Nevertheless, the absolute values of particle size change only about 20% (from ≈ 200 to ≈ 250) while the polymer concentration was ten times higher comparing sample **16l** and **16s**. Finally, one experiment applying a larger quantity of **16** and larger volumes of CH_2Cl_2 and PVA solution was carried out to evaluate the possibility to produce larger amounts of nanoparticles (**16t**). The particles obtained have a size and distribution very similar to the particles obtained by the smaller scaled experiments. From the direct comparison of the samples prepared under the same conditions from the the different cellulose esters (**16c**, **18a**, and **19a**) it can be noticed that the particle size and distribution is almost independent from the cellulose ester used for the emulsification-evaporation technique.

6.1.2. Solvent-displacement

The spontaneous particle formation by solvent-displacement is an alternative to the energy extensive formation of o/w emulsion by mechanical homogenization as preliminary stage of the nanoparticle formation. The techniques of solvent displacement are also known as nanoprecipitation, osmosis based precipitation, or solvent shifting.^[182–184] The particle formation is usually explained by an interfacial deposition of the polymer, initiated by boundary layer concentration fluctuations during the displacement of a water mixable organic solvent from the polymer solution (Figure 26).^[185] Practically, solvent-displacement can be carried out applying dialysis or a simple dropping technique.

Dialysis

Dialysis is based on the use of a physical barrier (dialysis membrane) that allows the passive transport of solvents and on the slow mixing of the polymer solution with the nonsolvent. The resulting solvent mixture is progressively less able to dissolve the polymer and the increasing interfacial tension drives the macromolecules to aggregate and finally precipitate as particles.^[184] When the precipitation process is slow enough

a so-called equilibrium morphology is reached, corresponding to the minimal free energy of the system. Thus, in the experiments reported in this work dialysis lead to spherical particles, since the most important thermodynamic parameter is the free interface energy. However, other shapes including disks, sponges and tubular rods are reported in literature as well.^[184,186]

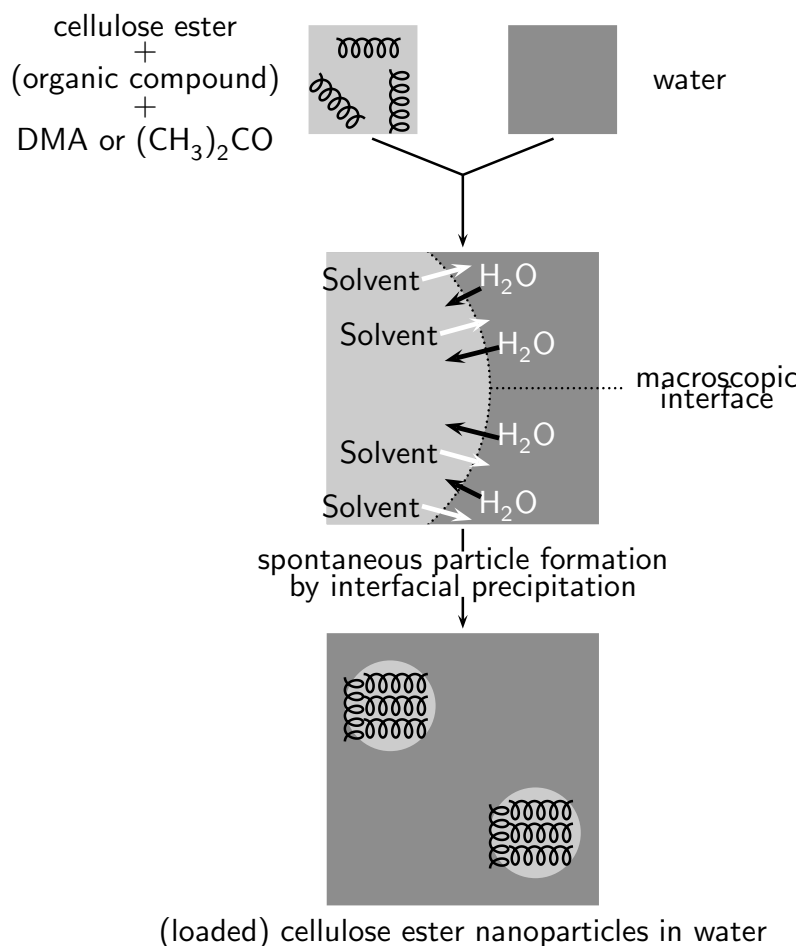


Figure 26: Principle of the preparation of polysaccharide nanoparticles by the solvent-displacement process, applying *N,N*-dimethylacetamide (DMA) or acetone as organic solvent, adapted from^[178]

The properties of the particles obtained by solvent-displacement in general and dialysis in particular are governed by the intrinsic physicochemical characteristics of the system. Namely the solvent solvation power, the hydrophobic-hydrophilic balance of the polysaccharide ester, and the polymer concentration have an influence on the particle formation and properties as well as on the particle morphology. Since the number of solvents that is applicable for dialysis is limited this work focusing on the polymer concentration and the hydrophobic-hydrophilic balance as parameters

for the control of the particle properties. For this purpose, **16** and **17** were dissolved in *N,N*-dimethylacetamide and dialyzed against the non-solvent water. Fig. 27 shows the dependency of the particle size (*z*-Average) and the polydispersity index (PDI) as a measure of the size distribution on the mass concentration (c_w) of the initial polymer solution. It can be noticed that in case of **16** (Fig. 27a) the particle size increases from ≈ 230 to ≈ 320 nm when increasing the polymer concentration from 1 to 6 mg/ml. Simultaneously the PDI increases from 0.090 to 0.164. Above the critical overlap concentration c^* , which was determined by plotting the reduced viscosity (η_{red}) over c_w , irregular precipitation occurs. In case of **17** (Fig. 27b) the particle size and distribution increases from ≈ 380 (0.077) to ≈ 420 nm (0.098) until c^* is reached. Above c^* larger particles are obtained and the PDI increases to 0.3, which indicates the change from a narrow size distribution to a very broad one.

The phenomenon of the formation of nano-scaled particles by solvent-displacement can be attributed to the nucleation of macromolecules due to concentration fluctuations caused by the interdiffusion of water and the solvent DMA. The initial nuclei tend to grow by capturing macromolecules from the solution. Simultaneously the polymer solution becomes progressively more supersaturated, since the ratio of water to DMA increases. Therefore the number of nuclei increases until they have frequent encounters that cause their aggregation.^[183] As a consequence of this *nucleation and growth*- and *nucleation and aggregation* mechanism the mean particle diameter and the size distribution tend to increase with the initial concentration of the polymer solution. The results of the dialysis of **16** and **17** can be explained by this model very well until c^* is reached. Beyond the c^* entanglements between the polymer chains are present and therefore macroscopic aggregates can be expected as it is observed in the case of **16**. The fact that in case of **17** still nanoparticles, albeit with a broad distribution, are obtained may be attributed to the molecular mass of **16** that is three times higher than that of **17**. Thus the entanglements of the polymer chains above c^* may result in more drastic effects with respect to irregular precipitation. However even in case of **17** macroscopic aggregates are obtained when starting with a polymer solution with a concentration higher than 26 mg/mL. Beside the different concentration dependency all particles obtained from **17** are larger than those from **16** even when the same polymer concentration is applied. For example, the particles obtained from a polymer solution with a concentration of 5 mg/mL yields particles of a size of ≈ 310 and ≈ 350 nm depending on if **16** or **17** was used.

This finding can be attributed to the more hydrophobic character of **16** which tends the particles to a more compact structure, which probably contains less water.

Dropping Technique

An alternative technique of solvent-displacement is the dropwise addition of water to the dilute polymer solution under stirring.^[187] Since the organic solvent is not removed during the nanoprecipitation as in case of dialysis, the application of volatile solvents mixable with water is favored. Therefore, cellulose acetate with a DS of 2.49 (**17**), which is soluble in acetone, was utilized to evaluate this technique. Since the mechanism of nanoprecipitation by dropwise addition of the nonsolvent is assumed to be similar to that of dialysis, the same dependency on c^* can be expected. The value of c^* of **17** in acetone was determined to be 14 mg/mL and all further experiments were carried out applying less concentrated polymer solutions to prevent any effects related to polymeric entanglements. Comparing to dialysis, the dropping technique is a more efficient path for the preparation of larger quantities of nanoparticles because of the low price and low toxicity of acetone compared to DMA. Furthermore, no dialysis membrane is needed. However, beside the concentration of the polymer solution two other formulation parameters namely the water/acetone ratio and the rate of water addition need to be controlled. Table 12 summarizes the conditions for and results of the preparation of nanoparticles from **17** by the addition of water to the polymer solution.

A first set of experiments was carried out to evaluate the influence of the ratio of water to acetone. For this purpose, the total volume of water added to a fixed volume of polymer solution (20 mL) was varied. It turned out that at all concentrations applied the size of the final particles increases with increasing amount of water added. This holds true until a certain water acetone ratio is reached and than no further increase in size can be observed. The direct comparison of the samples **17g-l** (c_{W17} 6 mg/mL) and **17m-r** (c_{W17} 4 mg/mL) suggests that amount of water needed to reach the final particle diameter decreases with decreasing polymer concentration. Moreover, the the absolute value of the final diameter decreases as well. This tendency can not be assumed as a sure fact, since the samples **17s-x** (c_{W17} 2 mg/mL) show no regular trend. In further experiments the influence of the rate of water addition was varied. By comparing samples **17a-f** (5 mL/min) and **17g-l** (10 mL/min) it can be noticed that a faster addition yields smaller particles. Since it is difficult to

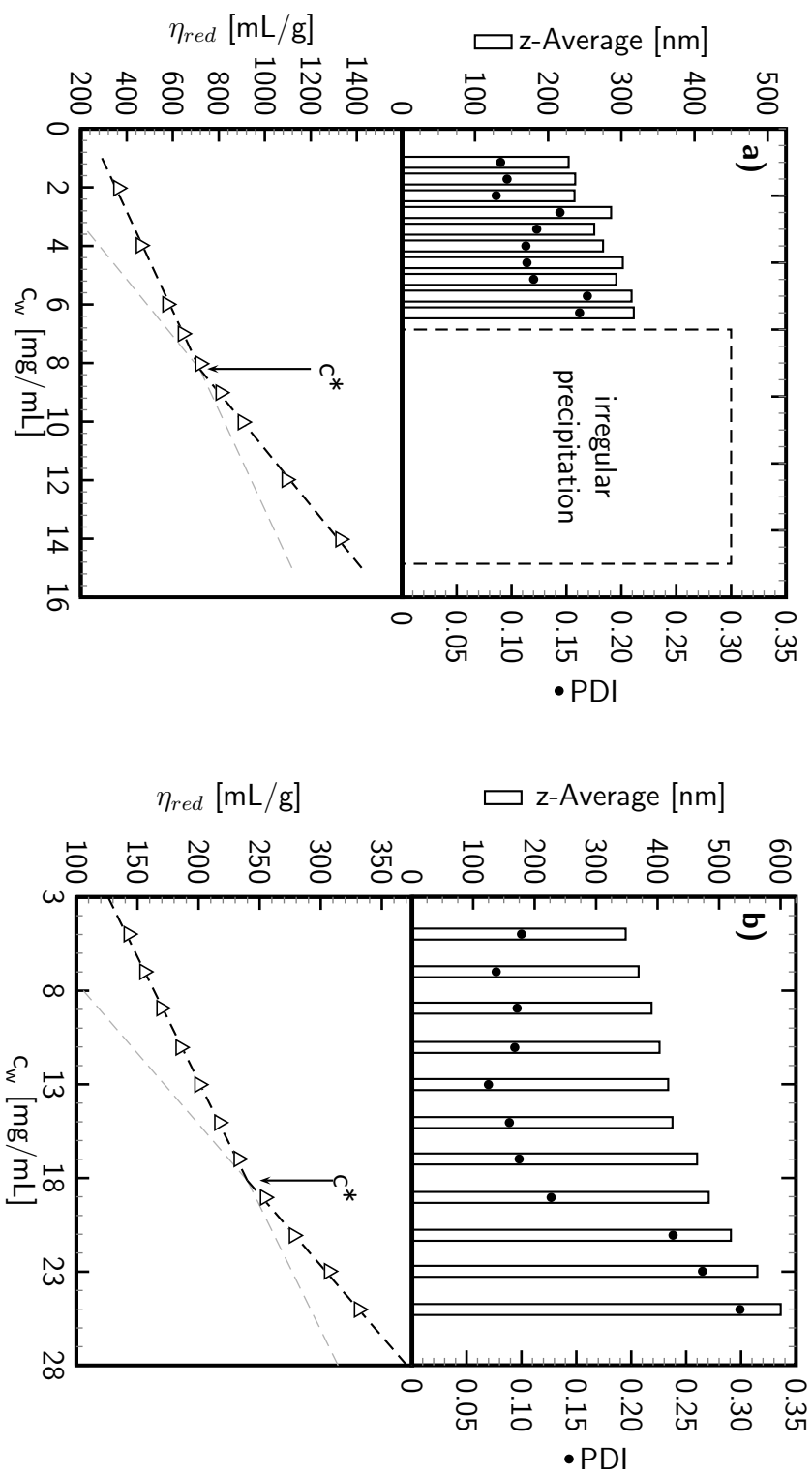


Figure 27 : Dependency of the particle size (z-Average) and polydispersity index (PDI) of nanoparticles obtained via dialysis (top) and reduced viscosity (η_{red} , bottom) on the concentration of **a)** cellulose triacetate (**16**) and **b)** cellulose acetate (**17**, DS 2.49) dissolved in N,N-dimethylacetamide; c^* denotes for the critical overlapping concentration.

guarantee an instant mixing of polymer solution and the water added, higher rates of water addition gave no reproducible results and are not reported for that reason.

Table 12: Conditions for and results of the preparation of nanoparticles (NP) from cellulose acetate with a DS of 2.49 (**17**) by the addition of water to a polymer solution; water mixable organic solvent: acetone ((CH₃)₂CO).

No.	Preparation conditions				NP properties ^a	
	m ₁₇ [mg]	V _{(CH₃)₂CO} [mL]	V _{H₂O} [mL]	rate of addition [mL/min]	Z-average [nm]	PDI
17a	120	20	20	5	310	0.066
17b	120	20	30	5	334	0.073
17c	120	20	40	5	362	0.080
17d	120	20	50	5	403	0.111
17e	120	20	60	5	425	0.112
17f	120	20	70	5	422	0.132
17g	120	20	20	10	285	0.065
17h	120	20	30	10	294	0.074
17i	120	20	40	10	295	0.061
17j	120	20	50	10	330	0.099
17k	120	20	60	10	328	0.104
17l	120	20	70	10	337	0.072
17m	80	20	20	10	226	0.086
17n	80	20	30	10	293	0.089
17o	80	20	40	10	310	0.104
17p	80	20	50	10	314	0.138
17q	80	20	60	10	307	0.090
17r	80	20	70	10	294	0.072
17s	40	20	20	10	281	0.132
17t	40	20	30	10	326	0.189
17u	40	20	40	10	240	0.135
17v	40	20	50	10	308	0.125
17w	40	20	60	10	250	0.231
17x	40	20	70	10	712	0.619

^a Mean values of whole sample determined by dynamic light scattering using cummulants method assuming spherical particle shape.

6.1.3. Conclusions

Comparing the methods of emulsification-evaporation and solvent-displacement, different advantages and disadvantages can be concluded. In case of emulsification-evaporation very small and uniformly (even monomodal) distributed particles can be obtained very fast and with an excellent reproducibility. The high concentrations that are applicable allow to prepare large amounts of nanoparticles very efficiently. However, the need of chlorinated solvents and stabilizing agents such as polyvinyl alcohol are the main drawbacks of this method in particular if biomedical applications are considered. Moreover, the thermal treatment of the initial nanoemulsion in order to generate the nanoparticles might have undesirable effects if polysaccharide derivatives are applied, which are more sensitive than cellulose acetate. Last but not least, ultrasonic treatment of polysaccharides and polysaccharide derivatives is known to induce polymer degradation.^[188] The solvent-displacement by dialysis or dropping technique is very easy to use and yields small narrowly distributed particles as well. Compared to emulsification-evaporation, the properties of the particles obtained by solvent-displacement are much more dependent on the concentration of the initial polymer solution. In particular, high a concentration above c^* is not applicable for the preparation of nanoparticles by dialysis and dropping technique. Moreover, solvent-displacement is much more dependent on the polymer properties. From the direct comparison of dialysis and dropping technique, it can be concluded that the latter is much faster and the use of an expensive dialysis membrane can be avoided on one hand. On the other, a thermal treatment of the samples is required if the organic solvent needs to be removed in case of the dropping technique, while dialysis yields solvent free particles from the outset.

6.2. Nanoparticles from highly substituted dextran

2-[(4-methyl-2-oxo-2*H*-chromen-7-yl)oxy] acetates

On the basis of the experience gained during the experiments described in the previous section, dialysis was applied simple and mild method for the preparation of nano-scaled particles from the photoactive dextran 2-[(4-methyl-2-oxo-2*H*-chromen-7-yl)oxy] acetates **10a-h**. The dextran samples were chosen for this experiments, since a broad DS range including highly substituted derivatives is accessible very efficiently. At first c^* of the samples **10a** and **10h** in DMA was determined to be 9 mg/mL and 11 mg/mL, respectively, and it was assumed that the c^* values of

10b-g are in the same range. Therefore, a concentration of 4 mg/mL was applied for dialysis to prevent any effects related to polymeric entanglements described above (subsection 6.1.2). Table 13 summarizes the results of the preparation of nanoparticles from **10a-h** via dialysis from DMA. It can be noticed that the diameter and the size distribution of the particles decreases with increasing DS. Below a DS of 0.38 (samples **10a-b**) no nanoparticles but irregular precipitation can be observed. In Fig. 28 scanning electron microscopy (SEM) images of the particles obtained from **10c** and **10h** are shown as representative examples. In accordance with the expected equilibrium morphology of hydrophobic particles in aqueous media both samples exhibit spherical particles which possess a minimal free interface energy. The trend of a decrease of the average particle size with increasing DS can also be noticed in the SEM images. Eye-catching is the more uniform distribution of the particles obtained from **10h** compared to those obtained **10c**. This finding qualitatively corresponds to the change of the PDI from 0.224 to 0.076 which was observed by dynamic light scattering.

Table 13: Conditions for and results of the preparation of nanoparticles from dextran 2-[(4-methyl-2-oxo-2H-chromen-7-yl)oxy] acetates (**10a-h**) via dialysis; water mixable organic solvent: *N,N*-dimethylacetamide; concentration of polymer solution: 4 mg/mL.

No.	DS	NP properties ^a	
		Z-average [nm]	PDI
10a	0.12	-	-
10b	0.25	-	-
10c	0.38	456	0.224
10d	0.47	314	0.135
10e	0.71	238	0.112
10f	0.90	213	0.098
10g	1.45	198	0.075
10h	2.01	150	0.076

^a Mean values of whole sample determined by dynamic light scattering using cummulants method assuming spherical particle shape.

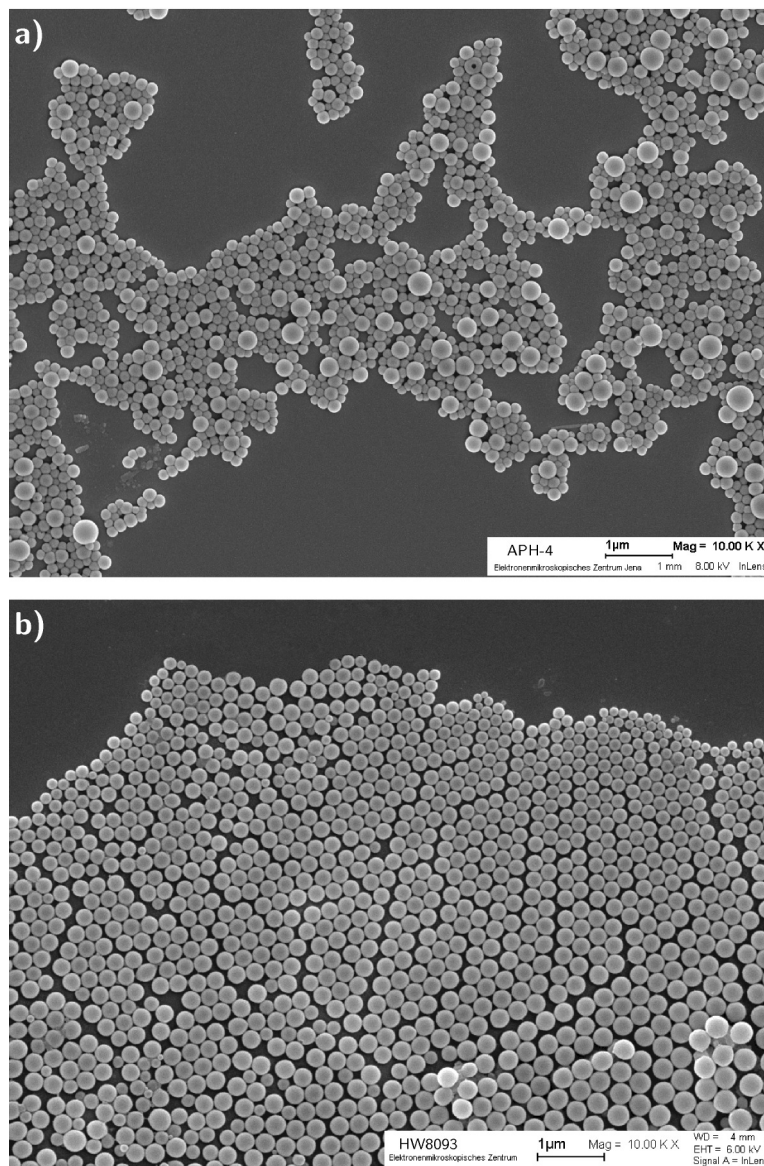


Figure 28: SEM images from nanoparticles obtained by dialysis of dextran [(4-methyl-2-oxo-2H-chromen-7-yl)oxy]acetates with a DS of **a)** 0.38 (**10c**) and **b)** 2.01 (**10h**).

7. Photochemical and photophysical behavior

The 2-[(4-methyl-2-oxo-2*H*-chromen-7-yl)oxy] acetate moieties, which were linked to different polysaccharides during the work reported in this thesis (see chapter 5), are typical coumarin-type chromophores. As pointed out by Trenor et al., the coumarin family attracts an increasing interest for the application in polymeric materials due to its intriguing photochemical and -physical properties.^[189] In particular, the fluorescence properties and the reversible photodimerization of coumarins provide the basis for novel applications including light harvesting and photo-cross-linkable tissue scaffolds. The light-induced processes of coumarins are summarized in Fig. 29. As a result of irradiation (usually) with UV-light the excited singlet state is formed. The energy gained can be released either radiatively via fluorescence and after inter-system-crossing by phosphorescence or is consumed by a $2\pi+2\pi$ cycloaddition reaction of the excited coumarin with a further ground state molecule.

As shown in Fig. 30, the photodimerization leads to four different dimers depending on the light intensity, the solvent, and the coumarin concentration.^[190] The structures obtained are termed for their stereo chemistry as *syn*-/*anti*- and *head to head*/*head to tail* dimers. The *syn*-/*anti*- nomenclature refers to the position of the former

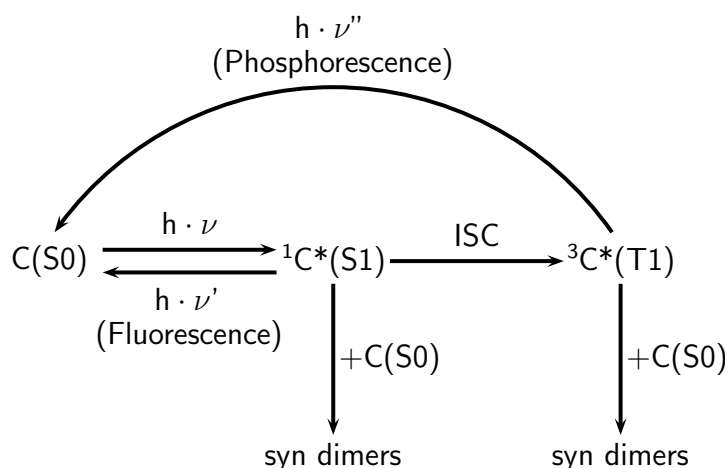


Figure 29: Schematic presentation of the light-induced processes of coumarin-type chromophores; C: coumarin in ground state; C*: coumarin in excited state; S: singlet state, T: triplet state, ISC: inter-system-crossing, adapted from Trenor et al.^[189]

coumarin moieties relative to the plane of the formed cyclobutane ring (same or opposite side) and the term *head to head/head to tail*- refers to their positions relative to each other. While the *syn*-adducts are formed from the excited singlet state (S1) the *anti*-dimers are obtained from the triplet state (T1). Therefore, the formation of *syn*-dimers is preferred in polar solvents, since the excited singlet-state dipole moment is stabilized.^[191] On the contrary, the use of nonpolar solvents or the addition of photosensitizers such as benzophenone lead predominately to anti-photodimers.^[192,193] In chlorinated solvents the lifetime of S1 is reduced by the heavy atom effect resulting in an increase of the relative concentration of T1 and thus also to a preferred formation of the *anti*-dimers.^[194] In solution the formation of the *head to head* or the *head to tail* structure depends mainly on the concentration of the chromophores while in solid state their alignment is of importance.^[195]

The reversibility of the photodimerization of coumarins was discovered by Schenck et al. in the late 1960s^[190]. However, the photochemical cleavage of the cyclobutane

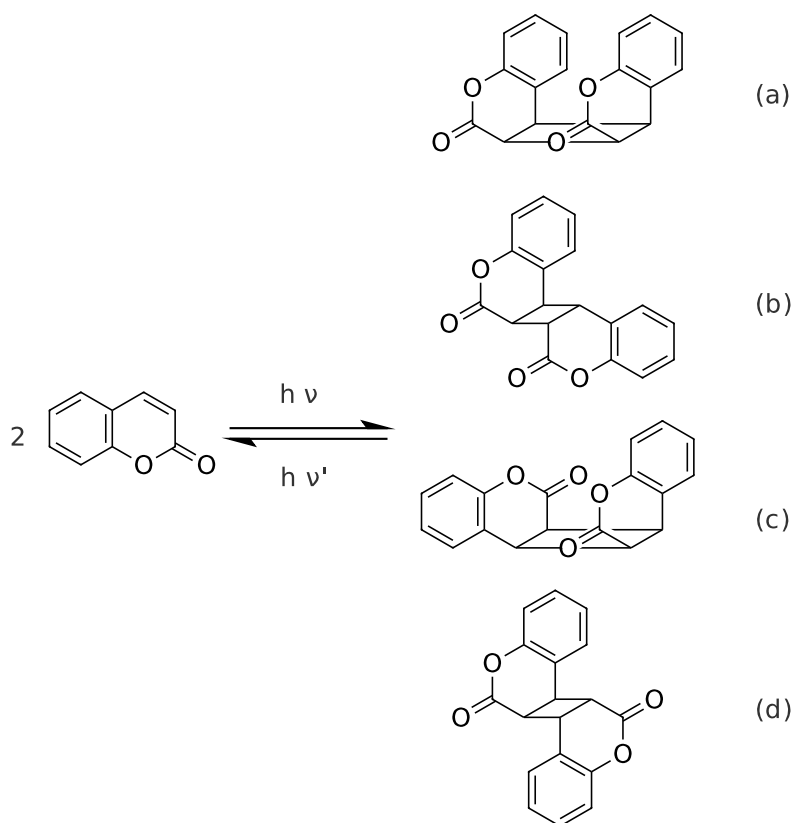


Figure 30: Schematic presentation of the $2\pi+2\pi$ cycloaddition of coumarin and the resulting different isomers; **a)** *syn-head to head*-dimer; **b)** *anti-head to head*-dimer; **c)** *syn-head to tail*-dimer; **d)** *anti-head to tail*-dimer.

ring has not been studied as extensive as the dimerization reaction, since the shorter wavelength required results in different problems. Namely the photodegradation of the phenyl ring or the cleavage of the internal ester may occur. Therefore, recent attempts focus on the cycloreversion of the coumarin dimers by two photon absorption.^[196]

The following sections describe the photochemical and photophysical behavior of photoactive polysaccharide derivatives as well in solution as in nano-particulate systems. Moreover, the insights into the morphology of the nanoparticles, provided by fluorescence measurements, will be emphasized.

7.1. Photochemical and photophysical behavior of photoactive polysaccharide derivatives in solution

The photochemical response of the cellulose-, dextran- and pullulan 2-[(4-methyl-2-oxo-2*H*-chromen-7-yl)oxy] acetates (**9-11**), the mixed 2-[(4-methyl-2-oxo-2*H*-chromen-7-yl)oxy]acetic acid- sulfuric acid half esters of dextran and pullulan (**12-13**), and the mixed 2-[(4-methyl-2-oxo-2*H*-chromen-7-yl)oxy]acetic acid- (3-carboxypropyl)trimethylammonium chloride esters of cellulose (**14**) was studied by means of UV-Vis spectroscopy. In case of **9-11** the perpropionylated derivatives were used in order to provide solubility in solvents, which are transparent for UV light with $\lambda < 300$ nm (e.g. acetonitrile). Since the photochemical behavior of **9-11**, **12-13**, and **14** is very similar, one representative example will be discussed in the following.

Figure 31 shows the results of the UV-Vis spectroscopic investigation of the photodimerization of the perpropionylated sample **10e**. Before irradiation the spectrum (Fig. 31a 0 sec) shows the typical $\pi \rightarrow \pi^* {}^1B$ transition below 250 nm, the $\pi \rightarrow \pi^* {}^1L_a$ transition as a shoulder at 290 nm, and the $\pi \rightarrow \pi^* {}^1L_b$ transition with a maximum at 316 nm.^[197] Upon irradiation with UV-light ($\lambda=333$ nm) the absorption at 316 nm decreases indicating the $2\pi+2\pi$ cycloaddition of the coumarin. Simultaneously the absorption below 256 nm increases as can be noticed from the differential spectra (Fig. 31b). The isosbestic point at 256 nm indicates the uniformity of the reaction. The kinetic of the photoreaction were studied by analyzing the time dependency of the change of the absorption maximum at 316 nm (Fig. 31c). The graphical plot according to $k \cdot t = \frac{1}{A} - \frac{1}{A_0}$ (Fig. 31d) proves a second-order reaction kinetic as expected for a bimolecular dimerization. Summing up the results obtained, it can be concluded that the photochemical dimerization of the 2-[(4-methyl-2-oxo-2*H*-chromen-7-yl)oxy]

acetate moieties linked to polysaccharides takes place very efficiently and can be described very well.

The photocycloreversion of the dimers formed during the irradiation at 333 nm was studied as well. UV-spectroscopy reveals that the initial coumarin chromophores are recovered by the irradiation with UV light with a wavelength of 254 nm. Exactly the reverse effects shown in Fig. 31a & b occur and the isosbestic point appears also at 256 nm. However, the complete cycloreversion could not be proved since the light sources available for the required wavelength provide not enough intensity.

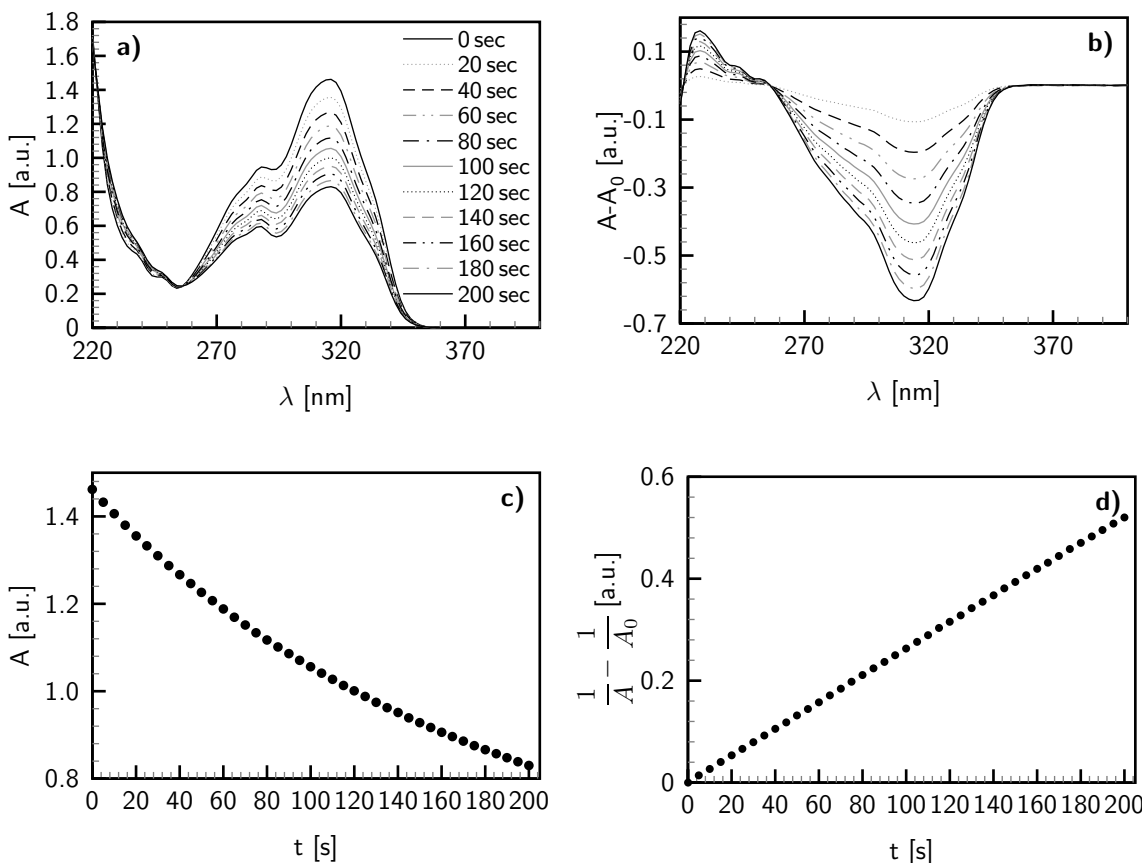


Figure 31: Results of the UV-Vis spectroscopic investigation of the photodimerization of the perpropionylated dextran 2-[(4-methyl-2-oxo-2*H*-chromen-7-yl)oxy] acetate **10e** ($DS_{\text{photo}} 0.71$): **a)** UV-Vis spectra measured after different irradiation times; **b)** differential spectra obtained from a) (same caption); **c)** time dependency of the change of the absorption maximum at 316 nm; **d)** graphical analysis of c) according to second-order reaction kinetics ($k \cdot t = \frac{1}{A} - \frac{1}{A_0}$)

Preliminary experiments about the photocontrol of solution properties were carried out by means of viscosity measurements. For this purpose, the reduced viscosity of several solutions with different concentrations of **10e** in DMA was determined

before and after irradiation. As shown in Fig. 32 the reduced viscosity (η_{red}) of the unirradiated samples increases linearly until the critical overlap concentration (c^*) is reached. At c^* (≈ 9.9 mg/mL) the slope of the increase becomes higher. In case of the irradiated samples two different effects can be noticed in the concentration ranges below and above c^* . The viscosity of the solutions with a concentration above c^* increases drastically and above 14 mg/mL precipitation is observed. Interestingly, the viscosity of the solutions with a concentration below c^* decreases upon irradiation.

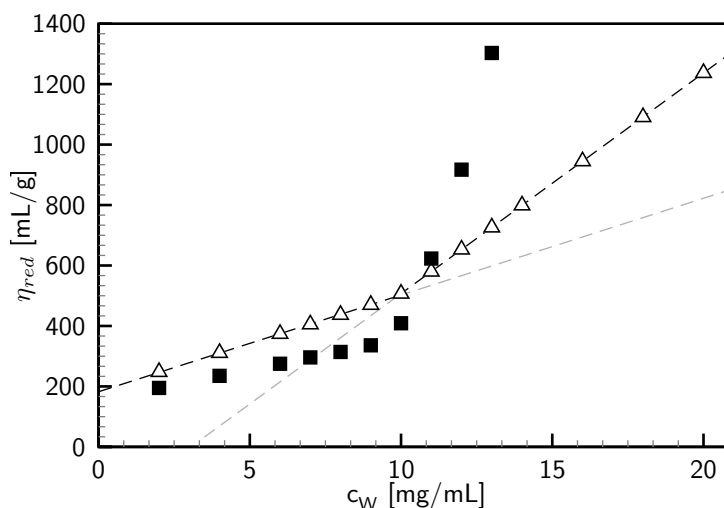


Figure 32: Dependency of the reduced viscosity (η_{red}) on the concentration of dextran 2-[(4-methyl-2-oxo-2*H*-chromen-7-yl)oxy] acetate **10e** in DMA (Δ) and viscosity of the same samples after irradiation for 2 h at 333 nm (\blacksquare)

Keeping in mind that above c^* there are frequent encounters between different polymer chains and moreover entanglements might be present, the increase of the viscosity and the precipitation upon irradiation of the solutions with $c_w > c^*$ can be understood intuitively as an intermolecular crosslinking. For the decrease of the viscosity below c^* it is difficult to give a definitive interpretation. It can be supposed that the photodimerization of the [(4-methyl-2-oxo-2*H*-chromen-7-yl)oxy] acetate moieties predominantly takes place within one polymer chain at this concentration. This may lead to a more compact polymer coil and thus a decrease of η_{red} . However, a determination of the radius of gyration, e.g., via the Fox-Flory theory, seems not reasonable since both plots tend to the same intrinsic viscosity. Therefore, additional informations for example the molar mass determined by static light scattering are needed for a more detailed understanding of the photochemical behavior of the photoactive polysaccharide derivatives in solution.

7.2. Light absorption and fluorescence for the characterization of photoactive polysaccharide based nanoparticles

The photophysical and photochemical characteristics of the particle suspensions obtained via dialysis from dextran 2-[(4-methyl-2-oxo-2*H*-chromen-7-yl)oxy] acetates **10d** (DS 0.47), **10f** (DS 0.90), **10g** (DS 1.45), and **10h** (DS 2.01), were studied by means of absorption- and fluorescence spectroscopy. The extinction (absorption + scattering) spectra were measured by placing the sample cuvette at the beam entrance of an integrating sphere. This setup reduces the effects of scattering of light by the nanoparticles significantly and thus the measured spectra are referred as absorption spectra,^[198] even though this is not the absorption in the physical correct sense. The particle suspensions were adjusted to contain approximately equal amounts of the polysaccharide derivatives by diluting them to 2% (v/v) and thus making it possible to compare the absorbance values between different particle samples. The absorbance spectra of the particles shown in Fig. 33a display the $\pi \rightarrow \pi^*$ transitions, which are typical for 7-alkoxy coumarins (see above). The absorbance increases with increasing DS, which is reasonable since there are more 2-[(4-methyl-2-oxo-2*H*-chromen-7-yl)oxy] acetate moieties for the same amount of polymer. The absorption maximum wavelength is the same (≈ 320 nm) for the particles from **10d**, **10f** and **10g** and is slightly blue-shifted (317 nm) for particles obtained from **10h**.

The fluorescence emission spectrum with a maximum at 399 nm of the particles obtained from **10h** is shown in Fig. 33b. The spectra of the particles obtained from the derivatives with different DS are qualitatively similar. Nevertheless, a comparison of the fluorescence intensities of different particle samples was not considered reliable, since the different particles sizes and distributions (see section 6.2) will cause different scattering characteristics. The fluorescence excitation spectra of particles prepared from **10d** and **10h** have a maximum at 320 and 317 nm, respectively. A comparison of the absorption- and fluorescence excitation spectra indicates that the setup with the integrating sphere produces precise results in the case of the smallest particles, but as the particle size increases the scattering causes minor differences between the absorption and fluorescence excitation spectra.

As pointed out, the fluorescence spectra of the different particle suspensions could not give a reliable comparison of fluorescence efficiencies of the particles with varying DS because of their different scattering properties. Therefore, the fluorescence decays

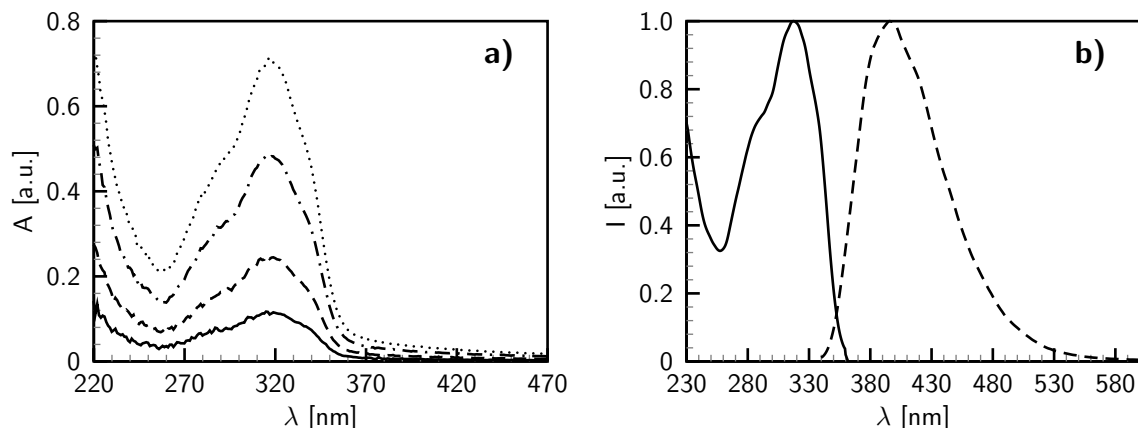


Figure 33: **a)** Absorption spectra of diluted nanoparticle suspensions (2 vol-%) obtained via dialysis from dextran 2-[(4-methyl-2-oxo-2H-chromen-7-yl)oxy] acetates **10d** (DS 0.47, solid line), **10f** (DS 0.90, dash), **10g** (DS 1.40 dot-dash), and **10h** (DS 2.01, dot); **b)** fluorescence emission- (excitation wavelength 320 nm) and excitation spectra (monitoring wavelength 400 nm) of nanoparticles from **10h**.

were measured and as can be noticed from the direct comparison of the particles prepared from **10d** and **10h** (Fig. 34a), the decay becomes faster as the DS increases. An optimal fit (minimized χ^2) of the decays according to

$$I(t) = a_0 + \sum_{i=1}^n a_i e^{-t/\tau_i} \quad (7.1)$$

requires a 3-exponential model and the average fluorescence lifetime (τ_{avg}) was calculated as:

$$\tau_{avg} = \left(\sum_{i=1}^3 a_i \tau_i \right) / \left(\sum_{i=1}^3 a_i \right) \quad (7.2)$$

As shown in Fig. 34b&c, the average fluorescence lifetime decreases moderately from 2.5 to 1.5 ns with increasing DS (0.47 to 2.01) or decreasing particle size (314 to 131 nm).

Two factors are known from literature that can cause a severe decline in the fluorescence quantum yield (or lifetime) of 7-alkoxy coumarins: aggregation in solid state and less polar environment compared to water.^[191,199–201] Since dextran is a very hydrophilic polysaccharide, possessing three hydroxyl groups per repeating unit, some relatively polar domains might be provided by the polymer backbone, especially in the particles with low DS. The modification of the hydroxyl groups with the hydrophobic chromophores decreases the polarity of the resulting derivative

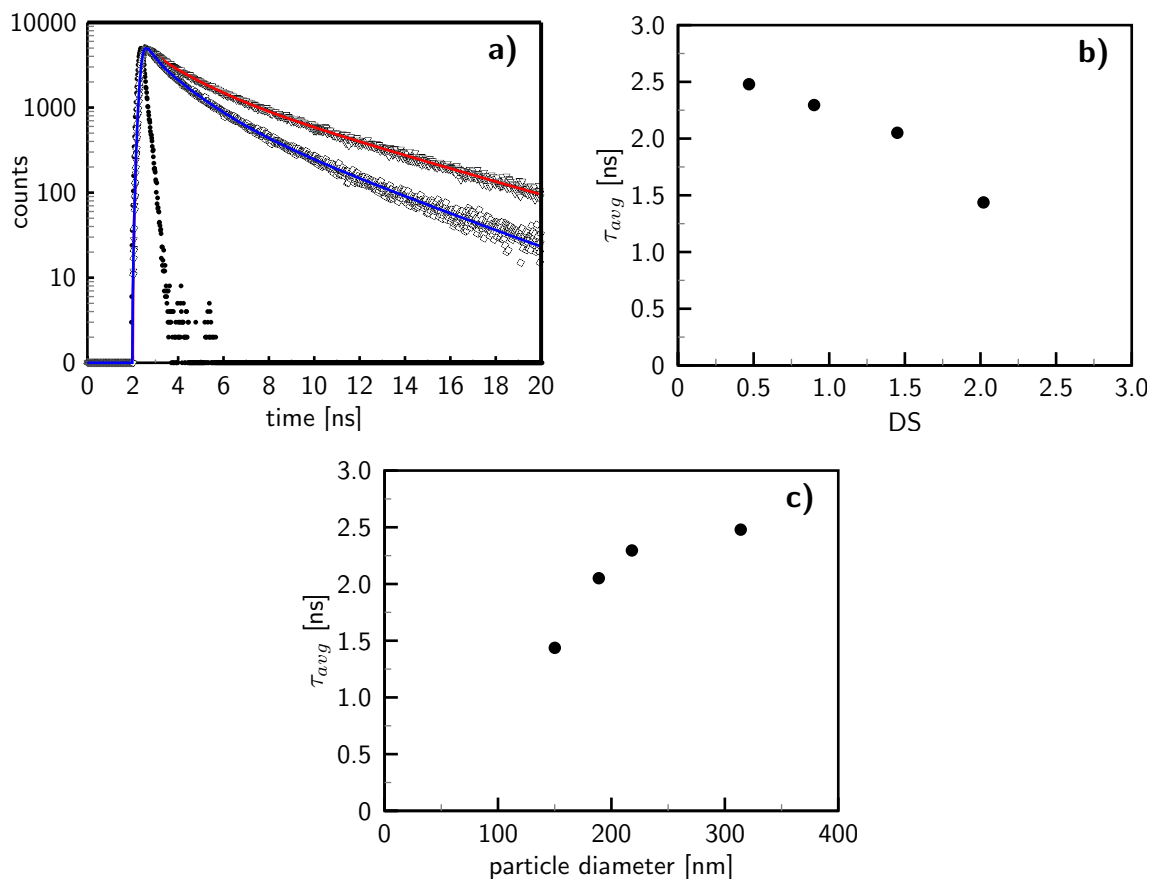


Figure 34: **a)** Fluorescence decay curves and their 3-exponential fits ($I(t) = a_0 + \sum_{i=1}^3 a_i \exp(-t/\tau_i)$) of particles obtained via dialysis from dextran 2-[(4-methyl-2-oxo-2H-chromen-7-yl)oxy] acetates **10d** (DS 0.47, triangles, red line) and **10h** (DS 2.01, squares, blue line), instrumental response shown as dotted line; **b)** average fluorescence lifetime ($\tau_{avg} = (\sum_{i=1}^3 a_i \tau_i) / (\sum_{i=1}^3 a_i)$) as function of the degree of substitution (DS) and **c)** of particle diameter.

and increases the concentration of coumarin moieties. Thus a decrease of 7-alkoxy coumarin fluorescence lifetime with increasing DS of the dextran derivative seems reasonable. However, it is important to note that a high increase of the coumarin DS, from 0.47 to 2.01 does not decrease the fluorescence lifetime excessively, which indicates that a high amount of coumarins can be incorporated in the particles without the loss of fluorescent properties. Moreover, it needs to be emphasized that the average fluorescence lifetimes determined in case of the dextran 2-[(4-methyl-2-oxo-2H-chromen-7-yl)oxy] acetate nanoparticles are in the range of the lifetime of

the low molecular weight model compound 7-methoxy-4-methyl-2*H*-chromen-2-one **20** in water ($\tau \approx 1.8$ ns).

The 3-exponential model used for the fit of the fluorescence decays is useful in obtaining the average fluorescence lifetime, but assigning three separate fluorescence lifetimes in a physically significant way is difficult. To get more information on the nature of the emitting coumarin species in the particles and more detailed information on the particle polarity and structure decay associated spectra from the particle suspensions obtained from **10h** was established by measuring the intensity decay across the whole emission spectrum. It turned out clearly that the fluorescence decays $I(\lambda, t)$ are not monoexponential. Therefore, different fits according to

$$I(\lambda, t) = \sum_i^n a_i(\lambda) e^{-t/\tau_i} \quad (7.3)$$

were tested with respect to two criteria: fit quality in terms of weighted mean square deviation (χ^2) and the meaningfulness of the fit. The values of χ^2 should be as close to one as possible and here values < 1.2 were considered acceptable. The two-exponential fit results in two components with fluorescence lifetimes of 1.4 and 4.4 ns (Fig. 35a), but this fit is of poor quality (Fig. 35d). The fit quality is improved by adding a third exponential, and a further increase in the number of exponentials did not improve the fit quality significantly. In the case of the three-exponential fit, the spectra of the components with shorter lifetimes (< 0.32 and 1.6 ns) have very similar shapes. In addition, though the polymer and particle environment is expected to alter the fluorescence lifetime of the coumarin molecules, three distinct lifetimes (or environments) are difficult to define. A more reasonable assumption is that the two shorter components obtained from the three-exponential fit are actually presenting the same fluorescent species, which has a distributed lifetime. Therefore, a stretched exponential, $e^{(-t/\tau)^\beta}$, was used to describe a lifetime distribution.^[202] In this model the stretching parameter β estimates the heterogeneity of the environment of the fluorophore. The model returns to exponential when $\beta=1$, and with decreasing values of β the lifetime distribution becomes broader. Fitting the data only with stretched exponential results in a very poor fit quality, but a combination of a stretched exponential decay for the shorter lifetime and an exponential decay for the longer lifetime according to

$$I(t) = a_1 \cdot e^{(-t/\tau_1)^\beta} + a_2 \cdot e^{-t/\tau_2} \quad (7.4)$$

yields almost the same fit quality as in case of the 3-exponential model (Fig. 35d). Attempts to include a distribution in the longer lifetime did not result in significant improvements of the fit and thus were omitted. The resulting decay associated spectra (Fig. 35c) reveal two components with lifetimes of 1.1 ns ($\beta = 0.77$) and 4.7 ns. Since the spectra of the two components have different shapes two different fluorescent species are confirmed in the particles, or in other words, the 2-((4-methyl-2-oxo-2*H*-chromen-7-yl)oxy) acetate chromophores are located in two different microenvironments.

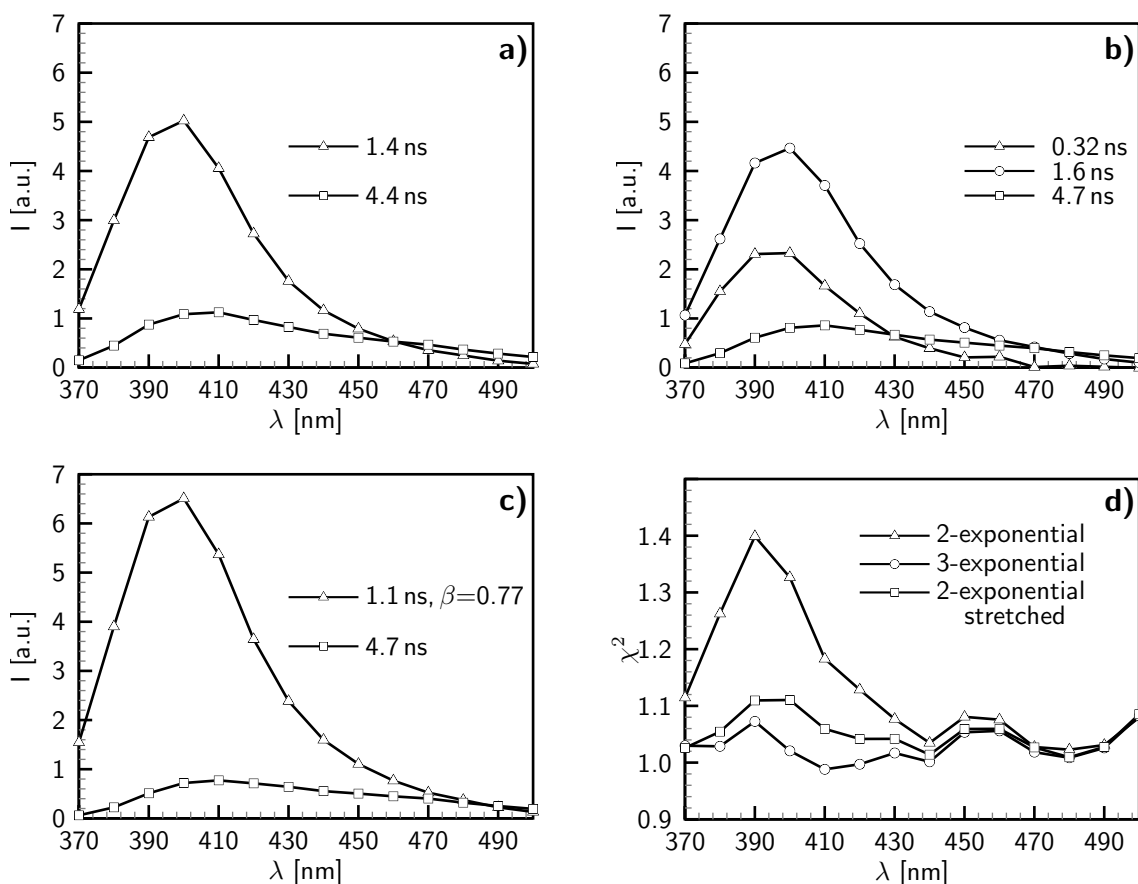


Figure 35: Decay associated fluorescence spectra of particles obtained via dialysis from dextran 2-[(4-methyl-2-oxo-2*H*-chromen-7-yl)oxy] acetate **10h** (DS 2.01): data analysis via **a)** two-exponential fit, **b)** three-exponential fit, and **c)** two-exponential fit, where the shorter component is fitted with a stretched exponential; **d)** weighted mean square deviation of the fits presented in **a)**-**c)**.

For a numerical analysis the distribution of the lifetime was calculated from the rate probability density function and its asymptotic form obtained by the saddle-point method:^[203]

$$\Phi(k) = \frac{\alpha\tau}{\sqrt{2\pi k}} \cdot (k\tau)^{[-1-\frac{\alpha}{2}]} \cdot e^{[-(k\tau)^{-\alpha}]}$$

$$\text{with } \alpha = \frac{\beta}{1-\beta} \text{ and } \tau = \frac{\tau_0}{\beta(1-\beta)^{\frac{1}{\alpha}}}$$
(7.5)

After the rate distribution is obtained, it can be converted to the lifetime distribution by taking the inverse of the rate. The lifetime distribution calculated using the values $\tau_0 = 1.1$ ns and $\beta = 0.77$ is shown in Fig. 36. The distribution of the 4.7 ns lifetime presented is calculated by approximating the distribution with a Gaussian a band with width of 0.2 ns, which is taken from the error of the fitted lifetime.

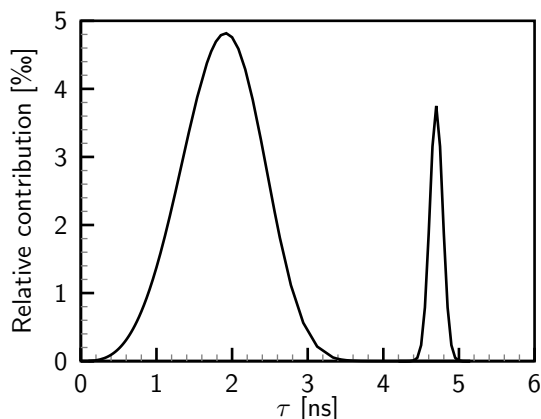


Figure 36: Fluorescence lifetime distribution of particles obtained via dialysis from dextran 2-[(4-methyl-2-oxo-2*H*-chromen-7-yl)oxy] acetate **10h** (DS 2.01) calculated on basis of two-exponential fit, where the shorter component is fitted with a stretched exponential.

The area under the curves in Fig. 35c and Fig. 36 are in good agreement and amounting the component with a lifetime of 1.1 ns to $\approx 84\%$ of the total intensity. Keeping in mind the lifetime of the low molecular weight model compound **20** to be ≈ 1.8 ns in water and ≈ 0.3 ns in DMSO it can be concluded that this fluorophores face a lower polarity compared to water, but yet a highly polar environment. Actually, with the distribution taken into account, the 1.1 ns component presents coumarins in a range of environments, varying from waterlike to relatively less polar. This indicates that water is penetrating inside the particles which are assumed to be

non-polar. The spectrum of the component with the longer lifetime (4.7 ns) is slightly red-shifted compared to that of the 1.1 ns component. As known from studies of **20** an increase in polarity of the solvent yields a red-shift of the fluorescence. Another possible reason for red-shifted fluorescence would be excimer emission, which has been reported for coumarin derivatives linked to polymers and in cellulose based host-guest systems.^[204,205] However, a broad excimer emission band would be expected to appear at wavelengths longer than 420 nm. Both the longer lifetime and the red-shift of the spectrum thus indicate that the 4.7 ns component belongs to coumarins in an environment of higher polarity compared to the ones with 1.1 ns lifetime. Unexpectedly, the lifetime of 4.7 ns exceeds the value measured for **20** in water and thus can need to be assigned to the chromophores located at the particle surface, which possesses a negative surface charge as indicated by the negative zeta (ζ) potential.

Summing up the fluorescence measurements described above it is possible to draw a tentative picture the nanoparticles prepared via dialysis from dextran 2-[(4-methyl-2-oxo-2*H*-chromen-7-yl)oxy] acetate **10h**. First it can be concluded from the decay associated spectra that the particles possess two domains with a medium (distributed)- and a very high polarity. From the comparison lifetimes of the fluorescent species located in these domains with a low molecular weight model it turned out that the chromophores at the surface face a polarity, which is higher than water. This is in accordance with the model of negative charged particle suggested by a negative ζ potential.^[47,206] The shorter lifetime possess a distribution indicating that the corresponding chromophores are located in environment of a polarity varying from relatively unpolar to waterlike. This finding suggests that water is penetrating into the particle interior. Therefore, the simple model of a hydrophilic shell and a hydrophobic core suggested by previous studies need to be reconsidered.^[47]

Beside the investigation of the particle morphology, the photocrosslinking of the 2-((4-methyl-2-oxo-2*H*-chromen-7-yl)oxy) acetate moieties in the particles was studied by fluorescence spectroscopy. Fig. 37 shows the fluorescence spectra of particles obtained via dialysis from dextran 2-[(4-methyl-2-oxo-2*H*-chromen-7-yl)oxy] acetate **10h** (DS 2.01) before (solid line) and after 300 sec of illumination at 333 nm (dashed line). The decrease of the fluorescence proves the reaction of the fluorescent coumarine moieties to the non-fluorescent dimers. Moreover a blue-shift of 13 nm of the fluorescence band is observed, which indicates that the coumarine moieties in the polar domains of the particles (proposed to be located at the surface) are preferably

cross linked. Interestingly, the particle properties, which are accessible by dynamic light scattering (size and ζ -potential) remain constant during the irradiation.

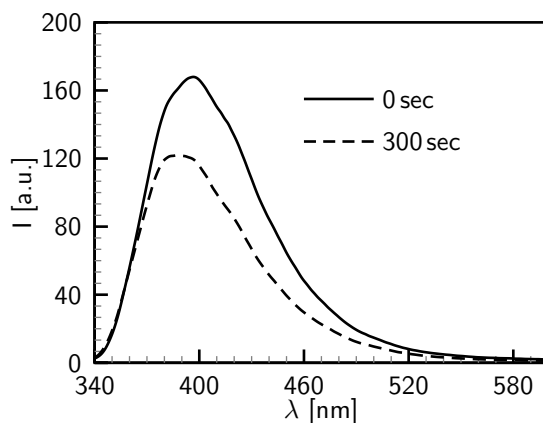


Figure 37: Fluorescence spectra ($\lambda_{ex}=320$ nm) of particles obtained via dialysis from dextran 2-[(4-methyl-2-oxo-2*H*-chromen-7-yl)oxy] acetate **10h** (DS 2.01) before (solid line) and after 300 sec of illumination at 333 nm (dashed line).

8. Summary

In this work it was illustrated how light can be applied as probe for the analytics of the structure of complex polysaccharide derivatives and how to implement photoactivity to polysaccharides by chemical modification. The photochemistry of the new derivatives was studied in the dissolved state as well as in nanoparticulate systems. Moreover, insights in the morphology of nanoparticles prepared from hydrophobic polysaccharide derivatives was gained.

As shown for aminocellulose sulfates, a novel class of zwitterionic polymers, UV-Vis spectroscopy is a valuable tool to gain the degree of substitution as an important structural parameter of novel multifunctional polysaccharide derivatives. It was demonstrated that compared to other methods, UV-Vis spectroscopy is a much faster method and lower DS values can be accurately determined if prerequisites like solubility in appropriate solvents are fulfilled. Combining UV-Vis spectroscopy with other methods including NMR- and FTIR spectroscopy not only the success of functionalization and the presence of the particular structural entities in new cellulose derivatives can be proved but also quantitative information about the constitution of the polymeric repeating units can be obtained.

In order to implement photoactivity to polysaccharides, highly engineered photoactive polysaccharide derivatives were synthesized applying modern esterification techniques. Namely cellulose, dextran and pullulan were functionalized with a fluorescent photocrosslinkable coumarin-type chromophore via the activation of the carboxylic acid with *N,N*-carbonyldiimidazole (CDI). Moreover, ionic functionalities were linked to the polymer via the introduction of sulfuric acid half esters or the esterification with a cationic carboxylic acid derivative. The reactions reported demonstrate how to obtain highly functionalized photoactive polysaccharide derivatives and how to prepare multifunctional derivatives thereof. It is important to emphasize that the reaction conditions applied for the second functionalization preserve the photochemical moieties. The structural characterization of the products obtained benefit from the experiences gained in case of the aminocellulose sulfates and thus, e.g., the influence of the polysaccharide backbone on the functionalization pattern with the specific chromophore was established.

The derivatives were applied for the preparation of nano-scaled particles. First different methods for the preparation of nanoparticles were evaluated applying conventional cellulose esters. By emulsification-evaporation very small and uniformly distributed particles can be obtained very fast and with an excellent reproducibility. However, a series of formulation parameters need to be optimized and the required ultrasonic- as well as the thermal treatment might have undesired side effects on the polymeric structure. The prerequisite for the application of the low (mechanical) energy method of solvent displacement via dropping technique or dialysis (requires also low thermal energy) is the knowledge of critical overlap concentration. Compared to emulsification-evaporation, the properties of the particles obtained by solvent displacement are less dependent on the formulation parameters but on the hydrophilic-hydrophobic balance of the particular polymer applied. As a result of the evaluation of the different methods, dialysis was chosen as simple method for the preparation of spherical nanoparticles from the photoactive polysaccharide esters. The particle properties were studied via dynamic light scattering and their dependency on the degree of substitution was established.

The $2\pi+2\pi$ cycloaddition and the corresponding cycloreversion of the coumarin moieties linked to the polysaccharide were shown in solution via UV-Vis spectroscopy. Moreover, it was demonstrated that the solution properties, namely the viscosity, can be controlled by this photodimerization although it was not possible to give a definitive explanation of the effects observed.

The environment depending fluorescence of the coumarin moieties was applied to study the properties of the nanoparticles prepared from the photoactive polysaccharide derivatives. From the results of time correlated single photon counting measurements a tentative picture of the particles was drawn. As a result the simple model of a hydrophilic shell and a hydrophobic core suggested by previous studies needs to be extended. In this regard the most important finding is penetration of water into the core of the particles that was believed to be very hydrophobic up to now.

Moreover, fluorescence measurements reveal that the photodimerization of the coumarin moieties described above takes place in the nanoparticles as well. It turned out that the coumarine moieties located at the surface of the particle are preferably cross linked.

9. Zusammenfassung

Im Rahmen der vorliegenden Arbeit wurde gezeigt wie Licht einerseits als Sonde für die Charakterisierung der Struktur komplexer Polysaccharidderivate genutzt werden kann und wie andererseits photoaktive Polysaccharidderivate durch chemische Modifizierung erhalten werden können. Die Photochemie der neuen Derivate wurde sowohl in Lösung als auch in Nanopartikeln untersucht. Darüber hinaus wurden neue Erkenntnisse über die Morphologie von Nanopartikeln gewonnen, die aus hydrophoben Polysaccharidderivaten hergestellt werden können.

Am Beispiel der Aminocellulosesulfate, einer neuen Klasse von zwitterionischen Polymeren, konnte gezeigt werden, dass sich die UV-Vis Spektroskopie hervorragend zur Bestimmung des durchschnittlichen Substitutionsgrades als wichtigen strukturellen Parameter neuer multifunktionaler Polysaccharidderivate eignet. Die UV-Vis Spektroskopie ist unter bestimmten Voraussetzungen, wie der Löslichkeit der Derivate in geeigneten Lösemitteln erheblich schneller und erlaubt die genaue Bestimmung sehr viel kleinerer DS Werte erlaubt. Die Kombination der UV-Vis Spektroskopie mit anderen Methoden wie NMR- oder FTIR Spektroskopie erlaubt es nicht nur den Erfolg einer Funktionalisierung und die Anwesenheit der entsprechenden Strukturen nachzuweisen, sondern liefert auch Informationen über die Konstitution der polymeren Wiederholungseinheiten.

Die Synthese photoaktiver Polysaccharidderivate wurde durch die Anwendung moderner Methoden zur Veresterung von Polysacchariden verwirklicht. So wurde die Funktionalisierung von Cellulose, Dextran und Pullulan mit fluoreszenten photovernetzbaaren Cumarinchromophoren über die Aktivierung der entsprechenden Carbonsäure mit N,N-Carbonyldiimidazol realisiert. Darüber hinaus wurden ionische Produkte durch die Einführung von Schwefelsäurehalbestern oder die Veresterung mit kationischen Carbonsäurederivaten synthetisiert. Die beschriebenen Reaktionen zeigen wie hochfunktionalisierte photoaktive Polysaccharidderivate und davon ausgehend multifunktionelle Polymere erhalten werden können. In diesem Zusammenhang ist die Erhaltung der Photoaktivität bei der Einführung weiterer Funktionalitäten besonderes hervorzuheben. Die Strukturcharakterisierung dieser Derivate erfolgte auf Basis der Erfahrungen, die im Fall der Aminocellulosesulfate gewonnen werden

konnten. So war es beispielsweise möglich den Einfluss des Polymerrückgrates auf die Funktionalisierung und die Substituentenverteilung zu ermitteln.

In der Folge wurde die Eignung der gewonnen hydrophoben Derivate für die Präparation von Nanopartikeln untersucht. Dazu wurden im ersten Schritt verschiedene Methoden zur Herstellung von Nanopartikeln aus konventionellen Celluloseestern erprobt. Durch die Erzeugung einer Nanoemulsion und das anschließende Abdampfen des organischen Lösemittels können sehr schnell und mit guter Reproduzierbarkeit kleine einheitliche Partikel erhalten werden. Allerdings müssen zahlreiche Parameter optimiert werden und die Notwendigkeit des Eintrags großer mechanischer Energien (Ultraschall) während der Präparation der Nanoemulsion bzw. die thermische Belastung während des Entfernens des Lösungsmittels können zu unerwünschten Effekten führen. Diese Nachteile können durch die alternative Möglichkeit des Lösemittelaustausches (Eintropfen oder Dialyse) zur Herstellung von Nanopartikeln weitgehend vermieden werden. Allerdings erfordert die Anwendung dieser Methoden genaue Kenntnisse über die Polymereigenschaften insbesondere muss die kritische Überlappungskonzentration bekannt sein. Darüber hinaus hat die Balance zwischen Hydrophobie und Hydrophilie des jeweiligen Derivats einen großen Einfluss auf die Eigenschaften der Nanopartikel, die durch Lösemittelaustausch erhalten wurden. Für die Präparation von Nanopartikeln aus den photoaktiven Polysaccharidderivaten wurde aufgrund ihrer Einfachheit die Dialyse als Methode ausgewählt. Die Eigenschaften der erhaltenen Partikel und deren Abhängigkeit vom Ausgangspolymer wurden mit Hilfe von dynamischer Lichtstreuung und Rasterelektronenmikroskopie untersucht.

Die photochemische $2\pi+2\pi$ Cycloaddition und die entsprechende Cycloreversion der polysaccharidgebundenen Cumarineinheiten wurde in Lösung mit Hilfe der UV-Vis Spektroskopie untersucht. Darüber hinaus wurde gezeigt wie die Viskosität der Lösung über die Photodimerisierung gesteuert werden kann. Eine abschließende Erklärung für alle beobachteten Effekte liegt allerdings noch nicht vor.

Die Umgebungsabhängigkeit der Fluoreszenz der polysaccharidgebundenen Cumarineinheiten wurde genutzt um die Eigenschaften der entsprechenden Nanopartikel zu untersuchen. Die Resultate der Fluoreszenzlebensdauer messungen liefern neue Informationen über die Morphologie der Nanopartikel und unterstreichen die Notwendigkeit das einfache Modell von einem hydrophoben Kern und einer hydrophilen Hülle zu erweitern. Der wichtigste Befund in diesem Zusammenhang ist

der Nachweis, dass Wasser auch in den bisher als sehr hydrophob beschriebenen Kern eindringt.

Ebenfalls mit Hilfe von Fluoreszenzmessungen konnte gezeigt werden, dass die oben beschriebene Photodimerisierung der Cumarineinheiten auch in den Nanopartikeln stattfindet. Dabei wurde festgestellt, dass vorwiegend die Cumarineinheiten vernetzt wurden, die an der Oberfläche der Partikel lokalisiert sind.

Part III.

Experimental Part

Materials

Microcrystalline cellulose Avicel[®] PH 101 **1** was purchased from Fluka (Neu-Ulm, Germany). Determination of the intrinsic viscosity according to ISO 5351 and size-exclusion chromatography of a carbanilated sample according to Terbojevich et al.^[207] yield a degree of polymerization DP_w (ISO) of 264, DP_n (SEC) of 78 and DP_w (SEC) of 281. Dextran (Fluka) **6** produced by *Leuconostoc mesenteroides* strain no. NRRL B-512(F) possesses a \overline{M}_w of 54,400 g/mol and a \overline{M}_n of 34,960 g/mol. Pullulan (Sigma) **7** produced by *Aureobasidium pullulans* possesses a \overline{M}_w of 137000 g/mol and a \overline{M}_n of 71600 g/mol. Cellulose and LiCl (Merck, Darmstadt, Germany) were dried for 6 h at 105 °C in vacuum over potassium hydroxide prior use. Methyl-6-O-tosyl- α -D-glucopyranoside was purchased from Wako Chemical, Ltd. Other chemicals were purchased from Sigma Aldrich (Deisenhofen, Germany) and were used without further treatment. Deuterated solvents for NMR spectroscopy were purchased from Euriso-Top (Saint Aubin Cedex, France)

Measurements

NMR spectra were acquired on a Bruker Avance 250 MHz, Avance 400 MHz, and Avance 600 MHz spectrometer with 16 scans for ¹H-NMR (room temperature) and up to 200,000 scans for ¹³C-NMR (70 °C) applying 25 mg sample per mL for ¹H-NMR and 100 mg sample per mL for ¹³C NMR studies.

FTIR spectra were recorded on a Nicolet AVATAR 370 DTGS spectrometer with the KBr technique.

Elemental analyses were performed by CHNS 932 Analyzer (Leco, Germany) or an Vario ELIII (Elementaranalysensysteme, Hanau, Germany) and the halogen content was determined by the procedure of Schöniger^[208].

For UV-Vis spectroscopic determination of the DS a PerkinElmer λ 10 UV-Vis Spectrometer and quartz glass cuvettes were used. The UV-Vis spectroscopic investigations of the photoreaction were carried out on Varian-Cary 5000 spectrometer

coupled with HBO 200 mercury, which was equipped with a high intensity concave grating monochromator (Zeiss) to get monochromatic light. Other irradiation experiments were carried out using a HBO 200 mercury lamp with a metal interference filter (Zeiss 333 nm) for UV light with wavelength 350–310 nm. Extinction spectra of the aqueous particle suspensions were measured using a Perkin-Elmer λ 900 spectrophotometer equipped with an integrating sphere (PELA-1000).

The relative viscosities were determined with an automatic Lauda PVS 1/2 viscometer equipped with a dilution Ubbelohde viscometer (capillary No. 1c, Schott Instruments, Mainz, Germany) in a temperature-controlled water bath (Lauda E 200, Lauda-Königshofen, Germany) at 20 °C.

The diameter and polydispersity of the nanoparticles were determined by dynamic light scattering using a Zetasizer Nano ZS (Malvern Instrument, Malvern, UK). The suspensions were diluted with deionized, filtered water to a concentration of about 0.005%. The mean particle size was approximated as the effective (*z*-average) diameter and the width of the distribution as the polydispersity index (PDI) obtained by the cumulants method assuming spherical shape.

For scanning electron microscopy (SEM) studies, one droplet nanoparticle suspension on a mica surface was lyophilized and covered with gold or platinum. The images were obtained with the SEM equipment LEO-1 450 VP (LEO, Oberkochen, Germany) operating at 15 kV or 8 kV.

Fluorescence spectra of the aqueous nanoparticle suspensions were measured using a Perkin-Elmer LS50B spectrofluorometer. A time-correlated single photon counting (TCSPC) system consisting of a PicoHarp 300 controller and a PDL 800-B driver was used for the time resolved fluorescence measurements. The excitation wavelength was 340 nm from a pulsed diode laser head PLS-8-2-295. The fluorescence signal was detected with a micro channel plate photomultiplier (Hamamatsu R2809U). The time resolution of the instrument was approximately 320 ps (full width, half maximum). The fluorescence decays were fitted to a multiexponential model. The average fluorescence lifetime was calculated as $\tau_{avg} = (\sum a_i \tau_i) / (\sum a_i)$. The decay associated spectra were obtained by measuring the decay curve at each monitoring wavelength with a constant data accumulation time and fitting the decays globally. The amplitudes were corrected by taking into account the wavelength sensitivity of the photomultiplier tube. The amplitudes at <390 nm may appear lower compared to the actual values, because an optical filter with a sharp change in transmittance at 380 nm was used for excluding the excitation light from the detector.

Synthesis

Tosyl cellulose 2a-c and tosyl cellulose sulfates 3a-c

Tosyl cellulose (**2**) were prepared under homogeneous reaction conditions according to Rahn et al.^[151]. Briefly, cellulose (**1**) was allowed to react with p-toluenesulfonyl chloride and triethylamine as a base within 24 h at 8 °C in *N,N*-dimethylacetamide (DMA)/LiCl, (4.3% cellulose content). Tosyl cellulose sulfates (TCS, **3**) were prepared under homogeneous reaction conditions as well. For this purpose **2** was allowed to react with sulfur trioxide pyridine complex in DMA as solvent.^[152]

6-deoxy-6-(4-aminoethyl)amino cellulose-2,3(6)-O-sulfate 4a-c, typical example:

TCS **3a** (15 g, 43.75 mmol) was dissolved in 105 mL H₂O to give a clear pale yellow solution. The solution was refluxed under inert conditions and 1,2-diaminoethane (DAE, 60 mL, 893 mmol) was added dropwise within 25 min. After 6 h the reaction mixture became a clear pale brown solution. The product was precipitated after cooling to room temperature into 1.5 L acetone and washed 4 times in acetone (each 300 mL). Subsequently, the final product **4a** was dried at 50 °C under vacuum. Yield: 12 g, 90.6%; **EA** [%]: C 26.39, H 4.05, N 3.79, S 12.92; DS_{AEA} 0.41, DS_{Tos} 0, DS_{Sulf} 1.25; **FTIR** (KBr) $\tilde{\nu}$ [cm⁻¹]: 3440 ν (-OH), 3240 ν (NH₂), 2947 ν (CH₂), 1468 ν (NH₂), 1237 ν (SO₂, sulfate), 1142- 1109 ν (C-N primary and secondary), 800 ν (S-O, sulfate). **¹³C-NMR** (D₂O) [ppm]: δ = 100.82 (C1), 83.37–72.50 (C2-C5), 66.59 (C6-OSO₃), 48.73 (C6-N), 45.48 and 38.35 (C7, C8).

6-deoxy-6-(2-(bis-N',N'-(2-aminoethyl)aminoethyl)) amino cellulose-2,3(6)-O-sulfate 5a-c, typical example:

To a solution of TCS **3a** (15 g, 43.75 mmol) in 105 mL H₂O 148 mL tris-(2-aminoethyl) amine (TAEA, 989 mmol) were added dropwise. The reaction mixture was kept at 100 °C for 6 h under a nitrogen atmosphere. After cooling to room temperature, the product was precipitated in acetone (1.5 L) and washed 4 times with acetone (each 300 mL). After filtration, the final product **5a** was dried at 50 °C under vacuum. Yield: 11.8 g, 86%; **EA** [%]: C 27.99, H 4.28, N 5.75, S 11.46, DS_{BAEA} 0.32, DS_{Tos} 0, DS_{Sulf} 1.21; **FTIR** (KBr) $\tilde{\nu}$ [cm⁻¹]: 3481 ν (-OH), 3148 ν (NH₂), 2960 ν (CH₂), 1490 ν (NH₂), 1253 ν (SO₂, sulfate), 1141-1066 ν (C-N primary, secondary and tertiary),

800 $\nu(\text{S-O, sulfate})$, $^{13}\text{C-NMR}$ (D_2O) [ppm]: $\delta = 100.40$ (C1), 81.73-72.40 (C2-C5), 66.45 (C6-OSO₃), 53.75- 48.92 (C8, C9), 45.46 (C6-N), 38.88-37.32 (C7, C10), 21.14 (C11').

2-[(4-Methyl-2-oxo-2*H*-chromen-7-yl)oxy]acetic acid methyl ester

To a solution of 2 g (11.4 mmol) 4-methylumbelliferone in 50 mL of acetone 1.74 g (11.4 mmol) methyl bromoacetate and 1.6 g (11.6 mmol) anhydrous potassium carbonate were added. The mixture was heated and kept at reflux for five hours. Subsequently, the solids were removed by filtration and the solvent was removed under reduced pressure. The pale yellow product was purified by recrystallization from ca. 100 mL absolute ethanol and dried at 40 °C under vacuum yielding a white solid. Yield: 2.54 g (10.23 mmol), 90%; **m.p.**: 158-160 °C; **EA** [%]: calculated/found C: 62.90/62.91 H: 4.83/4.81; **FTIR** (KBr) $\tilde{\nu}$ [cm^{-1}]: $\nu(\text{CH}_{\text{arom.}})$ 3091, 3071 (w), $\nu(\text{CH}_{\text{double bond}})$ 3021 (w), $\nu(\text{CH}_{\text{alkyl}})$ 2987, 2962, 2927 (w), $\nu(\text{C=O}_{\text{ester}})$ 1765 (s), $\nu(\text{C=O}_{\text{lactone}})$ 1726 (s), $\nu(\text{C=O}_{\text{ester}})$ 1765 (s), $\nu(\text{C=C}_{\text{konj.}})$ 1617 (s), $\nu(\text{C-O-C}_{\text{ester}})$ 1153 (s), $\delta(\text{CH}_{\text{arom.}})$ 858, 853, 804 (m); $^1\text{H-NMR}$ (250 MHz CDCl_3) [ppm]: $\delta = 7.52$ (1H, d, $J^3=8.8$ Hz, $\text{H}_{\text{CH-arom}}$), 6.90 (1H, dd, $J^3=8.8$ Hz, $J^4=2.6$ Hz, $\text{H}_{\text{CH-arom}}$), 6.77 (1H, d, $J^4=2.6$ Hz, $\text{H}_{\text{CH-arom}}$), 6.15 (1H, d, $J^4=1.2$ Hz, $\text{H}_{\text{CH-double bond}}$), 4.68 (2H, s, H_{CH_2}), 3.82 (3H, s, $\text{H}_{\text{CH}_3\text{-ester}}$), 2.39 (3H, d, $J^4=1.2$ Hz H_{CH_3}); $^{13}\text{C-NMR}$ (63 MHz CDCl_3) [ppm]: $\delta = 168.41$ ($\text{C=O}_{\text{ester}}$), 160.97 ($\text{C=O}_{\text{lactone}}$), 160.54 (quart. $\text{C-O}_{\text{ether}}$), 155.04 (quart. $\text{C-O}_{\text{lactone}}$), 152.35 ((quart. C-C_{CH_3}), 125.8 (C_{arom}), 114.44 (quart. C_{arom}), 112.51/112.47 ($\text{C}_{\text{double bond}}/\text{C}_{\text{arom}}$), 101.7 (C_{arom}), 65.21 (C_{CH_2}), 52.46 ($\text{C}_{\text{CH}_3\text{-ester}}$), 18.64 (C_{CH_3})

2-[(4-Methyl-2-oxo-2*H*-chromen-7-yl)oxy]acetic acid (8)

To a suspension of 1.5 g (6 mmol) 2-[(4-methyl-2-oxo-2*H*-chromen-7-yl)oxy]acetic acid methyl ester in 30 mL ethanol 2.5 mL sodium hydroxide solution was added (10% w/w). The mixture was heated and kept at reflux for two hours. Subsequently, the solvent was removed under reduced pressure and the residue was dissolved in 100 mL water. The crude product was isolated by adding aqueous HCl (2 M) until no precipitation occurs. After recrystallization from ca. 100 mL absolute ethanol a white solid was obtained. Yield: 1.38 g (5.9 mmol), 98.5%; **m.p.**: 208 °C; **EA** [%]: calculated/found C: 61.54/61.45 H: 4.27/4.23; **FTIR** (KBr) $\tilde{\nu}$ [cm^{-1}]: $\nu(\text{O-H}_{\text{acid}})$ 3200-2500 (vs), $\nu(\text{CH}_{\text{arom.}})$ 3090, 3070 (w), $\nu(\text{CH}_{\text{double bond}})$ 3023 (w), $\nu(\text{CH}_{\text{alkyl}})$ 2985, 2960, 2923 (w), $\nu(\text{C=O}_{\text{acid}})$ 1735 (s), $\nu(\text{C=O}_{\text{lactone}})$ 1722 (s), $\nu(\text{C=O}_{\text{ester}})$ 1765 (s),

$\nu(\text{C}=\text{C}_{\text{konj.}})$ 1608 (s), $\delta(\text{CH}_{\text{arom.}})$ 853, 850, 802 (m); **$^1\text{H-NMR}$** (250 MHz DMSO-d6) [ppm]: $\delta = 7.69$ (1H, d, $J^3=8.5$ Hz, $\text{H}_{\text{CH-arom}}$), 6.97 (2H, m, $J^4=2.6$ Hz, $\text{H}_{\text{CH-arom}}$), 6.22 (1H, d, $J^4=1.2$ Hz, $\text{H}_{\text{CH-double bond}}$), 4.82 (2H, s, H_{CH_2}), 2.39 (3H, d, $J^4=1.2$ Hz H_{CH_3}); **$^{13}\text{C-NMR}$** (63 MHz DMSO-d6) [ppm]: $\delta = 169.67$ ($\text{C}=\text{O}_{\text{acid}}$), 160.79 ($\text{C}=\text{O}_{\text{lactone}}$), 160.12 (quart. $\text{C}-\text{O}_{\text{ether}}$), 154.55 (quart. $\text{C}-\text{O}_{\text{lactone}}$), 153.37 (quart. $\text{C}_{\text{C-CH}_3}$), 126.50 (C_{arom}), 113.55 (quart. C_{arom}), 112.29/111.40 ($\text{C}_{\text{double bond}}/\text{C}_{\text{arom}}$), 101.51 (C_{arom}), 64.85 (C_{CH_2}), 18.13 (C_{CH_3})

2-[(4-Methyl-2-oxo-2H-chromen-7-yl)oxy] acetates of cellulose (9), typical example

Dry cellulose (**1**, 3 g 18,5 mmol) was suspended in 90 mL of dry *N,N*-dimethylacetamide (DMA) and stirred at 130 °C for 1 h. After the slurry had been allowed to cool to 100 °C, 5.4 g LiCl were added. By cooling to room temperature under stirring, the cellulose dissolves completely. In a separate flask 2,16 g 2-[(4-methyl-2-oxo-2H-chromen-7-yl)oxy] acetic acid (**8**, 9.25 mmol) and 1.5 g (9.25 mmol) *N,N*-carbonyldiimidazole (CDI) were dissolved in 25 mL DMA and kept at 70 °C until no gas evolution occurs. Subsequently this solution was added to the cellulose solution and the resulting mixture was allowed to react at 70 °C for 20 h under stirring. The product was precipitated in 500 mL water, washed four times with 300 mL water and once with 300 mL ethanol. After drying at 40 °C under vacuum, 4.21 g of a white solid were obtained. **FTIR** (KBr): $\tilde{\nu} [\text{cm}^{-1}] = 3600\text{-}2900$ (s, OH), 1721 (vs, C=O), 1615 (vs, C=O), 1100 (vs, C-O); **$^1\text{H-NMR}$** (250 MHz, DMSO-d6): δ [ppm] = 7.39, 6.76 (CH arom), 6.00 (CH lacton), 4.79 (CH_2 linkage), 2.16 (CH_3); 5.6-3.5 (CH AGU and OH)

2-[(4-Methyl-2-oxo-2H-chromen-7-yl)oxy] acetates of dextran (10) and pullulan (11), general procedure

To a solution of 0.5 g (3 mmol) dextran (**6**) or pullulan (**7**) in 15 mL dry DMSO 0.84 g (3 mmol) 2-[(4-methyl-2-oxo-2H-chromen-7-yl)oxy] acetic acid (**8**) and 0.5 g (3 mmol) CDI was added. The mixture heated was kept at 80 °C for 20 h under stirring. Subsequently, the product precipitated in 200 mL ethanol and washed four times with 150 mL ethanol. After drying at 40 °C under vacuum a white solid was obtained. Analytical values for typical sample **10c**: IR (KBr): 3600-2900 (s, OH), 1721 (vs, C=O), 1615 (vs, C=O), 1100 (vs, C-O); **$^1\text{H-NMR}$** (250 MHz, DMSO-d6): δ

= 7.39, 6.76 (CH arom), 6.00 (CH lactone), 4.79 (CH₂ linkage), 2.16 (CH₃); 5.6-3.5 (CH AGU and OH).

Perpropionylation, general procedure

To determine the DS of the polysaccharide esters by means of ¹H-NMR spectroscopy, perpropionylation was carried out. For this purpose 300 mg sample were allowed to react in 5 mL pyridine with 5 mL propionic anhydride in the presence of a catalytic amount of 4-(*N,N*-dimethylamino) pyridine at 80 °C for 20 h under stirring. The product was isolated by precipitation in 100 mL ethanol and purified by washing three times with 100 mL ethanol. The resulting solid was dried at 40 °C under vacuum. IR (KBr): no ν (OH).

Sulfation of 2-[(4-methyl-2-oxo-2*H*-chromen-7-yl)oxy] acetates of dextran (12) and pullulan (13), general procedure

The polysaccharide esters **10** and **11** were dissolved in *N,N*-dimethylformamide (0.05 g/ml). After adding 2-methyl-2-butene as a proton scavenger and SO₃/DMF complex, the solution was allowed to react for two hours at 30 °C under stirring. The reaction mixture was neutralized with a saturated aqueous NaHCO₃ solution and subsequently precipitated in ethanol. The product was purified via dialysis against water through a cellulose membrane (Spectra/Por[®]; MWCO = 3500 g/mol) and isolated by lyophilization.

Mixed [(4-methyl-2-oxo-2*H*-chromen-7-yl)oxy] acetic acid-(3-carboxypropyl)trimethylammonium chloride esters of cellulose (15), typical example

The polysaccharide ester **9** (2 g) was dissolved in DMA/LiCl as described for cellulose. In a separate flask 0.91 g (5 mmol) (3-carboxypropyl)trimethylammonium chloride (**14**) and 0,81 g (5 mmol) CDI were dissolved in 30 mL DMSO and kept at 70 °C until no gas evolution occurs. Subsequently this solution was added to the solution of **9** in DMA/LiCl and the resulting mixture was stirred at 70 °C for 20 h. The product was precipitated in 400 mL acetone, washed three times with 250 mL acetone and two times with 250 mL ethanol. For further purification, a dialysis against water through a cellulose membrane (Spectra/Por[®]; MWCO = 3500 g/mol) was carried out. Lyophilization yields 2.62 g of a white solid. ¹H NMR (400 MHz, D₂O):

δ [ppm] = 8.22–7.30 (CH arom), 6.73 (CH lactone), 3.83, 3.07, 2.60 (CH₂ 4), 3.61 (CH₃–N); ¹³C NMR (400 MHz, D₂O): δ [ppm] = 174.49, 173.35 (C=O), 127.10, 113.55, 111.78 (C arom), 66.16, 30.73, 18.54 (CH₂ 3CPTMA), 53.75 (CH₃–N), 102.93 (AGU-C1), 100.93 (AGU-C1'), 79.29–60.89 (AGU-C2–C6)

Nanoparticle preparation methods

Emulsification-evaporation

In a typical example, to a solution of 25 mg cellulose ester in 1 mL dichloromethane (CH₂Cl₂) 2 mL of an aqueous solution of polyvinyl alcohol (PVA) (3% w/v, M_w = 13000–23000 g/mol) were added. Emulsification was carried out with a Digital Sonifier[®] 250, (Branson Ultrasonics Corporation, Danbury, Connecticut, USA) equipped with a 102-C Converter unit, a 1/2" tapped disruptor horn, and a 1/8" tapered microtip. Depending on the specific sample time of sonification and quantity of energy was varied. The resulting emulsion was diluted with 10 mL of an aqueous solution of PVA (0.3% w/v). The nanoparticle suspension was obtained by stirring the samples at 30 °C until CH₂Cl₂ was completely removed (proved by head space GC). To remove an excess of PVA the particles were separated by centrifugation at 8000 rpm and redispersed in water. This procedure was repeated 4 times.

Solvent-displacement

Dialysis

As a typical example, a solution of 20 mg of the cellulose ester in 5 mL *N,N*-dimethylacetamide was placed in a dialysis tube (Spectra/Por 3, molecular weight cutoff: 3500 g/mol) of about 10 cm length. The filled tube was placed in 500 mL water and water was renewed five times after at least 3 h.

Dropping Technique

As a typical example, 20 mg of the cellulose ester was dissolved in 5 mL acetone. Subsequently, 15 mL of distilled water were added dropwise to the polymer solution. The resulting nanoparticle suspensions were stirred at 60 °C until acetone was completely removed from the aqueous suspension.

Part IV.

Back matter

Bibliography

- [1] P. G. Bahn, The making of a mummy, *Nature* 356 (1992) 109.
- [2] H. Gernsheim, The 150th anniversary of photography, *History of Photography* 1 (1977) 3–8.
- [3] L. M. Minsk, J. . G. Smithw, . P. V. Deusen, J. F. Wright, Photosensitive polymers. i. cinnamate esters of poly(vinyl alcohol) and cellulose, *Journal of Applied Polymer Science* 2 (1959) 302–307.
- [4] H. Böttcher, J. Bendig, M. A. Fox, G. Hopf, H.-J. Timpe, *Technical Applications of Photochemistry*, Deutscher Verlag für Grundstoffindustrie, Leipzig, 1991.
- [5] W. Schnabel, *Polymers and Light*, Wiley-VCH, Weinheim, 2007.
- [6] J. Bendig, H.-J. Timpe, Photostructuring, in: H. Böttcher (Ed.), *Technical applications of photochemistry*, Deutscher Verlag für Grundstoffindustrie, Leipzig, 1991, pp. 172–252.
- [7] B. L. Feringa, *Molecular Switches*, Wiley-VCH, Weinheim Germany, 2001.
- [8] H. Böttcher, Optical information recording, in:^[4], pp. 118–171.
- [9] A. Natansohn, P. Rochon, Azobenzene-containing polymers: Digital and holographic storage, *Photonic And Optoelectronic Polymers* 672 (1997) 236–250.
- [10] Schnabel, Polymers in optical memories, in:^[5], pp. 337–358. (chapter 12).
- [11] Schnabel, *Polymers and Light*, in:^[5], pp. 207–230. (chapter 8).
- [12] I. Willner, S. Rubin, Control of the structure and functions of biomaterials by light, *Angewandte Chemie, International Edition* 35 (1996) 367 –385.
- [13] C. J. Barrett, J. ichi Mamiya, K. G. Yagerc, T. Ikeda, Photo-mechanical effects in azobenzene-containing soft materials, *Soft Matter* 3 (2007) 1249–1261.

-
- [14] M. Behl, A. Lendlein, Actively moving polymers, *Soft Matter* 3 (2007) 58–67.
- [15] N. K. Viswanathan, D. Y. Kim, S. Bian, J. Williams, W. Liu, L. Li, L. Samuelson, J. Kumar, S. K. Tripathy, Surface relief structures on azo polymer films, *Journal of Materials Chemistry* 9 (1999) 1941–1955.
- [16] O. Pieroni, A. Fissi, G. Opova, Photochromic polypeptides, *Progress in Polymer Science* 23 (1998) 81–121.
- [17] O. Pieroni, F. Ciardelli, Photoresponsive polymeric materials, *Trends in Polymer Science* 3 (1995) 282–287.
- [18] T. Heinze, Chemical functionalization of cellulose, in: S. Dumitriu (Ed.), *Polysaccharides: Structural Diversity and functional versatility*, Marcel Dekker, New York, Basel, Hong Kong, 2004, 2nd edition, 2004, pp. 551–590.
- [19] N. Vekshin, *Photonics of Biopolymers*, Springer Verlag, Berlin-Heidelberg, 2002.
- [20] S. R. Martin, M. J. Schilstra, Circular dichroism and its application to the study of biomolecules, *Biophysical Tools For Biologists: Vol 1 In Vitro Techniques* 84 (2008) 263–293.
- [21] T. Heinze, T. Liebert, A. Koschella, *Esterification of Polysaccharides*, Springer Verlag, Heidelberg, 2006.
- [22] P. L. Bragd, H. van Bekkum, A. C. Besemer, Tempo-mediated oxidation of polysaccharides: survey of methods and applications, *Topics in Catalysis* 27 (2004) 49–66.
- [23] T. Heinze., New ionic polymers by cellulose functionalization, *Macromolecular Chemistry and Physics* 199 (1998) 2341–2364.
- [24] B. Philipp, D. Klemm, T. Heinze, U. Heinze, W. Wagenknecht, *Comprehensive Cellulose Chemistry*, volume 1 and 2, WILEY-VCH, Weinheim, 1998.
- [25] T. Heinze, T. Liebert, B. Heublein, S. Hornig, Functional polymers based on dextran, *Advances in Polymer Science* 205 (2006) 199–291.
- [26] D. Klemm, B. Heublein, H.-P. Fink, A. Bohn, Cellulose: Fascinating biopolymer and sustainable raw material, *Angewandte Chemie, International Edition* 44 (2005) 3358–3393.

- [27] D. Klemm, H.-P. Schmauder, T. Heinze, Cellulose, in: S. DeBaets, A. Steinbüchel, E. J. Vandamme (Eds.), *Biopolymers-Polysaccharides II*, Wiley, Weinheim, 2002, pp. 275–320.
- [28] M. Nakata, T. Kawaguchi, Y. Kodama, A. Konno, Characterization of curdlan in aqueous sodium hydroxide, *Polymer* 39 (1998) 1475–1481.
- [29] I. Giavasis, L. M. Harvey, B. McNeil, Scleroglucan, in: S. DeBaets, A. Steinbüchel, E. J. Vandamme (Eds.), *Biopolymers-Polysaccharides II*, Wiley, Weinheim, 2002, pp. 37–60.
- [30] U. Rau, Schizophyllan, in: S. DeBaets, A. Steinbüchel, E. J. Vandamme (Eds.), *Biopolymers-Polysaccharides II*, volume 6, Wiley, Weinheim, 2002, pp. 61–92.
- [31] K. I. Shingel, Current knowledge on biosynthesis, biological activity, and chemical modification of the exopolysaccharide, pullulan, *Carbohydrate Research* 339 (2004) 447–460.
- [32] T. D. Leathers, Dextran, in: S. DeBaets, A. Steinbüchel, E. J. Vandamme (Eds.), *Biopolymers-Polysaccharides I*, Wiley, Weinheim, 2002, pp. 299–346.
- [33] R. F. Tester, J. Karkals, Starch, in: S. DeBaets, A. Steinbüchel, E. J. Vandamme (Eds.), *Biopolymers-Polysaccharides II*, volume 6, Wiley, Weinheim, 2002, pp. 381–438.
- [34] R. L. Shogrun, Starch: Properties and material applications, in: D. L. Kaplan (Ed.), *Biopolymers from Renewable Resources*, Springer, Berlin, 1998, pp. 30–46.
- [35] A. Ebringerová, T. Heinze, Xylan and xylan derivatives - biopolymers with valuable properties 1. naturally occurring xylans: structures, isolation, procedure and properties, *Macromolecular Rapid Communications* 21 (2000) 542–556.
- [36] H. Maier, M. Anderson, C. Karl, K. Magnuson, R. L. Whistler, Guar, locust bean, tara, and fenugreek gums, in: J. N. BeMiller, R. L. Whistler (Eds.), *Industrial Gums: Polysaccharides and Their Derivatives*, Academic Pr Inc, 1993, pp. 181–205.

-
- [37] A. Franck, L. DeLeenheer, Inulin, in: S. DeBaets, A. Steinbüchel, E. J. Vandamme (Eds.), *Biopolymers-Polysaccharides II*, Wiley, Weinheim, 2002, pp. 439–480.
- [38] T. Uragami, S. Tokura, *Material Science of Chitin and Chitosan*, Springer, Berlin, 2006.
- [39] D. F. Day, Alginates, in: D. L. Kaplan (Ed.), *Biopolymers from Renewable Resources*, Springer, Berlin, 1998, pp. 119–143.
- [40] A. C. O’Sullivan, Cellulose-the structure slowly unravels, *Cellulose* 4 (1997) 173–207.
- [41] Y.-Z. Lai, Reactivity and accessibility of cellulose, hemicelluloses, and lignins, in: D. N.-S. Hon (Ed.), *Chemical Modification of Lignocellulosic Materials*, Marcel Dekker, New York, 1996, pp. 35–96.
- [42] T. Heinze, T. Liebert, Unconventional methods in cellulose functionalization, *Progress in Polymer Science* 26 (2001) 1689–1762.
- [43] R. P. Swatloski, R. D. Rogers, J. D. Holbrey, Dissolution and processing of cellulose using ionic liquids wo 03/029329 a3, patent, 2003.
- [44] T. Liebert, T. Heinze, Interactions of ionic liquids with polysaccharides: 5. solvents and reaction media for the modification of cellulose, *BioResources* 3 (2008) 576–601.
- [45] A. N. DeBelder, Medical applications of dextran and its derivatives, in: S. Dumitriu (Ed.), *Polysaccharides in medicinal applications*, Marcel Dekker, New York, 1996, pp. 505–524.
- [46] S. Hornig, T. Liebert, T. Heinze, Structure design of multifunctional furoate and pyroglutamate esters of dextran by polymer-analogous reactions, *Macromolecular Bioscience* 7 (2007) 297–306.
- [47] S. Hornig, T. Heinze, Nanoscale structures of dextran esters, *Carbohydrate Polymers* 68 (2007) 280–286.
- [48] I. Spiridon, V. I. Popa, *Polysaccharides structural diversity and functional versatility*, Marcel Dekker, 2005, p. 459.

- [49] K. C. Cheng, A. Demirci, J. M. Catchmark, Pullulan: biosynthesis, production, and applications, *Applied Microbiology and Biotechnology* 92 (2011) 29–44.
- [50] A. Bos, Uv spectra of cellulose and some model compounds, *Journal of Applied Polymer Science* 16 (1972) 2567–2576.
- [51] A. Beelik, J. K. Hamilton, Ultraviolet irradiation of model compounds related to cellulose, *Journal of Organic Chemistry* 26 (1961) 5074–5080.
- [52] R. H. Atalla, S. C. Nagel, Laser-induced fluorescence in cellulose, *Chemical Communications* 19 (1972) 1049–1050.
- [53] T. Rosenau, A. Potthast, W. Milacher, A. Hofinger, P. Kosma, Isolation and identification of residual chromophores in cellulosic materials, *Polymer* 45 (2004) 6437–6443.
- [54] T. Rosenau, A. Potthast, P. Kosma, H. U. Suess, N. Nimmerfroh, Isolation and identification of residual chromophores from aged bleached pulp samples, *Holzforschung* 61 (2007) 656–661.
- [55] T. Popoff, O. Theander, Formation of aromatic-compounds from carbohydrates .4. chromophores from reaction of hexuronic acids in slightly acidic, aqueous-solution, *Acta Chemica Scandinavica*, B 30 (1976) 705–710.
- [56] T. Popoff, O. Theander, Formation of aromatic-compounds from carbohydrates .3. reaction of d-glucose and d-fructose in slightly acidic, aqueous-solution, *Acta Chemica Scandinavica*, B 30 (1976) 397–402.
- [57] T. Popoff, O. Theander, E. Westerlund, Formation of aromatic-compounds from carbohydrates .6. reaction of dihydroxyacetone in slightly acidic, aqueous-solution, *Acta Chemica Scandinavica*, B 32 (1978) 1–7.
- [58] O. Theander, E. Westerlund, Formation of aromatic-compounds from carbohydrates .8. reaction of d-erythrose in slightly acidic, aqueous-solution, *Acta Chemica Scandinavica*, B 34 (1980) 701–705.
- [59] A. Vikkula, J. Valkama, T. Vuorinen, Formation of aromatic and other unsaturated end groups in carboxymethyl cellulose during hot alkaline treatment, *Cellulose* 13 (2006) 593–600.

-
- [60] I. Forsskahl, H. Tylli, C. Olkkonen, Participation of carbohydrate-derived chromophores in the yellowing of high-yield and tcf pulps, *Journal of Pulp and Paper Science* 26 (2000) 245–249.
- [61] T. Bikova, A. Treimanis, Uv-absorbance of oxidized xylan and monocarboxyl cellulose in alkaline solutions, *Carbohydrate Polymers* 55 (2004) 315–322.
- [62] P. E. G. Loureiro, A. J. S. Fernandes, M. G. V. S. Carvalho, D. V. Evtuguin, The assessment of chromophores in bleached cellulosic pulps employing uv-raman spectroscopy, *Carbohydrate Research* 345 (2010) 1442–1451.
- [63] A. S. Jääskeläinen, K. Toikka, A. Lahdetie, T. Liitia, T. Vuorinen, Reactions of aromatic structures in brightness reversion of fully-bleached eucalyptus kraft pulps, *Holzforschung* 63 (2009) 278–281.
- [64] K. Krainz, A. Potthast, U. Suess, T. Dietz, N. Nimmerfroh, T. Rosenau, Effects of selected key chromophores on cellulose integrity upon bleaching 10(th) ewlp, stockholm, sweden, august 25-28, 2008, *Holzforschung* 63 (2009) 647–655.
- [65] S. L. Tseng, A. Valente, D. G. Gray, Cholesteric liquid-crystalline phases based on (acetoxypentyl)cellulose, *Macromolecules* 14 (1981) 715–719.
- [66] S. N. Bhadani, D. G. Gray, Cellulose-based liquid-crystalline polymers - esters of (hydroxypropyl) cellulose, *Molecular Crystals and Liquid Crystals* 99 (1983) 29–38.
- [67] I. Rusig, M. H. Godinho, L. Varichon, P. Sixou, J. Dedier, C. Filliatre, A. F. Martins, Optical-properties of cholesteric (2-hydroxypropyl) cellulose (hpc) esters, *Journal of Polymer Science, Part B: Polymer Physics* 32 (1994) 1907–1914.
- [68] H. Q. Hou, A. Reuning, J. H. Wendorff, A. Greiner, Tuning of the pitch height of thermotropic cellulose esters, *Macromolecular Chemistry and Physics* 201 (2000) 2050–2054.
- [69] M. Müller, R. Zentel, Cholesteric phases and films from cellulose derivatives, *Macromolecular Chemistry and Physics* 201 (2000) 2055–2063.
- [70] H. DeVries, Rotatory power and other optical properties of certain liquid crystals, *Acta Crystallographica* 4 (1951) 219–226.

- [71] A. Greiner, H. Hou, A. Reuning, A. Thomas, J. H. Wendorff, S. Zimmermann, Synthesis and opto-electronic properties of cholesteric cellulose esters, *Cellulose* 10 (2003) 37–52.
- [72] I. Costa, D. Filip, J. L. Figueirinhas, M. H. Godinho, New cellulose derivatives composites for electro-optical sensors, *Carbohydrate Polymers* 68 (2007) 159–165.
- [73] J. R. Lakowicz, *Principles of Fluorescence Spectroscopy*, Springer Science+Business Media, LLC, 2006.
- [74] J. A. Olmstead, D. G. Gray, Fluorescence spectroscopy of cellulose lignin and mechanical pulp: A review, *Journal of Pulp and Paper Science* 23 (1997) J571–J581.
- [75] B. Albinsson, S. M. Li, K. Lundquist, R. Stomberg, The origin of lignin fluorescence, *Journal of Molecular Structure* 508 (1999) 19–27.
- [76] K. Radotic, A. Kalauzi, D. Djikanovic, M. Jeremic, R. M. Leblanc, Z. G. Cerovic, Component analysis of the fluorescence spectra of a lignin model compound, *J. Photochem. Photobiol.*, B 83 (2006) 1–10.
- [77] A. Castellan, V. Trichet, J. C. Pommier, A. Siohan, S. Armagnacq, Photo and thermal-stability of totally chlorine-free softwood pulps studied by uv/vis diffuse-reflectance and fluorescence spectroscopy, *Journal of Pulp and Paper Science* 21 (1995) J291–J296.
- [78] A. Castellan, R. Ruggiero, E. Frollini, L. A. Ramos, C. Chirat, Studies on fluorescence of cellulose, *Holzforschung* 61 (2007) 504–508.
- [79] S. Liukko, V. Tasapuro, T. Liitia, Fluorescence spectroscopy for chromophore studies on bleached kraft pulps, *Holzforschung* 61 (2007) 509–515.
- [80] M. Lewin, Oxidation and aging of cellulose, *Macromolecular Symposia* 118 (1997) 715–724.
- [81] N. Duran, E. Gomez, H. Mansilla, Biomass photo-chemistry. a review and prospects, *Polymer Degradation and Stability* 17 (1987) 131–141.

-
- [82] J. Röhring, A. Potthast, T. Rosenau, T. Lange, A. Borgards, H. Sixta, P. Kosma, A novel method for the determination of carbonyl groups in celluloses by fluorescence labeling. 2. validation and applications, *Biomacromolecules* 3 (2002) 969–975.
- [83] J. Röhring, A. Potthast, T. Rosenau, T. Lange, A. Borgards, H. Sixta, P. Kosma, Synthesis and testing of a novel fluorescence label for carbonyls in carbohydrates and celluloses, *Synlett* (2001) 682–684.
- [84] J. Röhring, A. Potthast, T. Rosenau, T. Lange, G. Ebner, H. Sixta, P. Kosma, A novel method for the determination of carbonyl groups in celluloses by fluorescence labeling. 1. method development, *Biomacromolecules* 3 (2002) 959–968.
- [85] A. Potthast, A. Röhring, T. Rosenau, A. Borgards, H. Sixta, P. Kosma, A novel method for the determination of carbonyl groups in celluloses by fluorescence labeling. 3. monitoring oxidative processes, *Biomacromolecules* 4 (2003) 743–749.
- [86] M. Kostic, A. Potthast, T. Rosenau, P. Kosma, H. Sixta, A novel approach to determination of carbonyl groups in dmac/licl-insoluble pulps by fluorescence labeling, *Cellulose* 13 (2006) 429–435.
- [87] R. Bohrn, A. Potthast, T. Rosenau, H. Sixta, P. Kosma, Synthesis and testing of a novel fluorescence label for carboxyls in carbohydrates and celluloses, *Synlett* 20 (2005) 3087–3090.
- [88] R. Bohrn, A. Potthast, S. Schiehser, T. Rosenau, H. Sixta, P. Kosma, The fdam method: Determination of carboxyl profiles in cellulosic materials by combining group-selective fluorescence labeling with gpc, *Biomacromolecules* 7 (2006) 1743–1750.
- [89] S. Hornig, C. Biskup, A. Grafe, J. Wotschadlo, T. Liebert, G. J. Mohr, T. Heinze, Biocompatible fluorescent nanoparticles for ph-sensing, *Soft Matter* 4 (2008) 1169–1172.
- [90] C. Legnani, C. Vilani, V. L. Calil, H. S. Barud, W. G. Quirino, C. A. Achete, S. J. L. Ribeiro, M. Cremona, Bacterial cellulose membrane as flexible substrate for organic light emitting devices, *Thin Solid Films* 517 (2008) 1016–1020.

- [91] Y. Okahisa, A. Yoshida, S. Miyaguchi, H. Yano, Optically transparent wood-cellulose nanocomposite as a base substrate for flexible organic light-emitting diode displays, *Composites Science And Technology* 69 (2009) 1958–1961.
- [92] A. C. Small, J. H. Johnston, Novel hybrid materials of cellulose fibres and doped zns nanocrystals, *Current Applied Physics* 8 (2008) 512–515.
- [93] M. J. Frampton, T. D. W. Claridge, G. Latini, S. Brovelli, F. Cacialli, H. L. Anderson, Amylose-wrapped luminescent conjugated polymers, *Chemical Communications* 24 (2008) 2797–2799.
- [94] M. Karakawa, M. Chikamatsu, C. Vakamoto, Y. Maeda, S. Kubota, K. Yase, Organic light-emitting diode application of fluorescent cellulose as a natural polymer, *Macromolecular Chemistry and Physics* 208 (2007) 2000–2006.
- [95] M. Karakawa, M. Chikamatsu, Y. Yoshida, R. Azumi, K. Yase, C. Nakamoto, Organic memory device based on carbazole-substituted cellulose, *Macromolecular Rapid Communications* 28 (2007) 1479–1484.
- [96] F. X. Redl, M. Lutz, J. Daub, Chemistry of porphyrin-appended cellulose strands with a helical structure: Spectroscopy, electrochemistry, and in situ circular dichroism spectroelectrochemistry, *Chemistry-A European Journal* 7 (2001) 5350–5358.
- [97] W. Holzer, A. Penzkofer, F. Redl, M. Lutz, J. Daub, Excitation energy density dependent fluorescence behaviour of a regioselectively functionalized tetraphenylporphyrin-cellulose conjugate, *Chemical Physics* 282 (2002) 89–99.
- [98] K. Sakakibara, Y. Ogawa, F. Nakatsubo, First cellulose langmuir-blodgett films towards photocurrent generation systems, *Macromolecular Rapid Communications* 28 (2007) 1270–1275.
- [99] K. Sakakibara, F. Nakatsubo, Fabrication of anodic photocurrent generation systems by use of 6-o-dihydrophytylcellulose as a matrix or a scaffold of porphyrins, *Cellulose* 15 (2008) 825–835.
- [100] K. Sakakibara, F. Nakatsubo, Effect of fullerene on photocurrent performance of 6-o-porphyrin-2,3-di-o-stearoylcellulose langmuir-blodgett films, *Macromolecular Chemistry And Physics* 209 (2008) 1274–1281.

-
- [101] M. Nowakowska, S. Zapotoczny, M. Sterzel, E. Kot, Novel water-soluble photosensitizers from dextrans, *Biomacromolecules* 5 (2004) 1009–1014.
- [102] M. Nowakowska, M. Sterzel, S. Zapotoczny, E. Kot, Photosensitized degradation of ethyl parathion pesticide in aqueous solution of anthracene modified photoactive dextran, *Applied Catalysis B-Environmental* 57 (2005) 1–8.
- [103] H. Tylli, I. Forsskahl, C. Olkkonen, A spectroscopic study of photoirradiated cellulose, *Journal of Photochemistry and Photobiology, A: Chemistry* 76 (1993) 143–149.
- [104] A. C. Bertolini, C. Mestres, J. Raffi, A. Buleon, D. Lerner, P. Colonna, Photodegradation of cassava and corn starches, *Journal of Agricultural and Food Chemistry* 49 (2001) 675–682.
- [105] R. A. Wach, H. Kudoh, M. L. Zhai, Y. Muroya, Y. Katsumura, Laser flash photolysis of carboxymethylcellulose in an aqueous solution, *Journal of Polymer Science, Part A: Polymer Chemistry* 43 (2005) 505–518.
- [106] J. Malesic, J. Kolar, M. Strlic, D. Kocar, D. Fromageot, J. Lemaire, O. Haillant, Photo-induced degradation of cellulose, *Polymer Degradation and Stability* 89 (2005) 64–69.
- [107] M. U. de la Orden, J. M. Urreaga, Photooxidation of cellulose treated with amino compounds, *Polymer Degradation and Stability* 91 (2006) 2053–2060.
- [108] D. Klemm, M. Schnabelrauch, A. Stein, Modification of o-trialkylsilylcellulose with cinnamic acid-containing side chains, *Macromolecular Chemistry* 191 (1990) 2985–2991.
- [109] A. R. Esker, H. Grül, G. Wegner, S. K. Satija, C. C. Han, Isotopic selectivity in ultrathin langmuir-blodgett membranes of a cross-linked cellulose derivative, *Langmuir* 17 (2001) 4688–4692.
- [110] U. Bora, P. Sharma, K. Kannan, P. Nahar, Photoreactive cellulose membrane - a novel matrix for covalent immobilization of biomolecules, *Journal of Biotechnology* 126 (2006) 220–229.
- [111] J. Delville, C. Joly, P. Dole, C. Bliard, Solid state photocrosslinked starch based films: a new family of homogeneous modified starches, *Carbohydrate Polymers* 49 (2002) 71–81.

- [112] J. Delville, C. Joly, P. Dole, C. Bliard, Influence of photocrosslinking on the retrogradation of wheat starch based films, *Carbohydrate Polymers* 53 (2003) 373–381.
- [113] J. Zhou, J. Zhang, Y. H. Ma, J. Tong, Surface photo-crosslinking of corn starch sheets, *Carbohydrate Polymers* 74 (2008) 405–410.
- [114] J. Zhou, Y. H. Ma, J. Zhang, J. Tong, Influence of surface photocrosslinking on properties of thermoplastic starch sheets, *Journal of Applied Polymer Science* 112 (2009) 99–106.
- [115] A. P. Kumar, R. P. Singh, Biocomposites of cellulose reinforced starch: Improvement of properties by photo-induced crosslinking, *Bioresource Technology* 99 (2008) 8803–8809.
- [116] E. A. AbdelRazik, Photoinduced graft copolymerization of ethyl acrylate, methyl methacrylate and methyl acrylate onto ethyl cellulose in homogeneous media, *Journal of Photochemistry and Photobiology, A: Chemistry* 107 (1997) 271–274.
- [117] Z. X. Li, L. G. Wang, Y. Huang, Photoinduced graft copolymerization of polymer surfactants based on hydroxyethyl cellulose, *Journal of Photochemistry and Photobiology, A: Chemistry* 190 (2007) 9–14.
- [118] M. Kamath, J. Kincaid, B. K. Mandal, Interpenetrating polymer networks of photocrosslinkable cellulose derivatives, *Journal of Applied Polymer Science* 59 (1996) 45–50.
- [119] C. K. Woo, B. Schiewe, G. Wegener, Multilayered assembly of cellulose derivatives as primer for surface modification by polymerization, *Macromolecular Chemistry and Physics* 207 (2006) 148–159.
- [120] J. Griffiths, Photochemistry of azobenzene and its derivatives, *Chemical Society Reviews* 1 (1972) 481–493.
- [121] K. G. Yager, C. J. Barrett, Novel photo-switching using azobenzene functional materials, *Journal of Photochemistry and Photobiology A: Chemistry* 182 (2006) 250–261.

-
- [122] K. Arai, H. Udagawa, Application of photoresponsive groups-containing cellulose as an adsorbent for thin layer chromatography, *Macromolecular Rapid Communications* 9 (1988) 797–800.
- [123] K. Arai, S. Sano, H. Satoh, Preparation of cellulose stilbene-4-carboxylate and its application to thin-layer chromatography, *Journal of Materials Chemistry* 2 (1992) 1257–1260.
- [124] K. Arai, S. Sano, Preparation of cellulose 2-methylstilbene-5-carboxylate and photoregulation of its properties, *Journal of Materials Chemistry* 4 (1994) 275–278.
- [125] K. Arai, Y. Kawabata, Changes in the sol-gel transformation behaviour of azobenzene moiety-containing methylcellulose irradiated with uv light, *Macromolecular Rapid Communications* 16 (1995) 875–880.
- [126] P. Zheng, X. Hu, X. Zhao, L. Li, K. C. Tam, L. H. Gan, Photoregulated sol-gel transition of novel azobenzene-functionalized hydroxypropyl methylcellulose and its α -cyclodextrin complexes, *Macromolecular Rapid Communications* 25 (2004) 678–682.
- [127] X. Hu, P. Zheng, X. Zhao, L. Li, K. Tam, L. Gan, Preparation, characterization and novel photoregulated rheological properties of azobenzene functionalized cellulose derivatives and their α -cd complexes, *Polymer* 45 (2004) 6219–6225.
- [128] W. Wang, M.-Z. Wang, Effect of cyclodextrin on the photoisomerization of azobenzene functionalized hydroxypropyl methylcellulose in aqueous solution, *Polymer Bulletin* 59 (2007) 537–544.
- [129] H. Wondraczek, T. Heinze, Efficient synthesis and characterization of new photoactive dextran esters showing nanosphere formation, *Macromolecular Bioscience* 8 (2008) 606–614.
- [130] S. Yang, M. M. Jacob, L. Li, A. L. Cholli, J. Kumar, S. K. Tripathy, Synthesis and characterization of novel azobenzene-modified polymers: Azocellulose, *Macromolecules* 34 (2001) 9193–9196.
- [131] S. Yang, M. M. Jacob, L. Li, K. Yang, A. L. Cholli, J. Kumar, S. K. Tripathy, Azobenzene modified cellulose, *Polymer News* 27 (2002) 368–372.

- [132] E. Yashima, J. Noguchi, Y. Okamoto, Photocontrolled chiral recognition by [4-(phenylazo)phenyl]carbamoylated cellulose and amylose membranes, *Macromolecules* 28 (1995) 8368–8374.
- [133] S. Patnaik, A. K. Sharma, B. S. Garg, R. P. Gandhi, K. C. Gupta, Photoregulation of drug release in azo-dextran nanogels, *International Journal of Pharmaceutics* 342 (2007) 184–193.
- [134] K. Arai, H. Satoh, Liquid crystalline phase-formation behavior of cellulose cinnamate, *Journal of Applied Polymer Science* 45 (1992) 387–390.
- [135] H. Murakami, A. Kawabuchi, K. Kotoo, M. Kunitake, N. Nakashima, A light-driven molecular shuttle based on a rotaxane, *Journal of the American Chemical Society* 119 (1997) 7605–7606.
- [136] S. Z. Yang, L. Li, A. L. Cholli, J. Kumar, S. K. Tripathy, Photoinduced surface relief gratings on azocellulose films, *Journal of Macromolecular Science, Part A: Pure and Applied Chemistry* 38 (2001) 1345–1354.
- [137] R. Guglielmetti, $4n+2$ systems: Spiroyrans, in: H. Dürr, H. Bouas-Laurent (Eds.), *Photochromism: Molecules and Systems*, Elsevier Science & Technology, Amsterdam, 2003, pp. 314–466.
- [138] R. C. Bertelson, Spiroyrans, in: J. C. Crano, R. J. Guglielmetti (Eds.), *Organic Photochromic and Thermochromic Compounds*, Plenum Press, New York-London, 1999, pp. 11–84.
- [139] R. C. Bertelson, Photochromic processes involving heterocyclic cleavage, in: G. H. Brown (Ed.), *Photochromism*, Wiley-Interscience, New York, 1971, pp. 45–431.
- [140] T. Heinze, U. Erler, U. Heinze, J. Camacho, U.-W. Grummt, D. Klemm, Synthesis and characterization of photosensitive 4,4'-bis(dimethylamino)diphenylmethyl ethers of cellulose, *Macromolecular Chemistry and Physics* 196 (1995) 1937–1944.
- [141] K. Arai, Y. Kawabata, Preparation of triphenylcarbinol moiety-containing cellulose derivative and its properties, *Macromolecular Chemistry and Physics* 196 (1995) 2139–2147.

- [142] K. Arai, Y. Shitara, T. Ohyama, Preparation of photochromic spiropyrans linked to methyl cellulose and photoregulation of their properties, *Journal of Materials Chemistry* 6 (1996) 11–14.
- [143] K. Arai, T. Ohyama, Y. Shitara, Preparation of a spironaphthoxazine moiety-containing methyl cellulose and photoregulation of its properties, *Polymer Journal* 29 (1997) 780–783.
- [144] M. H. Lee, X. D. Li, E. Kim, Preparation of photochromic cellulose derivatives containing spirobenzopyran, *Molecular Crystals and Liquid Crystals* 349 (2000) 51–54.
- [145] J. I. Edahiro, K. Sumaru, T. Takagi, T. Shinbo, T. Kanamori, Photoresponse of an aqueous two-phase system composed of photochromic dextran, *Langmuir* 22 (2006) 5224–5226.
- [146] A. B. Lowe, C. L. McCormick, Synthesis and solution properties of zwitterionic polymers, *Chem Rev* 102 (2002) 4177–4189.
- [147] S. E. Kudaibergenov, A. Ciferri, Natural and synthetic polyampholytes, 2 functions and applications, *Macromol Rapid Commun* 28 (2007) 1969–1986.
- [148] A. V. Dobrynin, R. H. Colby, M. Rubinstein, Polyampholytes, *J Polym Sci B: Polym Phys* 42 (2004) 3513–3538.
- [149] A. Ciferri, S. Kudaibergenov, Natural and synthetic polyampholytes, 1 theory and basic structures, *Macromol Rapid Commun* 28 (2007) 1953–1968.
- [150] T. Heinze, T. G. K. Petzold-Welcke, H. Wondraczek, Synthesis and characterization of aminocellulose sulfates as novel ampholytic polymers, *Cellulose* (2012) in press, DOI: 10.1007/s10570-012-9725-1.
- [151] K. Rahn, M. Diamantoglou, D. Klemm, H. Berghmans, T. Heinze, Homogeneous synthesis of cellulose p-toluenesulfonates in n,n-dimethylacetamide/licl solvent system, *Angew Makromol Chem* 238 (1996) 143–163.
- [152] T. Heinze, K. Rahn, The first report on a convenient synthesis of novel reactive amphiphilic polysaccharides, *Macromol Rapid Commun* 17 (1996) 675–681.
- [153] K. Petzold-Welcke, N. Michaelis, T. Heinze, Unconventional cellulose products through nucleophilic displacement reactions, *Macromol Symp* 280 (2009) 72–85.

- [154] J. Tiller, D. Klemm, P. Berlin, Designed aliphatic aminocellulose derivatives as transparent and functionalized coatings for enzyme immobilization, *Des Monomers Polym* 4 (2001) 315–328.
- [155] A. M. Bieser, J. C. Tiller, Mechanistic considerations on contact-active antimicrobial surfaces with controlled functional group densities, *Macromol Biosci* 11 (2011) 526–534.
- [156] M. Gericke, T. Liebert, T. Heinze, Interaction of ionic liquids with polysaccharides, 8 – synthesis of cellulose sulfates suitable for polyelectrolyte complex formation, *Macromol Biosci* 9 (2009) 343–353.
- [157] M. Nikolajski, J. Wotschadlo, J. H. Clement, T. Heinze, Amino functionalized cellulose nanoparticles: Preparation, characterization and interactions with living cells, *Macromol Biosci* (2012).
- [158] T. Heinze, S. Daus, M. Gericke, T. Liebert, Semi-synthetic sulfated polysaccharides - promising materials for biomedical applications and supramolecular architecture, in: A. Tiwari (Ed.), *Polysaccharides: Development, Properties and Applications*, Nova Science Publishers, 2010, pp. 213–259.
- [159] M. Gericke, A. Doliska, J. Stana, T. Liebert, T. Heinze, K. Stana-Kleinschek, Semi-synthetic polysaccharide sulfates as anticoagulant coatings for pet - i: Cellulose sulfate, *Macromolecular Bioscience* 11 (2011) 549–556.
- [160] S. Daus, K. Petzold-Welcke, M. Kötteritzsch, A. Baumgaertel, U. S. Schubert, T. Heinze, Homogeneous sulfation of xylan from different sources, *Macromolecular Materials and Engineering* 296 (2011) 551–561.
- [161] S. Daus, T. Heinze, Xylan-based nanoparticles: Prodrugs for ibuprofen release, *Macromol Biosci* 10 (2010) 211–220.
- [162] T. Heinze, M. Nikolajski, S. Daus, T. M. D. Besong, N. Michaelis, P. Berlin, G. A. Morris, A. J. Rowe, S. E. Harding, Protein-like oligomerization of carbohydrates, *Angew Chem, Int Ed* 50 (2011) 8602–8604.
- [163] J. Sirvio, A. Honka, H. Liimatainen, J. Niinimäki, O. Hormi, Synthesis of highly cationic water-soluble cellulose derivative and its potential as novel biopolymeric flocculation agent, *Carbohydr Polym* 86 (2011) 266–270.

- [164] P. Berlin, D. Klemm, A. Jung, H. Liebegott, R. Rieseler, J. Tiller, Film-forming aminocellulose derivatives as enzyme-compatible support matrices for biosensor developments, *Cellulose* 10 (2003) 343–367.
- [165] K. Schwikal, T. Heinze, B. Saake, J. Puls, A. Kaya, A. R. Esker, Properties of spruce sulfite pulp and birch kraft pulp after sorption of cationic birch xylan, *Cellulose* 18 (2011) 727–737.
- [166] J. H. Yang, Y. Liu, H. B. Wang, L. Liu, W. Wang, C. D. Wang, Q. Wang, W. G. Liu, The biocompatibility of fatty acid modified dextran-arginine bioconjugate gene delivery vector, *Biomaterials* 33 (2012) 604–613.
- [167] K. J. Edgar, C. M. Buchanan, J. S. Debenham, P. A. Rundquist, B. D. Seiler, M. C. Shelton, D. Tindall, Advances in cellulose ester performance and application, *Progress In Polymer Science* 26 (2001) 1605–1688.
- [168] K. J. Edgar, Cellulose esters in drug delivery, *Cellulose* 14 (2007) 49–64.
- [169] S. Boddohi, M. J. Kipper, Engineering nanoassemblies of polysaccharides, *Advanced Materials* 22 (2010) 2998–3016.
- [170] K. Janes, P. Calvo, M. Alonso, Polysaccharide colloidal particles as delivery systems for macromolecules, *Advanced Drug Delivery Reviews* 47 (2001) 83 – 97.
- [171] V. R. Sinha, A. K. Singla, S. Wadhawan, R. Kaushik, R. Kumria, K. Bansal, S. Dhawan, Chitosan microspheres as a potential carrier for drugs, *International Journal of Pharmaceutics* 274 (2004) 1–33.
- [172] M. Prabakaran, J. F. Mano, Chitosan-based particles as controlled drug delivery systems, *Drug Delivery* 12 (2005) 41–57.
- [173] Z. Liu, Y. Jiao, Y. Wang, C. Zhou, Z. Zhang, Polysaccharides-based nanoparticles as drug delivery systems, *Advanced Drug Delivery Reviews* 60 (2008) 1650–1662.
- [174] H. Peniche, C. Peniche, Chitosan nanoparticles: a contribution to nanomedicine, *Polymer International* 60 (2011) 883–889.

- [175] S. Hornig, H. Bunjes, T. Heinze, Preparation and characterization of nanoparticles based on dextran–drug conjugates, *Journal of Colloid and Interface Science* 338 (2009) 56–62.
- [176] T. Heinze, N. Michealis, S. Hornig, Reactive polymeric nanoparticles based on unconventional dextran derivatives, *European Polymer Journal* 43 (2007) 697–703.
- [177] E. M. Bachelder, T. T. Beaudette, K. E. Broaders, J. Dashe, J. M. J. Frechet, Acetal-derivatized dextran: An acid-responsive biodegradable material for therapeutic applications, *Journal of the American Chemical Society* 130 (2008) 10494–10495.
- [178] D. Horn, J. Rieger, Organic nanoparticles in the aqueous phase—theory, experiment, and use, *Angewandte Chemie International Edition* 40 (2001) 4330–4361.
- [179] T. Heinze, R. Dicke, A. Koschella, A. H. Kull, E.-A. Klohr, W. Koch, Effective preparation of cellulose derivatives in a new simple cellulose solvent, *Macromolecular Chemistry and Physics* 201 (2000) 627–631.
- [180] N. Anton, J.-P. Benoit, P. Saulnier, Design and production of nanoparticles formulated from nano-emulsion templates—a review, *Journal of Controlled Release* 128 (2008) 185 – 199.
- [181] P. Walstra, Principles of emulsion formation, *Chemical Engineering Science* 48 (1993) 333–349.
- [182] S. Schubert, J. T. Delaney, U. S. Schubert, Nanoprecipitation and nanoformulation of polymers: from history to powerful possibilities beyond poly(lactic acid) *Journal of Materials Chemistry* 21 (2010) 9649–9660.
- [183] J. Aubry, F. Ganachaud, J. P. C. Addad, B. Cabane, Nanoprecipitation of polymethylmethacrylate by solvent shifting: 1. boundaries, *Langmuir* 25 (2009) 1970–1979.
- [184] L. Chronopoulou, I. Fratoddi, C. Palocci, I. Venditti, M. V. Russo, Osmosis based method drives the self-assembly of polymeric chains into micro- and nanostructures, *Langmuir* 25 (2009) 11940–11946.

-
- [185] H. Fessi, F. Puisieux, J. Devissaguet, N. Ammoury, S. Benita, Nanocapsule formation by interfacial polymer deposition following solvent displacement, *International Journal of Pharmaceutics* 55 (1989) R1 – R4.
- [186] J. M. Stubbs, D. C. Sundberg, Nonequilibrium particle morphology development in seeded emulsion polymerization. iii. effect of initiator end groups, *Journal of Applied Polymer Science* 91 (2004) 1538–1551.
- [187] S. Hornig, T. Heinze, Efficient approach to design stable water-dispersible nanoparticles of hydrophobic cellulose esters, *Biomacromolecules* 9 (2008) 1487–1492.
- [188] N. Schittenhelm, W.-M. Kulicke, Producing homologous series of molar masses for establishing structure-property relationships with the aid of ultrasonic degradation, *Macromolecular Chemistry and Physics* 201 (2000) 1976–1984.
- [189] S. R. Trenor, A. R. Shultz, B. J. Love, T. E. Long, Coumarins in polymers: From light harvesting to photo-cross-linkable tissue scaffolds, *Chem Rev* 104 (2004) 3059–3078.
- [190] C. H. Krauch, S. Farid, G. O. Schenck, Photo-c4-cyclodimerisation von cumarin, *Chemische Berichte* 99 (1966) 625–633.
- [191] J.-J. Aaron, M. Buna, C. Parkanyi, M. S. Antonious, A. Tine, L. Cisse, Quantitative treatment of the effect of solvent on the electronic absorption and fluorescence spectra of substituted coumarins: Evaluation of the first excited singlet-state dipole moments, *Journal of Fluorescence* 5 (1995) 337–347.
- [192] G. S. Hammond, C. A. Stout, A. A. Lamola, Mechanisms of photochemical reactions in solution 25: Photodimerization of coumarin, *Journal Of The American Chemical Society* 86 (1964) 3103.
- [193] H. Morrison, H. Curtis, T. McDowell, Solvent effects on photodimerization of coumarin, *Journal Of The American Chemical Society* 88 (1966) 5415.
- [194] R. Hoffman, P. Wells, H. Morrison, Organic photochemistry .12. further studies on mechanism of coumarin photodimerization - observation of an unusual heavy atom effect, *Journal Of Organic Chemistry* 36 (1971) 102.

- [195] K. Gnanaguru, N. Ramasubbu, K. Venkatesan, V. Ramamurthy, A study on the photochemical dimerization of coumarins in the solid-state, *Journal Of Organic Chemistry* 50 (1985) 2337–2346.
- [196] H. C. Kim, S. Kreiling, A. Greiner, N. Hampp, Two-photon-induced cycloreversion reaction of coumarin photodimers, *Chemical Physics Letters* 372 (2003) 899–903.
- [197] P. S. Song, W. H. Gordon, Spectroscopic study of excited states of coumarin, *Journal of Physical Chemistry* 74 (1970) 4234–4240.
- [198] M. N. Merzlyak, K. R. Naqvi, On recording the true absorption spectrum and the scattering spectrum of a turbid sample: application to cell suspensions of the cyanobacterium *anabaena variabilis*, *Journal of Photochemistry and Photobiology B-biology* 58 (2000) 123–129.
- [199] S. Fery-Forgues, M. Cantuel, C. Fournier-Noel, Searching for fluorescent nanocrystals in aqueous solutions of 7-methoxycoumarin, *Dyes and Pigments* 87 (2010) 241–248.
- [200] K. Muthuramu, V. Ramamurthy, 7-alkoxy coumarins as fluorescence probes for microenvironments, *Journal of Photochemistry* 26 (1984) 57–64.
- [201] J. R. Heldt, J. Heldt, M. Ston, H. A. Dieh, Photophysical properties of 4-alkylcoumarin and 7-alkoxycoumarin derivatives - absorption and emission-spectra, fluorescence quantum yield and decay time, *Spectrochimica Acta Part A-molecular and Biomolecular Spectroscopy* 51 (1995) 1549–1563.
- [202] M. N. Berberan-Santos, E. N. Bodunov, B. Valeur, Mathematical functions for the analysis of luminescence decays with underlying distributions 1. Kohlrausch decay function (stretched exponential), *Chemical Physics* 315 (2005) 171–182.
- [203] G. Zatoryb, A. Podhorodecki, J. Misiewicz, J. Cardin, F. Gourbilleau, On the nature of the stretched exponential photoluminescence decay for silicon nanocrystals, *Nanoscale Research Letters* 6 (2011) 106.
- [204] E. Arici, A. Greiner, H. Q. Hou, A. Reuning, J. H. Wendorff, Optical properties of guest host systems based on cellulose derivatives, *Macromolecular Chemistry and Physics* 201 (2000) 2083–2090.

- [205] Y. Chen, R. T. Hong, Photopolymerization of 7,7'-coumarinyl polymethylene dicarboxylates: Fluorescence and kinetic study, *Journal of Polymer Science Part A-polymer Chemistry* 35 (1997) 2999–3008.
- [206] T. Liebert, S. Hornig, S. Hesse, T. Heinze, Nanoparticles on the basis of highly functionalized dextrans, *Journal of the American Chemical Society* 127 (2005) 10484–10485.
- [207] M. Terbojevich, A. Cosani, M. Camilot, B. Focher, Solution studies of cellulose tricarbanilates obtained in homogeneous phase, *J Appl Polym Sci* 55 (1995) 1663–1671.
- [208] W. Schöniger, Die mikroanalytische schnellbestimmung von halogenen und schwefel in organischen verbindungen, *Microchim Acta* 44 (1956) 869–876.

Publication List

Scientific publications in peer reviewed journals

1. "Enhanced Dewatering of Polyelectrolyte Nanocomposites by Hydrophobic Polyelectrolytes"
Joshua D. Kittle, Holger Wondraczek, Chao Wang, Feng Jiang, Maren Roman, Thomas Heinze, and Alan R. Esker
Langmuir (2012) in press: DOI: 10.1021/la3016996
2. "Synthesis and characterization of aminocellulose sulfates as novel ampholytic polymers"
Thomas Heinze, Taha Genco, Katrin Petzold-Welcke, Holger Wondraczek
Cellulose **19** (2012) 1305–1313
3. "Water soluble photoactive cellulose derivatives: Synthesis and characterization of mixed 4 2-[(4-methyl-2-oxo-2H-chromen-7-yl)oxy]acetic 5 acid-(3-carboxypropyl)trimethylammonium chloride esters of cellulose"
Holger Wondraczek, Annett Pfeifer, Thomas Heinze
Cellulose **19** (2012) 1327-1335.
4. "Syntheses and detailed structure characterization of dextran carbonates"
Thomas Elschner, Holger Wondraczek, Thomas Heinze
Carbohydrate Polymers (2012) in press: doi:10.1016/j.carbpol.2012.01.091
5. "Synthesis of highly functionalized dextran alkyl carbonates showing nanosphere formation"
Holger Wondraczek, Thomas Elschner, Thomas Heinze
Carbohydrate Polymers **83** (2011) 1112–1118
6. "Photoactive polysaccharides"
Holger Wondraczek, Anne Kotiaho, Pedro Fardim, Thomas Heinze
Carbohydrate Polymers **83** (2011) 1048–1061

7. "Synthetic photocrosslinkable polysaccharide sulfates"
 Holger Wondraczek, Annett Pfeifer, Thomas Heinze
European Polymer Journal **46** (2010) 1688–169
8. "Efficient Synthesis and Characterization of New Photoactive Dextran Esters Showing Nanosphere Formation"
 Holger Wondraczek, Thomas Heinze
Macromolecular Bioscience **8** (2008) 606–614

Oral presentations

1. "Polysaccharide-based nanoparticles"
 Holger Wondraczek, Melanie Nikolajski, Thomas Elschner, Thomas Heinze
 Tekes/FiDiPro Steering-group meeting: Polysaccharide-Based Biomaterials, Turku, Finland, November 30, 2011
2. "Structure and property design of polysaccharide-based nanoparticles"
 Holger Wondraczek, Melanie Nikolajski, Thomas Elschner, Thomas Heinze
 2nd International Polysaccharide Conference, EPNOE2011, Wageningen, The Netherlands, August 29-September 02, 2011
3. "Fluorescence studies of nanoparticles from coumarin-modified dextrans"
 Anne M. Kotiaho, Holger Wondraczek, Pedro Fardim, Thomas Heinze
 2nd International Polysaccharide Conference, EPNOE2011, Wageningen, The Netherlands, August 29-September 02, 2011
4. "On the incorporation of photoactive functions into biocomposites"
 Anne M. Kotiaho, Holger Wondraczek, Pedro Fardim, Thomas Heinze
 241st National Meeting & Exposition, American Chemical Society, Anaheim, CA, US, March 27-31, 2011
5. "Adsorption of derivatized dextran polyelectrolytes onto nanocrystalline cellulose probed via quartz crystal microbalance with dissipation monitoring and surface plasmon resonance"
 Joshua D. Kittle, Feng Jiang, Xiaosong Du, Holger Wondraczek, Andreas Koschella, Thomas Heinze, Maren Roman, Allan R. Esker
 241st National Meeting & Exposition, American Chemical Society, Anaheim, CA, US, March 27-31, 2011

6. "Design of photoactive polysaccharides"
Holger Wondraczek, Thomas Heinze
Tekes/FiDiPro workshop: Polysaccharide-Based Biomaterials, Jena, Germany,
July 6, 2010
7. "Polysaccharide-based nanoparticles: A novel approach for polymer prodrugs"
Thomas Heinze, Stephan Daus, Holger Wondraczek, Stephanie Hornig
104. ZELLCHEMING Hauptversammlung, Cellulose-Symposium, Wiesbaden,
Germany, June 23-24, 2009

Posters

1. "Structure-Activity Relationship of Dialkylaminoethyl-Dextrans for Gene Delivery"
Sofia Ochrimenko, Holger Wondraczek, Ulrich S. Schubert, Thomas Heinze,
Dagmar Fischer
European Symposium on Biomaterials and Related Areas, Jena, Germany,
April 13-14, 2011
2. "Synthesis and nanosphere formation of highly functionalized dextran alkyl carbonates"
Thomas Elschner, Holger Wondraczek, Thomas Heinze
Controlled Release Society German Chapter, Annual Meeting and International
Symposium of the Thuringian ProExcellence Initiative NanoConSens, Jena,
Germany, March 15-16, 2011
3. "Cellular internalization of nanoparticles in culture systems: A polarization microscopical study"
Annett Eitner, Holger Wondraczek, Thomas Heinze, Gustav F. Jirikowski,
Josef Makovitzky
52nd Symposium of the Society for Histochemistry, Prague, Czech Republic,
September 1-9, 2010
4. "Novel polysaccharid-based nanoparticles"
Holger Wondraczek, Stephanie Hornig, Thomas Heinze
First International Conference on Multifunctional, Hybrid and Nanomaterials,
Tours, France, March 15-19, 2009

5. "Nanostructures Based on Polysaccharides: Preparation and Characterization"
Nico Michaelis, Stephanie Hornig, Holger Wondraczek, Thomas Heinze
Fachgruppentagung "Makromolekulare Chemie" der GDCh, Aachen, Germany,
September 28-30, 2008

Acknowledgements/Danksagung

In the first place I am indebted to my supervisor Prof. Dr. Thomas Heinze for the possibility to prepare my Ph.D. thesis in his group. By his constant support, the numerous discussions, and by providing good general conditions he make the current work possible.

Moreover, special thanks goes to all coworkers of the *Center of Excellence for Polysaccharide Research* at the *Friedrich Schiller University of Jena* for the good working atmosphere and the general support. In particular, I am indebted to Annett Pfeifer, Dr. Katrin Petzold-Welcke, Taha Genco, and Thomas Elschner for the efficient cooperation.

For the financial support of my Ph.D. work, I thank the *German Science Foundation* (DFG, project HE 2054/11-1) and the *Thuringian Ministry for Education, Science, and Culture* (grant #B514-09051, NanoConSens). Moreover, I thank the *European Polysaccharide Network of Excellence (EPNOE)* for financing the participation at different international conferences.

Special thanks I would like to dedicate to the international cooperation partners Alan R. Esker and his coworker Joshua D. Kittle (*Department of Chemistry, Virginia Tech*), Maren Roman (*Department of Wood Science and Forest Products, Virginia Tech, Blacksburg, Virginia, USA*) and Pedro Fardim and his coworker Anne M. Kotiaho (*Åbo Akademi University, Turku, Finland*) for the inspiring cooperation and the insights into new methods and scientific fields.

Many thanks also to the employees of the *Institute of Organic Chemistry and Macromolecular Chemistry* of the *Friedrich Schiller University of Jena* and of the *Center of Electron Microscopy* at the *Jena University Hospital* for measuring my samples.

I thank Prof. Dr. Rainer Beckert for the preparation of the second review for this Ph.D. thesis.

Last but not least I thank my friends, my family, in particular my wife Evelyn for their support also beyond the Ph.D. work.

An erster Stelle danke ich meinem Betreuer Prof. Dr. Thomas Heinze für die Möglichkeit meine Doktorarbeit in seiner Arbeitsgruppe anzufertigen. Nur durch seine vielseitige Unterstützung, die zahlreichen Diskussionen und die Schaffung der entsprechenden Rahmenbedingungen ist die vorliegende Arbeit erst möglich geworden.

Ein großer Dank gebührt darüber hinaus allen Mitarbeitern des *Kompetenzzentrums für Polysaccharidforschung* an der *Friedrich-Schiller-Universität Jena* für gute die Arbeitsatmosphäre und die beständige Unterstützung. Im speziellen danke ich Annett Pfeifer, Dr. Katrin Petzold-Welcke, Taha Genco, und Thomas Elschner für die produktive Zusammenarbeit.

Für die Finanzierung meiner Arbeit danke ich der *Deutschen Forschungsgemeinschaft* (DFG, Projekt HE 2054/11-1) sowie dem *Thüringer Ministerium für Bildung, Wissenschaft und Kultur* (#B514-09051, NanoConSens). Darüber hinaus danke ich dem *European Polysaccharide Network of Excellence (EPNOE)* für die finanzielle Absicherung der Teilnahme an verschiedenen internationalen Tagungen.

Den internationalen Kooperationspartnern Alan R. Esker und seinem Mitarbeiter Joshua D. Kittle (*Department of Chemistry, Virginia Tech*), Maren Roman (*Department of Wood Science and Forest Products, Virginia Tech, Blacksburg, Virginia, USA*) sowie Pedro Fardim und seiner Mitarbeiterin Anne M. Kotiaho (*Åbo Akademi University, Turku, Finnland*) danke ich für die inspirierende Zusammenarbeit und die Einblicke in neue Methoden und Wissenschaftsfelder.

Beim technischen Personal des *Instituts für Organische Chemie und Makromolekulare Chemie* der *Friedrich-Schiller-Universität* und des *Elektronenmikroskopisches Zentrum am Universitätsklinikum Jena* danke ich für die durchgeführten Messungen und die Unterstützung bei deren Auswertung.

Prof. Dr. Rainer Beckert danke ich für die Anfertigung des Zweitgutachtens.

Zu guter Letzt danke ich meinen Freunden, meiner Familie und insbesondere meiner Frau Evelyn für die Unterstützung auch über die Arbeiten zur Promotion hinaus.

Declaration of Authorship / Selbständigkeitserklärung

I certify that the work presented here is, to the best of my knowledge and belief, original and the result of my own investigations, except as acknowledged. It has not been submitted in part or whole, as Ph.D. thesis to this or any other university.

Ich erkläre, dass ich die vorliegende Arbeit selbstständig und unter Verwendung der angegebenen Hilfsmittel, persönlichen Mitteilungen und Quellen angefertigt habe. Sie wurde weder im Ganzen noch in Teilen an dieser oder einer anderen Universität zur Erlangung des akademischen Grades *doctor rerum naturalium* (Dr. rer. nat.) vorgelegt.

Jena, den

Holger Wondraczek